The University Of Sheffield.

Characterisation of the essential transcription factor, WhiB1, from *Mycobacterium tuberculosis*

A thesis submitted in part fulfilment for the degree of Doctor of Philosophy.

Department of Molecular Biology and Biotechnology,

The University of Sheffield.

Laura Jayne Smith

MBiolSci (Hons) University of Sheffield

September 2012

Summary

Mycobacterium tuberculosis is a major human pathogen, infecting approximately one third of the world's population. The majority of infected individuals are asymptomatic, and in these cases *M. tuberculosis* is present in a non-replicating persistent state. *Mycobacterium tuberculosis* is capable of emerging from this persistent state and causing active disease. Extensive gene regulation facilitates the entry into and emergence from the persistent state, and understanding this reprogramming of genes may help provide novel methods of treatment. The cAMP receptor protein Rv3676 is a global gene regulator in *M. tuberculosis* that is required for virulence, regulating ~100 genes including *whiB1*. The *whiB1* gene encodes a member of the Wbl family of proteins, which are iron-sulphur cluster-containing transcription factors associated with a role in developmental processes in the actinomycetes. WhiB1, one of seven Wbl proteins encoded by *M. tuberculosis*, was the focus of this study. The *whiB1* gene was identified as being essential for *M. tuberculosis* survival. The WhiB1 protein incorporated a [4Fe-4S] cluster, ligated by four essential cysteine residues, which was stable in the presence of oxygen but reacted rapidly with nitric oxide in a multiphasic reaction forming an unusual octa-nitrosylated cluster. The reduced and oxidised apo-WhiB1 bound both the *whiB1* and *groEL2* promoter regions, but the [4Fe-4S] containing form of WhiB1 (holo-WhiB1) was unable to bind DNA. Treatment of holo-WhiB1 with nitric oxide led to restoration of DNA-binding. The DNA-binding capabilities of WhiB1 were found to be, in part, due to specific amino acid residues in the helix-turn-helix region of the protein. Transcription of *whiB1* is negatively-regulated by apo-WhiB1 in both the presence and absence of Rv3676, which has been identified as activating *whiB1* expression. Thus *whiB1* expression is regulated by two important infection signals *viz.* nitric oxide and cAMP, suggesting a role for WhiB1 in tuberculosis pathogenesis.

Acknowledgments

I have a number of people to thank for achieving the work presented here. Firstly and most importantly, I would like to thank my supervisor Professor Jeff Green for all his help, advice and support over the last four years as none of this would have been possible without him. A huge thanks also goes out to everybody in F10, past and present, for their help and in making it such a fun and great place to work. A special thanks goes to Dr Mel Stapleton for her endless patience, teaching me everything she knows and most importantly for all her radiation expertise that have made a lot of the work here possible. Thanks also go to Dr Robert Paramore for gel filtration experiments and Dr Arthur Moir for N-terminal sequencing. I also have to thank our collaborators at Mill Hill, especially Dr Roger Buxton and Debbie Hunt, for all the *in vivo* work. Thank you also to our collaborators at the University of East Anglia for their advice and use of equipment, in particular Dr Jason Crack for all his help with EPR and CD spectroscopy, as well as with both the experimental and analysis work associated with the kinetic experiments.

Thanks also to all my friends in Sheffield, within and outside of MBB, who over the past eight years have made it an excellent place to be and helped me to get to this point, you know who you all are! Lastly I'd like to thank my Mum and Dad for all their love and support, I couldn't have done it without you.

Publications and Presentations

Publications

Smith, L.J., Stapleton, M.R., Buxton, R.S. and Green, J. **(2012)** Structure-function relationships of the *Mycobacterium tuberculosis* transcription factor WhiB1. *Public Library of Sciences ONE* **7**: e40407.

Stapleton, M.R., **Smith L.J.**, Hunt, D.M., Buxton, R.S. and Green, J. **(2012)** *Mycobacterium tuberculosis* WhiB1 represses transcription of the essential chaperonin GroEL2. *Tuberculosis*, **92:** 328-332.

Crack, J.C., **Smith, L.J.**, Stapleton, M.R., Peck, J., Watmough, N.J., Buttner, M.J., Buxton, R.S., Green, J., Oganesyan, V.S., Thomson, A.J. and Le Brun, N.E. **(2011)** Mechanistic Insight into the Nitrosylation of the [4Fe-4S] Cluster of WhiB-like Proteins. *Journal of the American Chemical Society*, **133**: 1112-1121.

Smith, L.J., Stapleton, M.R., Fullstone, G.J.M., Crack, J.C., Thomson, A.J., Le Brun, N.E., Hunt, D.M., Harvey, E., Adinolfi, S., Buxton, R.S. and Green, J. **(2010)** *Mycobacterium tuberculosis* WhiB1 is an essential DNA-binding protein with a nitric oxide-sensitive iron-sulfur cluster. *Biochemical Journal*, **432**: 417-427.

Jeffrey Green, Jason C. Crack, Adrian J. Jervis, David P. Dibden, **Laura J. Smith**, Andrew J. Thomson and Nick E. Le Brun **(2010)**. Iron-sulphur cluster-based sensors. In Stephen Spiro and Ray Dixon (Ed.), *Sensory mechanisms in bacteria*. Caister Academic Press.

Presentations

Iron-Sulfur Meeting, NIMR Mill Hill (13 April 2012):

Talk presented: Structure-function relationships of the *Mycobacterium tuberculosis* transcription factor WhiB1.

FEMS 4th Congress of European Microbiologists, Geneva (26-30 June 2011):

Poster presented: Characterisation of WhiB1 from *Mycobacterium tuberculosis*.

Society for General Microbiology (SGM) Autumn Meeting, Nottingham (6-9 September 2010):

Talk presented: Characterisation of the WhiB1 protein from *Mycobacterium tuberculosis*.

Iron-Sulfur Meeting, NIMR Mill Hill (6 May 2010):

Talk and poster presented: Characterisation of WhiB1 from *Mycobacterium tuberculosis*.

List of Abbreviations

APS – Ammonium persulphate

cAMP – Cyclic adenosine monophosphate

CD spectroscopy – Circular dichroism spectroscopy

CRP – cAMP receptor protein

CMR – cAMP and macrophage regulator

DMS – Dimethyl sulphate

DNIC – Dinitrosyl iron complex

DTNB – 5,5'-dithiobis(2-nitrobenzoic acid)

DTT – Dithiothreitol

EHR – Enduring hypoxic response

EMSA – Electromobility shift assay

EPR spectroscopy – Electron paramagnetic resonance spectroscopy

Fe-S – Iron-sulphur cluster

kDa – Kilo Dalton

LB – Lennox broth

Mtb – *Mycobacterium tuberculosis*

NO – Nitric oxide

NOS2 – Nitric oxide synthase 2

NTB – 2-Nitro-5-thiobenzoic acid

OD – Optical density

PAGE – Polyacrylamide gel electrophoresis

PDIM – Phenolphthiocerol-dimycocerosate

P*whiB1* – *whiB1* promoter region

RNI – Reactive nitrogen intermediates

RPF – Resuscitation promoting factor A

RRE – Roussin's red ester

SDS – Sodium dodecyl sulphate

TCA – Trichloroacetic acid

TNF – Tumour necrosis factor

UV-vis spectroscopy – Ultra violet visible spectroscopy

Wbl – WhiB-like

Contents

1.0 Introduction

1.1 The lifestyle of Mycobacterium tuberculosis

1.1.1 Mycobacterium tuberculosis as the causative agent of tuberculosis

Mycobacterium tuberculosis is a member of the Mycobacterium genus within the actinomycetes, and is a Gram positive rod-shaped bacterium. *Mycobacterium tuberculosis* is slow growing with a doubling time of 15-20 hours, forming colonies on Petri dishes after 3-4 weeks. In 1882 Robert Koch isolated *M. tuberculosis* for the first time, and demonstrated that it was the causative agent of tuberculosis in humans (Daniel, 2006 and references therein). *Mycobacterium tuberculosis* is an obligate aerobe with a highly impermeable cell envelope containing a variety of unusual lipids that contribute to virulence; these include, mycolic acids (conferring the property of acid-fastness associated with Mycobacteria); glycolipids (including the inflammatory molecule lipoarabinomannan); and polyketides (including phenolphthiocerol, which forms a complex with mycocerosic acid to give the virulence factor phenolphthiocerol-dimycocerosate - PDIM) (Daffé and Draper, 1998). The properties of the *M. tuberculosis* bacillus and its resistance to a wide variety of antibiotics contribute to its virulence and continued presence as one of the world's biggest killers.

1.1.2 Prevalence of tuberculosis

Tuberculosis has been a strain on society for thousands of years, and remains a huge problem throughout the world today. The World Health Organisation estimated there were 8.8 million cases of tuberculosis in 2010 leading to 1.45 million deaths (WHO, 2011). It is also estimated that one third of the world's population (~ 2 billion) is infected with tuberculosis, creating a huge reservoir of *M. tuberculosis* (WHO, 2011). Of this infected population, individuals have a 5-10% risk of developing active tuberculosis. This risk is highly dependent on a number of factors, most significantly that of socio-economic and regional variation that is also impacted by the extent of HIV infection (Dye, 2006; Figure 1.1). Susceptibility to tuberculosis infection is considerably increased by HIV infection and diabetes. Co-infection of tuberculosis and

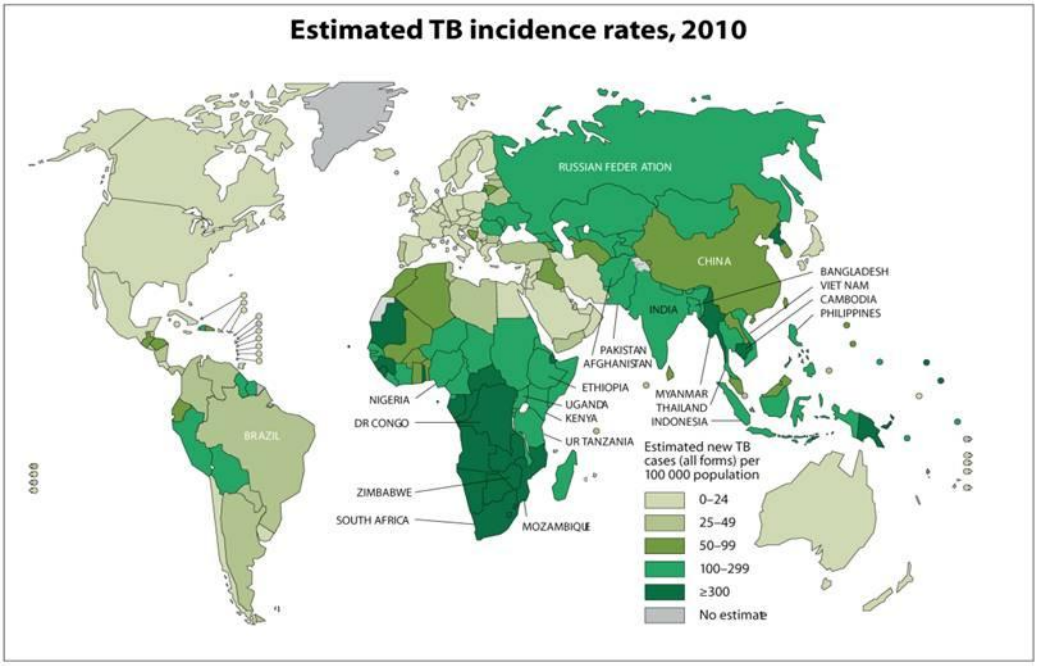

Figure 1.1: Global distribution of the estimated incidence rates of tuberculosis. Map shows the distribution of estimated new cases of tuberculosis in 2010. Numbers are based on cases per 100,000 of the population according to World Health organisation estimates. Map is from the WHO global tuberculosis report 2011 (WHO, 2011).

HIV in sub-Saharan Africa is a particular problem, while the increasing rates of diabetes in rapidly growing economies is also causing an increase in tuberculosis cases (Comas and Gagneux, 2009). Thus tuberculosis is a global problem and due to the increase in multidrug resistant strains continues to be so. Research into *M. tuberculosis* and new methods of treatment are therefore a necessity.

1.1.3 Control of tuberculosis

The continued presence of tuberculosis as a worldwide health problem is in part due to the current inadequate methods of diagnosis, treatment and prevention (Young *et al*., 2008). Diagnosis for both latent and active tuberculosis relies on methods derived in the 19th century with low sensitivity; the skin test for latent infections and sputum-smear microscopy for active tuberculosis infections (Daniel 2006 and references therein; Ehrlich, 1882). Prevention comes in the form of the BCG (bacillus Calmette-Guérin) vaccine derived from *Mycobacterium bovis*. Despite widespread use however, it is largely ineffective at preventing adult pulmonary disease (Young *et al*., 2008).

Mycobacteria are naturally resistant to the majority of antibiotics and chemotherapeutic agents. This is likely due to their highly hydrophobic cell envelope, which acts as an efficient permeability barrier (Nikaido *et al*., 2011). This offers a limited choice for tuberculosis treatment. The current treatment for tuberculosis infections, devised in the 1960s, involves the administration of four drugs over a period of 6-9 months. Chemotherapy comprises of an initial intensive phase of treatment with four drugs for two months, as discussed by Heym and Cole (1997). Here the mycobacteria specific drugs of isoniazid, pyrazinamide and ethambutol as well as the general antibiotic rifampicin, are administered to kill *M. tuberculosis* and prevent the emergence of resistant mutants. The second continuation phase involves treatment for four months with isoniazid and rifampicin to ensure full sterilisation of bacterial cells and the lesions infected by *M. tuberculosis* (Heym and Cole, 1997).

There are a number of problems associated with the current treatment of tuberculosis, including the need for drugs in forms which can be safely administered to children, and

that can be administered in combination with antiretroviral therapy for patients co-infected with tuberculosis and HIV (Swindells, 2012). The current method of treatment is also associated with a number of side effects, which can cause poor patient compliance. This, along with patients stopping their treatment when they begin to feel better, incorrect prescription and unreliable drug sources, leads to a worrying level of drug-resistant tuberculosis (Swindells, 2012). Drug-resistant tuberculosis is harder to treat, requiring a departure from the standard course often taking up to 30 months to administer (Matteelli *et al*., 2007). This treatment involves the use of second-line drugs which have limited efficacy, cause more severe side effects and are more expensive (Heym and Cole, 1997). The emergence of strains of *M. tuberculosis* resistant to several prescribed drugs highlights the problem further. Multidrug-resistant tuberculosis (MDR-TB), defined as strains resistant to isoniazid and rifampicin, is an increasing problem with 400,000 new cases per year (Matteelli *et al*., 2007). More worryingly, extensively resistant tuberculosis (XDR-TB), defined as MDR-TB plus resistance to a quinolone and one of the second-line anti-tuberculosis injectable drugs, for example kanamycin, is an emerging issue (Young *et al*., 2008).

It is clear that further research is required to find new methods of diagnosis, prevention and cure for tuberculosis as the current methods are insufficient. Drugs that can specifically target dormant *M. tuberculosis* cells for example, would not only help in preventing relapses, but may also help eliminate the organism from the huge latently infected population, which in turn would reduce the reservoir of disease (Heym and Cole, 1997).

1.1.4 Infection process of tuberculosis

Infection with *M. tuberculosis* begins with inhalation of the infectious bacilli as droplet nuclei from the atmosphere (Russell, 2001; 2007; Russell *et al*., 2010). These bacilli are known to remain airborne for several hours, and the minimum infectious dose is estimated at a single bacterium (Russell, 2007). Of those infected, between 5-10% develop primary tuberculosis. These individuals are usually children and those who are immunocomprimised (often due to co-infection with HIV), and primary tuberculosis is associated with the disseminated form of the disease (Bloom and Murray, 1992; Stewart

et al., 2003). The majority of people do however control this initial infection by mounting a cell-mediated response. The inhaled bacilli are phagocytosed by alveolar macrophages and are either killed directly or grow intracellularly to a limited extent in a localised lesion, the tubercle (Bloom and Murray, 1992). The formation of this lesion defining the disease and referred to as a granuloma, follows a set chain of events and is summarised here and in Figure 1.2 (Russell, 2001; 2007; Russell *et al*., 2010). The activated alveolar macrophages invade the subtending epithelial layer entering the blood vessels of the lungs. This then induces a localised inflammatory response characterised by the recruitment of mononuclear cells from neighbouring blood vessels, which provide fresh host cells for the expanding bacterial population. These cells become the building blocks of the granuloma, which appears as an unordered mass of monocytes, neutrophils and macrophages. The macrophages differentiate into specialised cell types including foamy macrophages, epithelioid macrophages and multinucleated giant cells. Development of the acquired immune response results in the arrival of lymphocytes, which in turn causes the granuloma to become more structured and organised. This in part is due to the production of tumour necrosis factor (TNF) by macrophages and T cells, which is believed to aid chemokine and adhesion-molecule regulation (Tufariello *et al*., 2003). The macrophage rich centre is surrounded by lymphocytes, and is often enclosed by a fibrous cuff (Russell, 2001; 2007; Russell *et al*., 2010). At this stage the granuloma has reduced blood supply and is generally thought to be hypoxic (Via *et al*., 2008). The arrival of the *M. tuberculosis*-specific lymphocytes 2-6 weeks post infection causes the end of rapid bacterial replication and the killing of some bacilli, resulting in a containment phase (Bloom and Murray, 1992; Russell *et al*., 2010). These lymphocytes are in the form of CD4 and CD8 T cells and B cells. The CD4 and CD8 T cells produce interferon γ, which activates the macrophages in the granuloma. The CD8 T cells can lyse the infected activated macrophages and kill intracellular bacteria (Tufariello *et al*., 2003). This prevents active disease, often with no symptoms being noticed, but can leave a residual population of viable bacteria in the walled-off lesion (Stewart *et al*., 2003). Hypoxia, as seen in the granulomas, has been shown to induce a non-replicative persistence state in *M. tuberculosis* cultures, which explains how a residual population remains (Russell *et al*., 2010; Via *et al*., 2008).

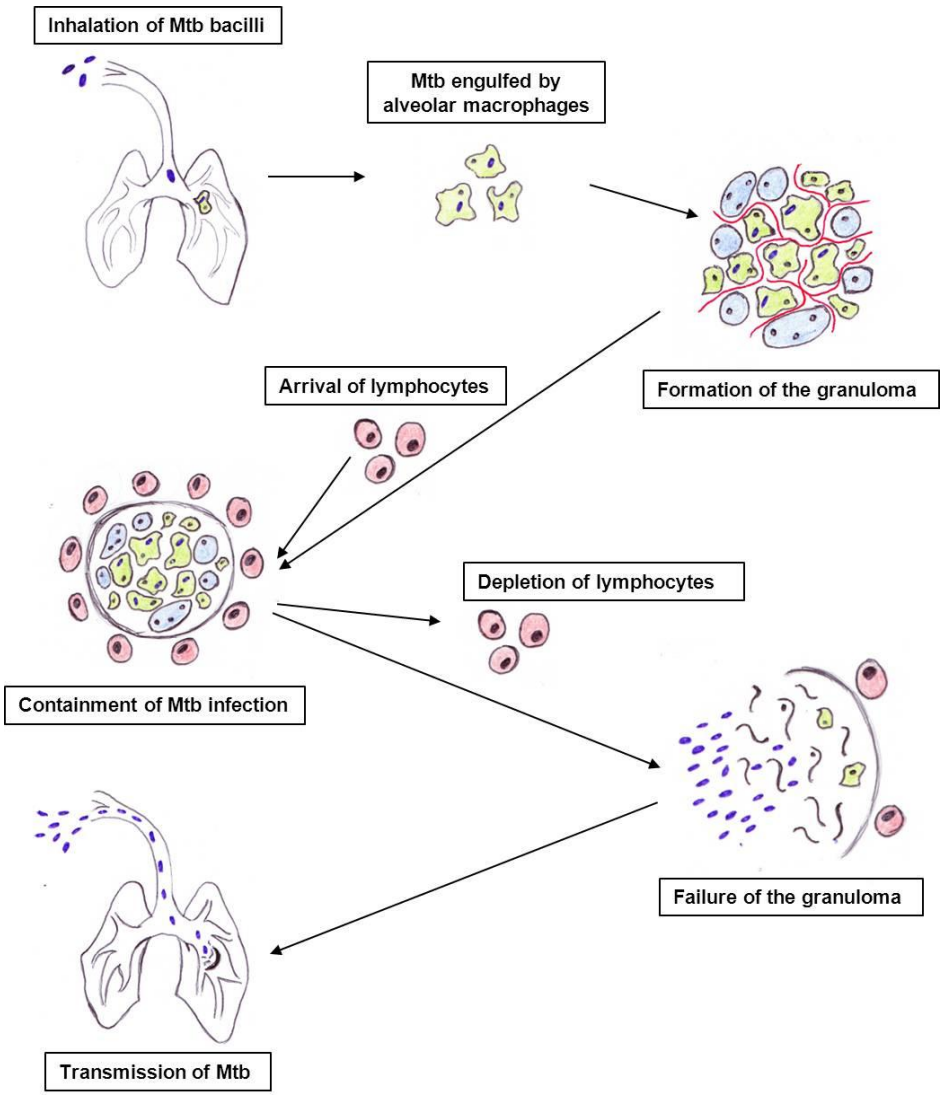

Figure 1.2: Infection process of tuberculosis. The inhaled *M. tuberculosis* (Mtb) bacilli are engulfed by alveolar macrophages (green cells), resulting in a local inflammatory response. Fresh macrophages arrive for the expanding bacterial population, forming the building blocks of the granuloma, which is serviced by numerous blood vessels (red lines). This core is surrounded by differentiated macrophages (blue cells) including foamy macrophages, giant multinucleated cell and epithelioid macrophages. Development of the acquired immune response leads to the arrival of lymphocytes (red cells). This results in a more ordered structure and containment of the infection. The granuloma becomes walled-off by a fibrous cuff and is no longer serviced by blood vessels, thus becoming hypoxic. Depletion of lymphocytes as a result of immunocomprimisation causes the granuloma to no longer be able to contain the infection. Reactivation of Mtb causes rapid replication and the failure of the granuloma. The lesion ruptures spilling infectious bacilli into the airway and the effective transmission of Mtb.

Due to the presence of viable bacteria in the granuloma, post-primary tuberculosis can develop in later life by the reactivation of these bacterial cells or failure to control a second infection (Stewart *et al*., 2003). This occurrence is usually a result of the individual becoming immunocomprimised, causing a reduction in CD4 T cells. Depletion of these T cells results in a reduced ability of the granuloma to contain the bacilli. There is a decrease in the production of interferon γ, which leads to decreased activation of macrophages. This in turn allows *M. tuberculosis* cells to multiply, leading to reactivation of the disease (Tufariello *et al*., 2003). Neutralisation of TNF can also have an effect as it leads to disorder of the granuloma, possibly by deregulating chemokine and adhesion molecule production (Tufariello *et al*., 2003). The granuloma can no longer contain the infection and ruptures releasing thousands of viable bacilli into the airways, creating the characteristic productive cough associated with tuberculosis and efficient aerosol transmission of infectious bacilli (Figure 1.2). This form of tuberculosis is predominately a pulmonary disease, which causes extensive lung damage (Stewart *et al*., 2003).

1.1.5 The role of *Mycobacterium tuberculosis* during infection

In Section 1.1.4, the role of the immune system in controlling *M. tuberculosis* infections is discussed. The bacillus itself however, plays an important role in establishing an infection by its ability to evade the immune response and set up a persistent infection. In doing this, it can survive for extended periods of time in a non-replicating dormant state until conditions are favourable for replication. This then leads to successful transmission, which is the ultimate aim. *Mycobacterium tuberculosis* experiences a variety of hostile environments in its life-cycle of infection and has adopted a number of methods of evasion and survival. Once the *M. tuberculosis* bacilli are engulfed by macrophages, they have the ability to survive and grow intracellularly within a safe niche. They do this by employing a number of methods to prevent being killed by the macrophage itself and evading detection by lymphocytes, which in turn kill the infected macrophage.

Mycobacterium tuberculosis evades two of the major antimicrobial mechanisms of the macrophages; generation of nitric oxide and reactive nitrogen intermediates (RNIs), and the fusion of the phagosomes and lysosomes (Tufariello *et al*., 2003). RNIs are produced by the nitric oxide synthase NOS2, and are essential for controlling *M. tuberculosis* infection in humans (Rich *et al*., 1997). As the host is often unable to eliminate the bacteria, *M. tuberculosis* must express a number of genes to cope with the bactericidal and bacteriostatic effects of these RNIs and persist in the host. This ability will be discussed in detail in Section 1.2. Macrophages engulf bacteria into a compartment referred to as the phagosome. To kill the bacilli the phagosome must mature by fusion with a lysosome forming the phagolysosome, an acidic compartment with bactericidal activity (reviewed in Vieira *et al*., 2002). *Mycobacterium tuberculosis* is capable of interfering with this fusion to form the phagolysosome, thus avoiding the bactericidal activity of the reactive oxygen and nitrogen intermediates, lysozymal enzymes, toxic peptides and the acidic pH (reviewed in Deretic *et al*., 2006; Rohde *et al*., 2007b; Russell, 2001; Smith, 2003; Tufariello *et al*., 2003). As well as this, *M. tuberculosis* also prevents the acidification of the phagosome, restricting it to pH 6.4 not pH 4.8 (Russell, 2007).

As mentioned, *M. tuberculosis* can evade intracellular killing by the macrophages it occupies. The bacilli also produce a number of molecules, including a 19 kDa lipoprotein and a 25 kDa glycolipoprotein, which can interfere with the pathway for processing and presenting of MHC class II antigens by infected macrophages (Noss *et al*., 2001; Wadee *et al*., 1995). Successful presentation of antigens in this manner alerts CD4 T cells, and is thus essential for the priming and effector functions of these lymphocytes (Tufariello *et al*., 2003). *Mycobacterium tuberculosis* is therefore capable of preventing this and can remain safe in the macrophage and evades killing by the acquired immune response, which in turn aids in its persistence (Tufariello *et al*., 2003).

In addition to the evasion of the immune system by occupying a safe niche in the macrophage, *M. tuberculosis* can survive for years in the hypoxic walled-off lesion described in Section 1.1.4. The bacilli do not replicate in this lesion due to its acidic nature, low oxygen levels and the presence of toxic fatty acids, but persist in a non-replicating dormant-like state (Smith, 2003). To remain in the granuloma without being cleared by the immune system, it is thought that the infection is sustained by this

population of non-replicating bacilli and that the immune response mainly targets antigens produced by a small population of actively growing *M. tuberculosis* cells (Russell *et al*., 2009). As well as avoiding the immune response, non-replicating cells avoid the anti-tuberculosis drugs administered. This dormant state of *M. tuberculosis*, bought on by the stress conditions in the granuloma, confers innate immunity to the drugs which target actively growing cells (Russell *et al*., 2009). To survive in the granuloma in the non-replicating state, *M. tuberculosis* must employ mechanisms to cope with the environmental stresses and lack of nutrients. Changes in gene expression are key to this ability. To cope with nutrient starvation for example, genes are induced by *M. tuberculosis* to oxidise fatty acids, which are then used as the main carbon and energy source (Sassetti and Rubin, 2003). There are also sophisticated genetic mechanisms employed to sense and cope with the environmental stresses of hypoxia, nitric oxide and changes in redox potential, which will be discussed in more detail in Section 1.2 (Talaat *et al*., 2004).

It is clear that *M. tuberculosis* is a highly successful pathogen, capable of setting up a persistent infection for extended periods of time. Its ability to evade killing by macrophages and switch from active growth to a non-replicating latent state is key in its success. To do this it must transmit the signals associated with infection, including hypoxia and nitric oxide, to alter its gene expression.

1.2 Transcriptional regulation in M. tuberculosis *during infection*

Following initial infection, *M. tuberculosis* can persist in a non-replicating state from which it may emerge when conditions are more favourable (e.g. in periods of immunosuppression) (Stewart *et al*., 2003). Understanding the persistent state may be key in finding novel ways of controlling tuberculosis. Extensive and appropriate gene regulation is necessary for establishing the non-replicating state (dormancy) and for emerging from it, and a number of studies have explored the expression profiles of *M. tuberculosis* genes associated with infection (Rengarajan *et al*., 2005; Rohde *et al*., 2007a; Sassetti and Rubin, 2003; Schnappinger *et al*., 2003; Talaat *et al*., 2004). Some of the transcriptional regulation mechanisms employed by *M. tuberculosis* in response

to the signals associated with infection, namely hypoxia, nitric oxide and cAMP, will be discussed here.

1.2.1 The transcriptional regulatory network in *M. tuberculosis*

The *M. tuberculosis* genome has over 140 genes encoding regulatory proteins and signal transduction pathways that control gene expression, which are essential for adaption to the variety of stressful environments the bacteria encounters (Cole *et al*., 1998). In addition, *M. tuberculosis* encodes 13 sigma factors that govern gene expression at the transcriptional level, 11 pairs of sensor histidine kinases and response regulators, and 6 serine-threonine protein kinases, all involved in gene regulation (Cole *et al*., 1998). Characterising the function of these regulatory proteins will provide insights into how *M. tuberculosis* relays environmental signals into altered gene expression. What is known currently about a number of the key regulators is discussed below.

1.2.2 Gene regulation in response to hypoxia and nitric oxide

Mycobacterium tuberculosis experiences both hypoxia and the presence of nitric oxide during the infection process. These two important signals of infection need to be relayed to changes in gene expression to allow survival and entrance into the dormant state. Adaption in response to these signals is mediated by the DosR/S/T (dormancy survival regulator) regulon. The dormancy regulon responds to hypoxia, and controls the expression of about 50 genes (Boon and Dick, 2002; Park *et al*., 2003; Voskuil *et al*., 2004). The DosR/S/T regulon controls the shift from aerobic to anaerobic metabolism during *M. tuberculosis* infection, allowing the bacilli to survive during hypoxia-induced dormancy, and facilitates the reversal to replication upon re-exposure to oxygen (Gengenbacher and Kaufmann, 2012; Leistikow *et al*., 2010; Rustad *et al*., 2009). The two sensor kinases of the three component system, DosS (redox sensor) and DosT (hypoxia sensor), have been shown to bind nitric oxide, carbon monoxide and oxygen (Kumar *et al*., 2007). These signals are then relayed to alter gene expression through the DosR regulator. Non-toxic concentrations of nitric oxide induce a 48 gene regulon, via the response regulator DosR, to inhibit aerobic respiration and slow the replication of

cells (Voskuil *et al*., 2003). The individual contributions of the genes induced by the DosR/S/T regulon in aiding *M. tuberculosis* survival in the dormant state are unknown. The DosR/S/T regulon is also thought to be under the control of a number of different transcription factors which, like Dos R/S/T, may respond to the infection signals of hypoxia and nitric oxide as well as oxidative stress and carbon monoxide, both in macrophages and the granuloma.

The role of DosR in response to the infection signal of hypoxia appears to be key in controlling a large network of genes to aid *M. tuberculosis* survival within the host. One study has suggested that there is another response to hypoxia that is independent of DosR. This enduring hypoxic response (EHR) showed a change in 230 genes, including 30 transcriptional regulators, which were significantly induced at four and seven days of hypoxia (Rustad *et al*., 2008). This paper suggests that the EHR may have an important role in controlling bacteriostasis, and that the importance of DosR may not be as significant as previously thought. Identification of the genes regulated by EHR may help shed more light on the changes in gene expression in response to hypoxia.

PhoPR is a two-component system with a role in transcriptional regulation, whereby the PhoR sensor histidine kinase relays yet unidentified stimuli to the PhoP regulator (Gonzalo-Asensio *et al*., 2006). Inactivation of the *phoP* regulator leads to attenuation of *M. tuberculosis*, with impaired growth in macrophages and mice models, and reduced virulence due to reduced secretion of the major T-cell antigen ESAT-6 (Frigui *et al*., 2008; Pérez *et al*., 2001). Transcriptome analysis has identified PhoP to, in part, control the DosR regulon (Gonzalo-Asensio *et al*., 2008). This was further confirmed as the *phoP* mutant showed downregulation of the DosR regulated α-crystallin protein, which is involved in protecting partially folded proteins during long periods of non-replicative growth (Gonzalo-Asensio *et al*., 2008; Sherman *et al*., 2001; Voskuil *et al*., 2003). PhoP is therefore believed to regulate dormancy through cross talk with DosR. Regulation of a subset of genes in the EHR by PhoP also suggests an important role in linking both the initial and enduring hypoxic responses. In addition to its regulation of genes involved in the response to hypoxia, PhoP was also identified as regulating genes encoding proteins with a role in the general stress response, persistence, respiratory metabolism, synthesis of lipids and virulence. These were differentially expressed in response to macrophage

infection, thus PhoP is believed to control many key functions for intracellular survival (Gonzalo-Asensio *et al*., 2008).

It is clear that gene regulation in response to nitric oxide and hypoxia is extremely complex involving an overlapping and vast transcriptional network. It is likely that there are many other regulators involved which are yet to be identified.

1.2.3 Gene regulation in response to cAMP

Cyclic AMP is a universal second messenger, which relays external environmental signals from membrane receptors to effectors within the cell (McDonough and Rodriguez, 2011). The regulatory effects of cAMP in bacteria are through interactions with cAMP receptor proteins. This results in changes in the DNA-binding properties of the regulators and thus alterations in gene expression (McDonough and Rodriguez, 2011). Cyclic AMP is considered as an important signalling molecule in *M. tuberculosis* as suggested by the presence of 15-17 genes encoding adenylyl cyclases, the generators of cAMP (Cole *et al*., 1998). Cyclic AMP is believed to play an important role in the infection process because concentrations increase 50-fold upon *M. tuberculosis* infection of macrophages (Bai *et al*., 2009). This increase upon infection occurs through a mycobacterial-derived cAMP burst, and has been shown to promote bacterial survival by interfering with host signalling pathways (Agarwal *et al*., 2009). The adenylyl cyclases that produce the cAMP show increased activity upon exposure to the infection signals of pH and fatty acids (as seen in the macrophages), and hypoxia and nutrient starvation (as seen in the granuloma) (Bai *et al*., 2011). The production of cAMP by the adenylyl cyclase, Rv0386, has been shown to have a direct link to survival and virulence as deletion of the gene leads to decreased pathology and attenuated virulence in mouse models of infection (Agarwal *et al*., 2009). Furthermore, the importance of cAMP as a signalling molecule to affect gene regulation in promoting survival and virulence has been demonstrated (Gazdik and McDonough, 2005; Rickman *et al*., 2005; Stapleton *et al*., 2010).

This gene regulation is mediated by two members of the cAMP receptor protein (CRP) family of transcription factors, encoded in the *M. tuberculosis* genome (Cole *et al*., 1998). The best characterised is Rv3676, referred to as CRP^{MT}, and has been shown to be a DNA-binding transcriptional regulator of more than 100 genes (Agarwal *et al*., 2006; Bai *et al*., 2005; Rickman *et al*., 2005; Stapleton *et al*., 2010). Rv3676 is necessary for virulence, whereby deletion of the *Rv3676* gene resulted in attenuated growth in macrophages and mice, as well as reduced virulence in mice (Rickman *et al*., 2005). Transcriptome analysis in the form of whole genome microarrays of the H37Rv strain of *M. tuberculosis* revealed that there were significant changes in the *Rv3676* mutant strain compared to the wild-type. Eight genes were identified with a >2.4 fold increase in the abundance of their transcripts in the wild-type compared to the *Rv3676* mutant, and eight genes identified with a >2.4 fold increase in the abundance of their transcripts in the mutant (Rickman *et al*., 2005). Two genes of particular interest were *rpfA* and *whiB1*. The *rpfA* gene encodes resuscitation promoting factor A (RpfA), a member of a group of Rpf proteins that may be involved in the regulation of persistent infection and in the reactivation process (Mukamolova *et al*., 2002). The *whiB1* transcript, encoded by *Rv3219*, was 3.41 fold more abundant in the wild-type strain (Rickman *et al*., 2005). WhiB1 is a member of the Wbl family of proteins. The Wbl family are thought to function as transcription factors, with a role in regulating developmental processes and survival within the host (den Hengst and Buttner, 2008). Thus, Rv3676, in complex with cAMP, regulates genes involved in the formation of *M. tuberculosis*' persistent state and emergence from dormancy (Stapleton *et al*., 2010). Previous studies have shown that *whiB1* is transcribed under the control of Rv3676 and that it is regulated by varying cAMP levels (Agarwal *et al*., 2006). They showed how cAMP-activated Rv3676 directly binds a consensus site adjacent to the *whiB1* promoter, leading to *whiB1* transcription. Further studies by Stapleton *et al.* (2010) have shown that the Rv3676 dimer can bind two molecules of cAMP and that it binds at two adjacent sites in the *whiB1* promoter. At low cAMP concentrations, only the upstream binding site is occupied by Rv3676 causing activation. At high cAMP concentrations, both sites are occupied leading to repression of *whiB1* transcription (Stapleton *et al*., 2010). The role of WhiB1 will be further analysed in this thesis.

Mycobacterium tuberculosis possesses a second member of the cAMP receptor protein family, Rv1675c (Cmr – cAMP and macrophage regulator) (McCue *et al*., 2000).

Rv1675c has not been as well characterised as Rv3676, but it has been identified as a cAMP-responsive transcription factor, regulating four cAMP-induced genes (Gazdik and McDonough, 2005; Gazdik *et al*., 2009). Of these four genes, Rv1675c bound the promoters of *mdh* (encoding a malate dehydrogenase), *groEL2* and *Rv1265* (a gene of unknown function) (Gazdik *et al*., 2009), suggesting direct regulation similar to that seen for Rv3676 of *whiB1*. Gazdik *et al*. (2009) suggest that Rv1675c is a transcription factor that regulates cAMP-induced genes within the macrophage and may be important in *M. tuberculosis* pathogenesis. The role of Rv1675c will be further analysed in this thesis.

1.3 The Wbl family of proteins

WhiB1 is a member of the Wbl (WhiB-like) family of proteins. They are found exclusively in the actinomycetes and play an important role in developmental processes, where they are thought to act as transcription factors (den Hengst and Buttner, 2008). The first member of the family to be identified and characterised was encoded by the *whiB* gene from *Streptomyces coelicolor*, whereby a mutant showed white colonies (the '*whi'* phenotype) opposed to the grey colour associated with the wild-type (Chater, 1972). It was identified in a screen for mutants that abolished sporulation, and thus the grey polyketide pigment associated with it, showing abnormally long, tightly-coiled aerial hyphae that were unable to form septa (Chater, 1972; Davis and Chater, 1992). Genome sequencing has revealed 270 Wbl homologues in the actinomycetes. In *S. coelicolor* there are 14 *wbl* genes, 11 encoded in the chromosome and 3 on the giant linear plasmid, SCP1 (Bentley *et al*., 2002; Bentley *et al*., 2004). Of these, 5 (WhiB, WhiD, WblA, WblC and WblE) are conserved in the actinomycetes. *Mycobacterium tuberculosis* encodes seven Wbl proteins (WhiB1-7) (Cole *et al*., 1998; Soliveri *et al*., 2000). Here the current literature available on the roles of Wbl proteins, as well as their structural and functional characteristics, is discussed.

1.3.1 Structural features of the Wbl proteins

The Wbl family of proteins are characterised by their small size, ranging from 81-122 amino acid residues in length, with the exception of WblP σ factor fusion protein from *S. coelicolor* (den Hengst and Buttner, 2008). The Wbl family have four highly conserved cysteine residues in the N-terminal domain with the central two forming a CXXC motif and a general alignment of Cys-X_{14-22}-Cys-X_2-Cys-X_5-Cys (Soliveri *et al*., 2000). The only exception to this is WhiB5 of *M. tuberculosis*, which has a Cys-X_3-Cys motif (Soliveri *et al*., 2000). The role of the four cysteine residues is considered to be in the binding of a metal co-factor. Another interesting feature of the Wbl proteins, first identified for WhiB from *S. coelicolor*, is the presence of a weakly predicted helix-turn-helix structure in the C-terminal domain (Davis and Chater, 1992). The loop region between the two helices has a conserved GV/IWGG motif, which may be exposed and play a role in interaction with RNA polymerase (Soliveri *et al*., 2000). The predicted helix-turn-helix feature suggests that Wbl proteins function as DNA-binding transcription factors, although there is no strong DNA-binding motif. Wbl proteins all have a high overall hydrophilicity, suggesting a cytoplasmic location. They also have an overall negative charge, but with a positively charged carboxy-region, again highlighting a possible role for them as DNA-binding proteins (Davis and Chater, 1992; Soliveri *et al*., 2000). The function of Wbl proteins, and the role of these structural features, will be discussed in Sections 1.3.2 and 1.3.3.

The presence of four highly conserved cysteine residues in the Wbl proteins suggest that they coordinate a metal co-factor, which is a feature of some DNA-binding proteins. A number of members of the Wbl family from *S. coelicolor* and *M. tuberculosis* have been shown to bind iron-sulphur clusters (Alam *et al*., 2007; 2009; Jakimowicz *et al*., 2005; Rybniker *et al*., 2010; Singh *et al*., 2007). The seven Wbl proteins from *M. tuberculosis* were shown to bind [2Fe-2S] clusters when aerobically expressed and purified, but following anaerobic reconstitution bound [4Fe-4S] clusters (Alam *et al*., 2009). Similar observations were made for WhiD from *S. coelicolor* (Jakimowicz *et al*., 2005). The iron-sulphur clusters, bound by the four cysteine residues, have been shown to be redox sensitive and react with oxygen and nitric oxide (Alam *et al*., 2009; den Hengst and Buttner, 2008; Jakimowicz *et al*., 2005). It is believed that the presence of the iron-sulphur cluster in the Wbl proteins will prove to be essential in controlling function, as

seen for the DNA-binding proteins SoxR and FNR of *Escherichia coli* (summarised by Crack *et al*. (2012)).

1.3.2 Roles of Wbl proteins in *Streptomyces*

As mentioned, the Wbl proteins from the actinomycetes are believed to play a role in developmental processes. The Streptomycetes, of which *S. coelicolor* is a member, are soil-dwelling, spore-forming bacteria which are an important source of antibiotics. Sporulation occurs when conditions are unfavourable for growth, and members of the Wbl family (WhiB and WhiD) have been shown to be important in this process (Chater, 1972; Davis and Chater, 1992; Flärdh *et al*., 1999; McVittie, 1974; Molle *et al*., 2000). WhiB, as discussed in Section 1.3, is essential for the proper septation of spores (Chater, 1972). WhiD is required for the later stages of sporulation, and *whiD* mutants produce spores that are heat-sensitive, prone to lysis and show size and shape irregularities (McVittie, 1974; Molle *et al*., 2000). Other Wbl proteins in *S. coelicolor*, have been shown to have roles in antibiotic production (WblA) and resistance (WblC). WblC was shown to control multidrug resistance in *S. coelicolor* as well as *Streptomyces lividans*, whereby a *wblC* mutant in *S. lividans* was sensitive to a wide variety of antibiotics (Morris *et al*., 2005). WblA was seen to act as a pleiotropic regulator of antibiotic biosynthesis in *Streptomyces peucetius*, down-regulating the anti-cancer drug doxorubicin, and in *S. coelicolor*, down-regulating the synthesis of a number of antibiotics including actinorhodin (Kang *et al*., 2007). Mutants in *wblA* of *S. coelicolor* also showed an ability to overproduce pigmented antibiotics, which were present in the aerial hyphae (Fowler-Goldsworthy *et al*., 2011). WblA of *S. coelicolor*, like WhiB and WhiD, was also shown to have a role in sporulation and development. A detailed study described a *wblA* mutant strain as having a delay in shutting off rapid growth as nutrients approached starvation levels (Fowler-Goldsworthy *et al*., 2011). This is similar to the findings by Flärdh *et al*. (1999), whereby a *whiB* mutant strain lacked controlled growth cessation. The role of WblE, the remaining conserved member in *S. coelicolor*, remains unknown as a *wblE* mutant strain showed no obvious phenotype (Homerová *et al*., 2003). It is clear that the Wbl proteins in the *Streptomyces* species have diverse roles, but are essential in developmental processes. The importance of WhiB, WhiD and WblA in stopping rapid growth when conditions are unfavourable

and in sporulation, indicates a regulatory role, potentially by acting as transcriptional regulators.

There is little direct evidence for the Wbl proteins in the *Streptomyces* species acting as transcription factors. The diverse phenotypes seen in Wbl mutants, as well as information on their structural features (Section 1.3.1), does however suggest a role in gene regulation. In addition, the unusual WblP σ factor fusion protein from *S. coelicolor* encodes an RNA polymerase sigma factor at its C-terminus as well as the conserved Wbl features at the N-terminus (Bentley *et al*., 2004). Detailed biochemical knowledge of these proteins in *Streptomyces* is limited, with WhiD being the most studied. As mentioned in Section 1.3.1, WhiD from *S. coelicolor* binds a [4Fe-4S] cluster which is sensitive to oxygen (Crack *et al*., 2009; Jakimowicz *et al*., 2005). It is thought that the Wbl proteins act as transcription factors and that the presence, absence or state of the cluster may play a vital role in their regulatory ability, possibly by relaying signals associated with changing environments (e.g. low oxygen conditions). Studies to identify possible genes regulated by WhiD, as well as the other members of the Wbl family in *S. coelicolor*, and whether this regulation is direct, will provide new insights to the biochemical function of these proteins.

1.3.3 Roles of Wbl proteins in *Mycobacterium* species

Mycobacterium tuberculosis, as discussed in Section 1.1.5, experiences a persistent state in its life-cycle of infection, whereby the bacilli undergo huge changes in gene expression to survive in this non-replicating latent state. The Wbl family of proteins have been implicated in the ability of *M. tuberculosis* to persist within the host for extended periods of time in the granuloma, despite the low oxygen and nutrient conditions, and survive within the macrophages, despite the presence of nitric oxide (Banaiee *et al*., 2006; Rohde *et al*., 2007a). The bacilli also have a substantial tolerance to a wide variety of antibiotics, and the Wbl proteins have also been implicated in this (Morris *et al*., 2005). The seven Wbl proteins therefore appear to be important in the remarkable ability of *M. tuberculosis* to survive in the harsh environment of the host, and moreover have been shown to be expressed under stress conditions (Geiman *et al*.,

2006; Larsson *et al*., 2012). Here, what is known of the roles of the seven Wbl proteins in *M. tuberculosis* is summarised.

WhiB1, the focus of this study, is regulated by CRP^{MT} (Rv3676) and studies on *whiB1* expression have shown it to be induced by cAMP (Agarwal *et al*., 2006; Larsson *et al*., 2012; Rickman *et al*., 2005; Stapleton *et al*., 2010). Although WhiB1 binds an iron-sulphur cluster (Alam *et al*., 2009), there is little detailed knowledge about its biochemical properties and function. Interestingly, an alternative role for WhiB1 has been suggested rather than it acting as a transcription factor. A group has presented evidence that the Wbl proteins in *M. tuberculosis* (with the exception of WhiB2), act as general protein disulphide reductases, reducing the substrate insulin (Alam *et al*., 2007; 2009; Garg *et al*., 2007). WhiB1 was also shown to interact with the α (1,4)-glucan branching enzyme (GlgB) reducing its intra-molecular disulphide bond (Garg *et al*., 2009).

WhiB2 is homologous to both WhiB from *S. coelicolor* and WhmD from *M. smegmatis* (den Hengst and Buttner, 2008). Both *whiB2* and *whmD* are essential genes and have been shown to be functionally equivalent (Gomez and Bishai, 2000; Raghunand and Bishai, 2006a; 2006b). Controlled depletion experiments have shown an essential role for them in proper septation and cell division of *Mycobaterium* (Gomez and Bishai, 2000; Raghunand and Bishai, 2006a). The *whmD* conditional mutant in *M. smegmatis* showed filamentous and branched growth with diminished septum formation, whereas when *whmD* was overexpressed there was growth retardation and hyperseptation (Gomez and Bishai, 2000). Similar observations were seen for *whiB2* of *M. tuberculosis* (Raghunand and Bishai, 2006a). These studies show the importance of WhiB2 and WhmD in *Mycobacterium* growth, and their similar roles to that of WhiB in *S. coelicolor*. The *whiB2* gene has been shown to be expressed during nutrient starvation, in macrophages and in the presence of cAMP, indicating its essential role during the infection process (Betts *et al*., 2002; Keiser *et al*., 2011; Larsson *et al*., 2012). There is direct evidence that WhiB2 from *M. tuberculosis* acts as a DNA-binding protein from the Rybniker group (2010). WhiB2 was shown to bind its own promoter region, regulating its own synthesis. This binding was affected by the presence of the iron-sulphur cluster, whereby the apo-form of the protein bound the promoter DNA (Rybniker *et al*., 2010). Interestingly, the Mycobacteriophage TM4 encodes a Wbl

protein (WhiBTM4), which acts a transcriptional inhibitor of WhiB2. WhiBTM4 is capable of binding to the WhiB2 promoter, and expression of *whiBTM4* led to hindered septation, similar to that of a *whiB2* mutant (Rybniker *et al*., 2010). It has recently been suggested that WhiB2 has properties similar to that of a chaperone, suppressing the aggregation of several model substrates including luciferase (Konar *et al*., 2012). This paper suggests that, although having the same features as the other Wbl proteins, WhiB2 has evolved differently to the other members and serves a very different function (Konar *et al*., 2012). This contradicts the findings of others that WhiB2 is a transcriptional regulator (Raghunand and Bishai, 2006a; Rybniker *et al*., 2010).

WhiB3 from *M. tuberculosis* is the best studied of the Wbl proteins and has been identified as a DNA-binding protein, which can sense redox and control several aspects of virulence (Guo *et al*., 2009; Saini *et al*., 2012; Singh *et al*., 2007; 2009; Steyn *et al*., 2002). Expression of *whiB3* is induced in macrophages and the mouse lung, indicating that *M. tuberculosis* regulates *whiB3* expression in response to environmental signals associated with infection (Banaiee *et al*., 2006). This idea has been supported by the findings whereby acid stress, hypoxia and nitric oxide induced *whiB3* expression (Geiman *et al*., 2006; Larsson *et al*., 2012). WhiB3 has also been shown to play a role in virulence, as mice infected with a *whiB3* null mutant showed increased survival (Steyn *et al*., 2002). WhiB3 incorporates a [4Fe-4S] cluster, which reacts with the dormancy signals oxygen and nitric oxide, suggesting it acts as a sensor of these physiologically significant gases (Singh *et al*., 2007). This study also demonstrated the role of WhiB3 in regulating the intermediary metabolism of *M. tuberculosis*, as it was essential for survival during nutrient starvation. This indicates that WhiB3 acts as an intracellular redox sensor, relaying signals through its iron-sulphur cluster to the regulation of metabolism (Singh *et al*., 2007). A number of studies have demonstrated that during exposure to hypoxia and nitric oxide, *M. tuberculosis* responds by accumulating the fatty acid triacylglycerol (Daniel *et al*., 2004; Sirakova *et al*., 2006). WhiB3 has been identified as regulating lipid and polyketide biosynthesis, including triacylglycerol and the virulence factor PDIM (Section 1.1.1), in response to activated macrophages (Guo *et al*., 2009; Singh *et al*., 2007; 2009). Thus WhiB3 has been implicated in *M. tuberculosis* survival and virulence. This is achieved by regulating lipid anabolism in response to oxido-reductive stress associated with infection, thus maintaining redox balance (Singh *et al*., 2009). Triacylglycerol has previously been identified as being under the control

of the DosR/S/T regulon (Daniel *et al*., 2004; Reed *et al*., 2007), and the finding that WhiB3 also regulates triacylglycerol production highlights a link between the dormancy regulon and this redox-sensing transcription factor (Singh *et al*., 2009). WhiB3 acts as a direct DNA-binding protein at the *pks2* and *pks3* promoter regions, encoding genes necessary for polyketide biosynthesis (Singh *et al*., 2009). It has also been shown to interact with the RpoV sigma factor, further confirming its role as a transcription factor (Steyn *et al*., 2002). Its DNA binding is independent of the presence or redox state of the iron-sulphur cluster, but reduction of apo-WhiB1 abolished DNA binding whereas oxidation encouraged it (Singh *et al*., 2009). This confirmed that WhiB3 regulation of fatty acid metabolism was redox-dependent. In summary, WhiB3 has been identified as a transcriptional regulator of fatty acid synthesis and thus accumulation, which is an essential virulence feature of *M. tuberculosis* during latent infection of the host.

Further evidence for the role of the Wbl proteins in the infection life-cycle of *M. tuberculosis* has come from recent work on WhiB5. A *whiB5* mutant showed attenuated infection abilities in the mouse lung with lower bacilli numbers and was unable to resume growth after reactivation from a chronic infection (Casonato *et al*., 2012). This is of significant interest, suggesting WhiB5 controls the expression of genes involved in reactivation from the latent state (Casonato *et al*., 2012). WhiB5 was also shown to influence the expression of a number of genes including *sigM*, encoding an alternative sigma factor, and genes encoding constituents for the ESX-2 and ESX-4 secretion systems, highlighting the role of WhiB5 in virulence (Casonato *et al*., 2012).

WhiB7 from *M. tuberculosis*, like WblC from *S. coelicolor*, has been linked with a role in antibiotic resistance (Morris *et al*., 2005). WhiB7 is induced by treatment with sub-inhibitory levels of antibiotics (erythromycin, tetracycline and streptomycin), and a number of stress conditions associated with infection (Geiman *et al*., 2006; Larsson *et al*., 2012; Morris *et al*., 2005). WhiB7 expression is also induced by fatty acids that *M. tuberculosis* accumulates and encounters during infection (Morris *et al*., 2005). A *whiB7* null mutant is hyper-sensitive to antibiotics, whereas overexpression of *whiB7* led to increased resistance (Morris *et al*., 2005). Morris and co-workers (2005) showed that WhiB7 provided this drug resistance by activating the expression of a regulon of genes involved in ribosomal protection and drug efflux. These data taken together suggest that *whiB7* is expressed during infection of the host and plays a role as a

transcriptional activator to help *M. tuberculosis* survive antibiotic treatment. WhiB7, as has been demonstrated for WhiB2, autoregulates its own transcription in response to antibiotics and changes in redox homeostasis (Burian *et al*., 2012). WhiB7 therefore appears to act as a transcription factor regulating antibiotic resistance, possibly by the iron-sulphur centre sensing redox changes.

There is little known about WhiB4 and WhiB6 of *M. tuberculosis*. They have both been shown to bind an iron-sulphur cluster similar to that of the other Wbl proteins (Alam *et al*., 2009), and have been implicated in having protein disulphide activity (Alam *et al*., 2007; 2009). They are also induced by cAMP and expressed during stress conditions (Geiman *et al*., 2006; Larsson *et al*., 2012).

1.4 Aims of the project

The information provided above clearly shows that *M. tuberculosis* is a major worldwide healthcare problem. Its ability to enter a persistent state, resulting in an enormous reservoir of infection, and to subsequently emerge from this state are key features of tuberculosis pathogenesis. This transition and the ability to survive the harsh environment within macrophages and the tubercle requires significant reprogramming of gene expression. As discussed, hypoxia, nitric oxide, carbon monoxide and cAMP signals all play major roles in bringing about this reprogramming through the actions of the DosR/S/T, PhoPR, CRP^{MT} and Cmr regulators. It is likely however, that we only have a partial picture of the signals and regulators involved in these complex processes. Wbl proteins play roles in developmental processes in actinomycetes but they are largely uncharacterised. The general properties of Wbl proteins and the regulation of *M. tuberculosis whiB1* by the cAMP-Rv3676 complex suggests however, that WhiB1 could play a role in development (transitions between replicating and persistent states). Based on current evidence, the hypothesis is that *M. tuberculosis* WhiB1 is an iron-sulphur cluster containing transcription factor that regulates gene expression in response to a redox signal. The experiments described in this thesis were carried out to test this hypothesis using a range of molecular biology and biochemical approaches.

2.0 Materials and Methods

2.1 Strains and plasmids

The strains of *Escherichia coli* used in this study are listed in Table 2.1 and the plasmids in Table 2.2.

Table 2.1: Strains of *Escherichia coli* used in this study

Strain	Relevant characteristics	Source or reference
BL21 λ(DE3)	*Escherichia coli* BL21 λ(DE3) lysogen carrying a copy of the T7 RNA polymerase under the control of the IPTG-inducible *lacUV5* promoter	Novagen
JRG2357	DH5α Δ*lacZYA-argF, lacZΔM15*	Invitrogen
JRG5923	DH5α /pGS2164	This work
JRG6050	BL21 λ(DE3)/pGS2164	This work
JRG5652	DH5α /p2060	This work
JRG5733	DH5α /pGS2103	This work
JRG5871	DH5α /p2126	This work
JRG6494	DH5α /p2365	This work
JRG6495	DH5α /p2366	This work
JRG6496	DH5α /p2367	This work
JRG6439	DH5α /p2344	This work
JRG6221	DH5α /pGS2300	This work
JRG6222	DH5α /pGS2301	This work
JRG6223	DH5α /pGS2302	This work
JRG6224	DH5α /pGS2303	This work
JRG6225	DH5α /pGS2304	This work
JRG6226	DH5α /pGS2305	This work
JRG6227	DH5α /pGS2306	This work
JRG6228	DH5α /pGS2307	This work
JRG6229	DH5α /pGS2308	This work

JRG6230	DH5α /pGS2309	This work
JRG6232	DH5α /pGS2311	This work
JRG6233	DH5α /pGS2312	This work
JRG6234	DH5α /pGS2313	This work
JRG6481	DH5α /pGS2358	This work
JRG6482	DH5α /pGS2359	This work
JRG6483	DH5α /pGS2360	This work
JRG6484	DH5α /pGS2361	This work
JRG6485	DH5α /pGS2362	This work
JRG6486	DH5α /pGS2363	This work
JRG6487	DH5α /pGS2364	This work

Table 2.2: Plasmids used in this study

Plasmid	**Relevant characteristics**	**Source or reference**
pET28a	His_6-tag overexpression vector; Kan^R	Novagen
pGS2164	pET28a-WhiB1; Kan^R	This work
pGS2103	pET28a-Rv1675c; Kan^R	This work
pCR4Blunt-TOPO	Cloning Vector; Kan^R and Amp^R	Invitrogen
p2060	pCR4Blunt-TOPO-P*whiB1*; Kan^R and Amp^R	Buxton, NIMR
p2126	pCR4Blunt-TOPO-P*groEL2*; Kan^R and Amp^R	Buxton, NIMR
p2365	pCR4Blunt-TOPO-P*rv2007c*; Kan^R	Buxton, NIMR
p2366	pCR4Blunt-TOPO-P*rv2032*; Kan^R	Buxton, NIMR
p2367	pCR4Blunt-TOPO-P*rv3133c*; Kan^R	Buxton, NIMR
p2344	pCR4Blunt-TOPO-P*rv3134c*; Kan^R	Buxton, NIMR
pGS2300	pGS2164 with C9A mutation	This work
pGS2301	pGS2164 with C37A mutation	This work
pGS2302	pGS2164 with C40A mutation	This work
pGS2303	pGS2164 with C46A mutation	This work
pGS2304	pGS2164 with P41S mutation	This work
pGS2305	pGS2164 with E45L mutation	This work

pGS2306	pGS2164 with P41S/E45L mutation	This work
pGS2307	pGS2164 with K72E mutation	This work
pGS2308	pGS2164 with R73E mutation	This work
pGS2309	pGS2164 with R74E mutation	This work
pGS2311	pGS2164 with R77E mutation	This work
pGS2312	pGS2164 with K79E mutation	This work
pGS2313	pGS2164 with R81E mutation	This work
pGS2358	pGS2164 with S57E mutation	This work
pGS2359	pGS2164 with G58E mutation	This work
pGS2360	pGS2164 with V59E mutation	This work
pGS2361	pGS2164 with W60E mutation	This work
pGS2362	pGS2164 with G61E mutation	This work
pGS2363	pGS2164 with G62E mutation	This work
pGS2364	pGS2164 with D13A mutation	This work

2.2 Media and chemical suppliers

Bacterial growth media components were sourced from Oxoid Ltd. Chemicals were supplied by BDH Chemicals Ltd., Fisher Scientific, Melford Laboratories Ltd. and Sigma. Kits for DNA purification were purchased from Qiagen. Restriction enzymes were sourced from Roche, Fermentas and Promega. DNase enzyme was supplied from Promega and Klenow enzyme from Fermentas. HiTrap columns were from GE Healthcare. Kanamycin antibiotic was sourced from Melford Laboratories Ltd. Proli NONOate was sourced from Alexis Biochemicals and Cayman Chemicals. Protein assay reagent was obtained from Bio-Rad. Isotopes were sourced from Perkin Elmer.

2.3 Growth media and conditions

2.3.1 Rich media

Escherichia coli was cultured in Lennox broth (LB) medium.

	LB (g/l)	LB Agar (g/l)
Tryptone	10	10
Yeast extract	5	5
NaCl	5	5
Agar bacteriological	-	15

These ingredients were made up to 1 litre with distilled water and autoclaved (121°C, 15 psi) to sterilise.

Once the LB medium was cooled to 50°C the appropriate antibiotics were added. Molten agar was poured into petri dishes (25 ml/dish) and allowed to cool and set. Plates were stored at 4°C for up to 1 month.

2.3.2 Growth of *Escherichia coli*

Escherichia coli was typically cultured in LB with the appropriate antibiotics at 37°C with shaking (250 rpm), until the desired optical density at 600 nm (OD_{600}) was reached. Overnight cultures (5 ml) were prepared by inoculating a single colony from a LB agar plate and were either used directly or to inoculate larger cultures.

2.3.3 Measurement of bacterial growth

Escherichia coli growth was estimated by measuring the OD_{600} of 1 ml of the culture using the Eppendorf Biophotometer, with LB as a blank.

2.3.4 Supplementation of growth media

Media were supplemented as indicated with kanamycin, 20 µg/ml. IPTG was added to a final concentration of 120 µg/ml for protein overexpression.

2.3.5 Storage of strains

Strains were stored on solid media at 4°C for up to one month. For long term storage strains were kept in the form of glycerol stocks, made as follows; 5 ml overnight cultures were centrifuged and cell pellets were resuspended in 1.25 ml LB, 1 ml sterile 80% (v/v) glycerol and the appropriate antibiotics. These were stored at -20°C.

2.3.6 Production of chemically competent cells

A single colony of the appropriate strain from a LB agar plate was inoculated in 0.25 ml of LB and incubated overnight at 37°C with rocking. This was then used to inoculate 25 ml LB containing $MgSO_4$ (final concentration of 20 mM) at 37°C with shaking (250 rpm). Once the OD_{600} reached 0.4, the cells were pelleted by centrifugation at 4500 x*g* for 5 minutes at 4°C. The pellet was then gently resuspended in 10 ml of chilled filter sterilised TFB1 (pH 5.8), i.e. 2/5 volume of original culture.

Cells were kept on ice for the following steps and all pipettes, Eppendorf tubes and flasks were chilled. The cells were incubated on ice for 5 minutes and pelleted at 4500 x*g* for 5 minutes at 4°C. Cells were then resuspended in 1 ml chilled filter sterilised TFB2 (pH 6.5), i.e. 1/25 of original culture volume.

TFB1 (pH 5.8):		TFB2 (pH 6.5)	
Potassium acetate	30 mM	MOPS	10 mM
$CaCl_2$	10 mM	$CaCl_2$	75 mM
$MnCl_2$	50 mM	RbCl	10 mM
RbCl	100 mM	Glycerol	15% (v/v)
Glycerol	15% (v/v)		

Cells were incubated on ice for 30 minutes, then aliquoted as 200 µl samples for storage at -70°C.

2.3.7 Transformation of chemically competent cells

Chemically competent cells were thawed on ice and 50 µl was placed into a chilled eppendorf tube. The desired plasmid (up to 1 µg) was added and chilled on ice for 30 minutes. Cells were subjected to heat shock at 42°C for 90 seconds and returned to ice for 2 minutes. LB (1 ml) was added and incubated at 37°C for 1 hour. Cells were then centrifuged for 30 seconds at 16060 x*g* in a bench-top centrifuge. The pellet was resuspended in a small volume of LB (~100 µl) and spread on a LB agar plate with the correct antibiotic.

2.3.8 Production of electrically competent cells

LB (100 ml) was inoculated with an overnight culture (1%) and grown at 37°C with shaking (250 rpm) until the OD_{600} reached 0.6. Cells were pelleted at 4°C (4500 x*g* for 15 minutes) and washed three times in sterile ice-cold water. The cell pellet was then resuspended in 300 µl of 10% (v/v) glycerol, and stored as 50 µl aliquots at -70°C.

2.3.9 Transformation of electrically competent cells

Plasmid DNA (up to 1 µg) was added directly to 50 µl aliquots of electrically competent cells. The mixtures were kept on ice for 30 minutes and then transformed by electroporation using a Hybaid Cell Shock unit (1800 V, 1 mm path length) and a chilled cuvette. LB (1 ml) was added and the cells were incubated at 37°C for 1 hour. Cells were plated onto LB agar containing the correct antibiotic.

2.4 Nucleic acid methods

2.4.1 Storage

Purified plasmids and genomic DNA were stored in either Qiagen EB buffer (10 mM Tris-HCl, pH 8.5) or deionised water at -20°C.

2.4.2 Measurement of DNA concentration

DNA concentration was measured using the double stranded DNA programme on an Eppendorf Biophotometer with dH_2O as a blank.

2.4.3 Plasmid purification

Plasmid DNA was typically purified from 5 ml overnight cultures of *E. coli* using the Qiagen QIAprep® Spin Miniprep kit, in accordance with the manufacturer's instructions.

2.4.4 Digestion of DNA with restriction endonucleases

Restriction enzymes were used in conjunction with the appropriate 10X buffer in accordance with manufacturer's instructions. Digests were usually performed in 10-100 µl reaction volumes containing DNA and the enzyme(s) at 1:10 of the reaction volume. Reactions were incubated at 37°C usually for 2 hours. The desired DNA fragments were purified by PCR purification (Section 2.4.9) and analysed by agarose gel electrophoresis (Section 2.4.5).

2.4.5 Agarose gel electrophoresis

Agarose gel electrophoresis was used for visualising DNA fragments. Agarose (1% (w/v)) was added to 1X TAE buffer and dissolved by heating in a microwave oven. Once sufficiently cooled, GelRed™ solution, provided by Biotium, was added to the gel at a 1:10000 dilution before casting. Prior to loading, DNA samples were mixed with 6X loading dye provided by Fermentas. A 1 kb ladder 'Generuler™' was used for size calibration supplied by MBI Fermentas. Gels were electrophoresed in 1X TAE buffer at 100 V for 1 hour. DNA fragments were visualised using a UVItech photodocumentation system.

50X TAE Buffer:

Tris	242 g
Glacial acetic acid	57.1 ml
EDTA (0.5 M, pH 8)	100 ml
dH_2O to 1 litre	

2.4.6 Gel Extraction

When required, specific DNA fragments were removed from agarose gels (Section 2.4.5) and purified using the QIAquick® Gel Extraction Kit from Qiagen according to the manufacturer's instructions.

2.4.7 Primer Design

Primers were designed for site-directed mutagenesis (Section 2.4.10) and are listed in Table 2.3 below, with the altered bases indicated in red. They were between 30-45 base pairs in length with a GC content of >70% and ideally with a T_m of ≥75ºC. Primers were produced by Eurofins MWG Synthesis GmbH.

Table 2.3: Primers used for site-directed mutagenesis

Primer	Mutation	Sequence	Direction
LS1	C9A	GCCACAAGGCGGTCGCTCGTGACGAGGATCC	Forward
LS2	C9A	GGATCCTCGTCACGAGCGACCGCCTTGTGGC	Reverse
LS3	C37A	GCGAAACTGGTCGCTAATCGGTGCCCGGTC	Forward
LS4	C37A	GACCGGGCACCGATTAGCGACCAGTTTCGC	Reverse
LS5	C40A	GGTCTGTAATCGGGCCCCGGTCACCACAGAG	Forward
LS6	C40A	CTCTGTGGTGACCGGGGCCCGATTACAGACC	Reverse
LS7	C46A	GGTCACCACAGAGGCCCTCAGCTGGGCACTG	Forward
LS8	C46A	CAGTGCCCAGCTGAGGGCCTCTGTGGTGACC	Reverse
LS9	P41S	GGTCTGTAATCGGTGCTCGGTCACCACAGAG	Forward
LS10	P41S	CTCTGTGGTGACCGAGCACCGATTACAGACC	Reverse
LS11	E45L	GCCCGGTCACCACACTGTGCCTCAGCTGGG	Forward
LS12	E45L	CCCAGCTGAGGCACAGTGTGGTGACCGGGC	Reverse
LS15	K72E	GCGGCGCGCGCTGGAGCGTCGCAACGCCCGC	Forward
LS16	K72E	GCGGGCGTTGCGACGCTCCAGCGCGCGCCGC	Reverse
LS17	R73E	GCGGCGCGCGCTGAAGGAACGCAACGCCCGC	Forward
LS18	R73E	GCGGGCGTTGCGTTCCTTCAGCGCGCGCCGC	Reverse
LS19	R74E	GCGCGCTGAAGCGTGAAAACGCCCGCACGAAAG	Forward
LS20	R74E	CTTTCGTGCGGGCGTTTTCACGCTTCAGCGCGC	Reverse

LS23	R77E	GAAGCGTCGCAACGCCGAAA CGAAAGCCCG	Forward
LS24	R77E	CGGGCTTTCGTTTCGGCGTTG CGACGCTTC	Reverse
LS25	K79E	GCAACGCCCGCACGGAAGCC CGTACCGGG	Forward
LS26	K79E	CCCGGTACGGGCTTCCGTGCG GGCGTTGC	Reverse
LS27	R81E	GCCCGCACGAAAGCCGAAAC CGGGGTCTG	Forward
LS28	R81E	CAGACCCCGGTTTCGGCTTTC GTGCGGGC	Reverse
LS29	P41S/E45L	GGTCTGTAATCGGTGCTCGGT CACCACACTGTGCCTCAGCTG GG	Forward
LS30	P41S/E45L	CCCAGCTGAGGCACAGTGTG GTGACCGAGCACCGATTACA GACC	Reverse
LS31	S57E	GAATACCGGCCAGGACGAGG GCGTCTGGGG	Forward
LS32	S57E	CCCCAGACGCCCTCGTCCTGG CCGGTATTC	Reverse
LS33	G58E	GGCCAGGACTCGGAGGTCTG GGGAGGCATG	Forward
LS34	G58E	CATGCCTCCCCAGACCTCCGA GTCCTGGCC	Reverse
LS35	V59E	GGCCAGGACTCGGGCGAGTG GGGAGGCATG	Forward
LS36	V59E	CATGCCTCCCCACTCGCCCGA GTCCTGGCC	Reverse
LS37	W60E	GGACTCGGGCGTCGAGGGAG GCATGAGCGAAG	Forward
LS38	W60E	CTTCGCTCATGCCTCCCTCGA CGCCCGAGTCC	Reverse
LS39	G61E	GGACTCGGGCGTCTGGGAAG GCATGAGCGAAG	Forward
LS40	G61E	CTTCGCTCATGCCTTCCCAGA CGCCCGAGTCC	Reverse
LS41	G62E	GGGCGTCTGGGGAGAGATGA GCGAAGACGAG	Forward
LS42	G62E	CTCGTCTTCGCTCATCTCTCCC CAGACGCCC	Reverse

LS43	D13A	GTCTGTCGTGACGAGGCTCCG GAACTGTTC	Forward
LS44	D13A	GAACAGTTCCGGAGCCTCGTC ACGACAGAC	Reverse

2.4.8 Polymerase Chain Reaction (PCR)

Reactions for analytical PCR typically contained (unless stated otherwise):

Plasmid DNA (~0.1 μg/μl)	1 μl
Primer 1 (100 pmol/μl)	1 μl
Primer 2 (100 pmol/μl)	1 μl
Extensor PCR Master Mix 1 (Thermo Scientific)	25 μl
dH_2O	22 μl

PCR was carried out using a Techne TC-3000 with the following typical reaction profile, unless stated otherwise. Samples were then run on agarose gel electrophoresis for analysis (Section 2.4.5) or purified (Section 2.4.9).

Initial denaturation	95ºC – 5 minutes	
Denaturation	95ºC – 30 seconds	25 Cycles
Annealing	50ºC – 30 seconds	
Extension	72ºC – 1 minutes	
Final extension	72ºC – 5 minutes	

2.4.9 DNA purification

DNA was typically purified using the Qiagen QIAquick® Purification kit, in accordance with the manufacturer's instructions.

2.4.10 Site-Directed Mutagenesis (SDM)

SDM was carried out using QuikChange® II XL Site-Directed Mutagenesis Kit from Stratagene. The manufacturer's instructions were followed.

2.5 Protein Methods

2.5.1 Measurement of protein concentration

Protein concentration was typically calculated using the Bio-Rad reagent (Bradford, 1976). A protein assay standard curve for a 5 ml reaction volume was used. Absorbance was measured at 595 nm using a Unicam HEλIOS spectrophotometer.

2.5.2 Denaturing gel electrophoresis (SDS-PAGE)

SDS-PAGE was performed as described by (Laemmli, 1970). Analysis was completed using 15% (w/v) resolving gel, and 5% (w/v) stacking gel as detailed below.

	15% Resolving gel (ml):	5% Stacking gel (ml):
30% (w/v) Acrylamide	3.8	1.7
3 M Tris-HCl (pH 8.3)	0.95	-
0.5 M Tris-HCl (pH 6.8)	-	1.25
dH_2O	2.7	6.95
10% (w/v) SDS	0.075	0.1
10% (w/v) APS	0.1	0.1
TEMED	0.02	0.02

The glass plates and spacers were set up in the clamps ready for pouring the gel. The resolving gel was poured, leaving space for the stacking gel to be added on top. Water-saturated butanol was applied to the top of the gel. Once the gel had set, the butanol was rinsed off with dH_2O. The stacking gel was then poured and a comb inserted to form the wells. The comb was removed once the gel had set. The gel, sandwiched between the

glass casting plates, was placed in the tank with 1X SDS running buffer. Samples were mixed with loading buffer at a 1:1 ratio and boiled for 10 minutes at 95°C before loading.

Protein size markers (Precision Plus Protein™ Standards from Bio-Rad) were also loaded to allow determination of molecular weight. Electrophoresis was carried out at 200 V for 45 minutes, until the dye front reached the base of the gel.

2X SDS loading buffer:		1X SDS running buffer:	
Glycerol	20% (v/v)	Tris	3 g
Tris-HCl (0.5 M pH 6.8)	100 mM	SDS	1 g
SDS	4% (v/v)	Glycine	14.4 g
Bromophenol blue	0.02% (v/v)	dH_2O to 1 litre	
2-Mercaptoethanol	200 mM		

After electrophoresis, the gel was removed from its glass plate and immersed in Coomasie Blue stain for 30 minutes followed by destain overnight.

	Coomassie Blue stain:	Destain:
Coomassie Brilliant Blue (R250)	1.15 g/l	-
Methanol	400 ml	400 ml
Acetic acid	100 ml	100 ml
dH_2O to 1 litre		

2.5.3 Overproduction of WhiB1 and Rv1675c

WhiB1 and Rv1675c were typically overproduced by culturing the host strain in a 2 litre flask containing 500 ml of LB and kanamycin, inoculated at 1:100 from an overnight culture. The culture was grown aerobically at 37°C with shaking (250 rpm) until an OD_{600} of 0.6-0.9 was reached. IPTG was added to a final concentration of 120 µg/ml. Cultures were then grown at 25°C with shaking (250 rpm), post induction, for 2 hours. Cells were then pelleted by centrifugation at 11900 x*g* for 30 minutes at 4°C. Pellets were either frozen overnight at -20°C or used immediately to produce cell-free extracts (Section 2.5.4).

2.5.4 Production of cell-free extracts

Cell pellets were typically resuspended in 10 ml of binding buffer A (Section 2.5.5). Resuspended cells were lysed by two passages through a French pressure cell at 16000 psi. The soluble and insoluble fractions were separated by centrifugation at 39190 x*g* for 15 minutes at 4°C. The soluble fraction was used immediately for purification of proteins.

2.5.5 Purification of recombinant WhiB1 and Rv1675c by affinity chromatography

WhiB1 and Rv1675c were purified using the engineered histidine tag. Purification used the soluble fractions after the French press step. Purification was carried out using the His-tag purification programme on the AKTA™ prime machine (GE Healthcare), and either a 1 or 5 ml HiTrap™ chelating column (GE Healthcare). The appropriate reagents were prepared and the machine was configured according to the manufacturer's instructions. The cell-free extracts (10 ml for the 1 ml column or 20 ml for the 5 ml column) were injected and the fractions (1 ml) eluting from the column were collected. The fractions which corresponded to the second absorption peak (280 nm) after addition of the elution buffer were collected and samples were separated by SDS-PAGE to locate the target protein. Fractions were stored at -20°C, with 1 mM DTT for WhiB1, until required.

Binding buffer A (pH 7.4):	
Sodium phosphate	20 mM
NaCl	0.5 M
dH_2O to 1 litre	

Elution buffer A (pH 7.4):	
Sodium phosphate	20 mM
NaCl	0.5 M
Imidazole	0.5 M
dH_2O to 1 litre	

Ni-Loading eluent:	
$NiSO_4$	100 mM

2.5.6 Refolding

Protein refolding was necessary for WhiB1 mutant proteins which were in the insoluble pellet after preparation of cell-free extracts. This was achieved using the refolding programme on the AKTA™ prime machine and a 1 ml HiTrap™ chelating column. The appropriate reagents were prepared and the machine was configured according to the manufacturer's instructions. The insoluble pellet was resuspended in 10 ml binding buffer B (recipe below) and agitated at 4˚C overnight to solubilise the proteins. The sample was then centrifuged at 39190 x*g* for 15 minutes at 4°C to separate soluble and insoluble fractions. The soluble sample was then applied to the column and the fractions (1 ml) collected. The fractions which corresponded to the absorption peak (280 nm) after addition of the elution buffer were collected and samples separated on SDS-PAGE to locate the protein. Fractions were stored at -20°C with 1 mM DTT until required.

Binding buffer B (pH 8):		Solubilisation buffer (pH 8):	
Guanidine hydrochloride	6 M	Urea	6 M
Tris-HCl	20 mM	Tris-HCl	20 mM
NaCl	0.5 M	NaCl	0.5 M
Imidazole	5 mM	Imidazole	5 mM
2-Mercaptoethanol	1 mM	2-Mercaptoethanol	1 mM
dH_2O to 1 litre		dH_2O to 1 litre	

Elution buffer B (pH 8):		Refolding buffer (pH 8):	
Tris-HCl	20 mM	Tris-HCl	20 mM
NaCl	0.5 M	NaCl	0.5 M
Imidazole	0.5 M	Imidazole	5 mM
2-Mercaptoethanol	1 mM	2-Mercaptoethanol	1 mM
dH_2O to 1 litre		dH_2O to 1 litre	

Ni-Loading eluent:	
$NiSO_4$	100 mM

2.5.7 Transfer of proteins onto Immuno-Blot™ PVDF membrane

Proteins were first separated using SDS-PAGE (Section 2.5.2), before blotting onto the Immuno-Blot™ PVDF membrane (BioRad). The membrane was soaked in methanol for a few seconds and then transferred to electroblotting buffer (10 mM CAPS in 10% (v/v) methanol; pH 11). The gel was removed from the electrophoresis cell and soaked in electroblotting buffer for 5 minutes. The transblotting sandwich was assembled and electroblotted at 50 V for 30 minutes at room temperature, using a BioRad Mini Trans-Blot Electrophoretic Transfer Cell.

2.5.8 N-Terminal sequencing

The Immuno-Blot™ PVDF membrane was removed from the transblotting sandwich (Section 2.5.7) and briefly rinsed with dH_2O. It was then submerged in 100% methanol for a few seconds prior to staining with Coomassie brilliant blue R250 (0.1% (w/v) in 40% (v/v) methanol and 1% (v/v) acetic acid) for 1 minute. The membrane was then destained in 50% (v/v) methanol and extensively rinsed in dH_2O before being allowed to dry at room temperature. The polypeptides of interest were excised from the membrane and sequences were determined by Dr A. J. G. Moir (Krebs sequencing and synthesis facility) using the Applied Biosystems protein sequencer.

2.5.9 Total amino acid analysis

Amino acid analysis was carried out by Alta Bioscience (University of Birmingham, UK) by complete acid hydrolysis for 24 h at 110ºC of aliquots of WhiB1 that had been previously assayed for protein concentration (Section 2.5.1).

2.5.10 Estimation of molecular mass by gel filtration

A calibrated Shodex KW805 column, equilibrated with 50 mM sodium phosphate buffer (pH 6.0) containing 150 mM NaCl was used. Both apo- and holo-WhiB1 samples (50 μM) were prepared and purified using heparin chromatography, eluted into 20 mM

sodium phosphate buffer, pH 7.4 with 0.5 M NaCl, and treated with the indicated reagents. Samples were compared to a standard curve using proteins of known molecular mass.

2.5.11 Estimation of reactive sulphydryl groups

The method described by Thelander (1973) was used. The reaction was performed in a 1 ml volume containing 700 μl 0.1 M Tris-HCl and 0.01 M EDTA (pH 7.6) and 200 μl of a solution containing 0.2 ml 0.4% 5,5'-dithiobis(2-nitrobenzoic acid) (DTNB) in ethanol and 1.8 ml of 1 M Tris-HCl (pH 8). WhiB1 (50 μg) in 100 μl of 25 mM Tris-HCl, pH 7.4 was added and the absorbance measured at 412 nm immediately. Protein samples were treated with 1% SDS where indicated. Buffer (25 mM Tris-HCl, pH 7.4) was used as the control. The reactive sulphydryl groups were then determined using the following formula.

$A = E_{412}c1$ A = Absorbance at 412 nm

E = Molar coefficient of NTB: 13,600 $M^{-1}cm^{-1}$

c = Concentration of NTB (M)

1 = Path length (cm)

$$\text{Reactive sulphydryl groups} = \frac{\text{Concentration of NTB (M)}}{\text{Concentration of WhiB1 (M)}}$$

2.5.12 Protein disulphide reductase activity assay

The protein disulphide reductase activity of WhiB1 was determined using the assay first described by Holmgren (1979). The assay relies on the ability of protein disulphide reductases to reduce the disulphide bonds that covalently hold the two chains of insulin together in a DTT-mediated manner. Release of the insoluble β-chain of insulin can be measured at 600 nm.

Insulin was prepared to a final concentration of 1.3 mM by the addition of 50 mM Tris-HCl (pH 8), adjusting the pH to 2-3 with 1 M HCl and then rapidly titrating back to pH 8. Aliquots were stored at -20°C until required.

The assay was carried out with varying concentrations of WhiB1 (apo-, holo- and NO-treated), or *E. coli* thioredoxin as a *bone fide* general protein disulphide reductase. Reactions were completed in 100 µl reaction volumes, in quadruplet in 50 mM Tris (pH 8) with 1 mM DTT and 100 mM NaCl. The 96 well plates containing the reactions and the insulin were pre-incubated separately for 1 hour at 25°C prior to addition of the insulin. Precipitation was monitored at OD_{600} using a plate reader maintained at 25°C, every 30 seconds for 115 minutes.

Enzyme activity was calculated by dividing the slope of the linear phase of the curve by the time required to reach the onset of precipitation (defined as an increase in absorbance ≥ 0.05).

2.6 Iron-sulphur cluster methods

2.6.1 Reconstitution of the iron-sulphur cluster of WhiB1

Purified WhiB1 (Section 2.5.5) was used for iron-sulphur cluster reconstitution. Reconstitution was carried out in a MK3 anaerobic workstation from Don Whitley Scientific Limited using anaerobic buffers and all solutions were allowed to become anaerobic before use. The typical reaction composition is listed below.

Purified WhiB1 (~50-600 µM)	1000 µl
Tris-HCl buffer (25 mM, pH 7.4)	1000 µl
Solution 1 (2.5 mM DTT and 1 mM L-cysteine)	20 µl
Solution 2 (100 mM ammonium ferrous sulphate)	10X Protein concentration
NifS (22.5 µM)	20 µl

Reactions were typically left to reconstitute in the cabinet overnight. Reconstituted WhiB1 was then cleaned-up to remove any non-integrated iron as detailed in Section 2.6.2.

2.6.2 Clean-up of reconstituted protein

Reconstituted WhiB1 was cleaned-up using either a 1 ml or 5 ml HiTrap™ heparin HP column. The reconstituted protein sample was loaded onto the column, washed with the anaerobic Tris buffer (25 mM, pH 7.4) and eluted with Tris buffer (25 mM, pH 7.4) containing 0.5 M NaCl into clean tubes.

2.6.3 Preparation of Proli NONOate

Proli NONOate (Cayman Chemicals or Alexis Biochemicals) was regularly used as a NO donor for sensitivity experiments. It was dissolved in 1 M NaOH and stored in 50 µl aliquots at a concentration of 22.8 mM at -20°C until required (unless otherwise stated).

2.6.4 Scanning spectroscopy

A Cary 50 Bio UV Vis Spectrophotometer was used. Protein samples were typically scanned in a Hellma® 10 mm cuvette, made of either special optical glass or quartz with a screw-cap lid to maintain anaerobic conditions. A baseline was created using the appropriate buffers, depending on the protein sample to be scanned. The absorption spectrum of the protein was obtained by scanning between wavelengths 200-800 nm. Stress reagents were added by injection into the cuvette through the Hellma® silicone seal in the lid with a Hamilton syringe.

2.6.5 Kinetic spectroscopy

Rapid rate kinetics was carried out at the University of East Anglia with Dr Jason Crack as described in Crack *et al*. (2011). The reaction of WhiB1 with NO was measured

using a Bio-sequential DX.17 MV UV-Vis Stopped-flow spectrometer with a 1 cm path length (Applied Photophysics). Absorption changes were detected with a photomultiplier set at a single wavelength. Reactions were carried out in 25 mM Tris, 0.5 M NaCl, 10 % (v/v) glycerol (pH 7.4), using gas-tight syringes (Hamilton). The stopped-flow system was flushed with anaerobic buffer prior to use. All solutions used for stopped-flow experiments were stored and manipulated inside an anaerobic cabinet (Belle Tech). The Proli NONOate used for NO generation was stored in 25 mM NaOH and quantified optically ($\varepsilon_{252\ nm}$ 8400 M/cm). An aliquot was combined with the assay buffer and allowed to decompose in a gastight syringe to achieve the desired concentration. The change in absorbance at 364 nm and 420 nm was measured at 24°C as a function of time. Absorbance data were fitted using Origin (Microcal) and Dynafit to the exponential function $y=y_0 + (y_{max}-y_0)\ (1-e^{[-k_{obs.}\ x]})$, where y = absorbance at any given time, y_0 = initial absorbance, y_{max} = maximum absorbance, and k_{obs} = the observed rate constant.

2.6.6 Electron paramagnetic resonance spectroscopy

Electron paramagnetic spectroscopy (EPR) was carried out by Dr Jason Crack at the University of East Anglia on samples prepared in Sheffield, as described in Smith *et al*. (2010). WhiB1 samples (17 µM) were prepared in 25 mM Tris buffer (pH 7.4) containing 1 mM DTT. Where indicated, a 27-fold molar excess of Proli NONOate was added. Samples were transferred to EPR tubes and frozen in liquid nitrogen before analysis. EPR spectra were recorded with a Bruker EMX spectrometer equipped with a TE-102 microwave cavity and an ESR-900 helium flow cryostat (Oxford Instruments). Spectra were recorded at both 20 K and 77 K. The microwave power was 2 mW with a frequency of 9.68 GHz, and the field modulation amplitude was 1 mT. Spectra were normalised to the same receiver gain. Spin intensities of paramagnetic samples were estimated by double integration of EPR spectra using 1 mM Cu(II) and 10 mM EDTA as the standard (Smith *et al*., 2010).

2.6.7 Circular Dichroism (CD) Spectroscopy

Circular dichroism (CD) spectroscopy was carried out at the University of East Anglia with Dr Jason Crack. CD measurements were made using a Jasco J810 spectropolarimeter and holo-WhiB1 (196 µM) in 20 mM sodium phosphate buffer (pH 7.4).

2.6.8 Iron assay

Protein samples post iron-sulphur reconstitution and clean-up using heparin chromatography (Section 2.6.2) were boiled in 1% (w/v) trichloroacetic acid (TCA) and dH_2O for 5 minutes. Samples were then centrifuged at 16060 x*g* in a bench-top centrifuge for 1 minute and the supernatant retained. The supernatant was then used in the following reaction:

Sample and dH_2O	480 µl
Saturated sodium acetate	400 µl
10% (w/v) Bathophenanthroline sulphonic acid	30 µl
20% (w/v) Fresh sodium ascorbate	90 µl

Once the sample had turned red after the addition of sodium ascorbate, the samples were centrifuged for 15 minutes and the absorbance measured at 535 nm and compared to a standard curve prepared with an iron standard solution (BDH) at 18 mM. The number of moles of iron in the sample was then calculated.

2.7 DNA-Protein Interactions

2.7.1 Radiolabelling of DNA

DNA fragments from PCR amplification (Section 2.4.8) were digested with the relevant restriction endonucleases (Section 2.4.4). The reaction mix was then purified (Section

2.4.9) and the DNA concentration measured (Section 2.4.2). A typical labelling reaction is detailed below and reactions were left for 1-2 hours at room temperature to complete.

DNA	150-600 ng
dNTPs (if required)	2.5 mM
Klenow buffer	1X
Klenow enzyme	1 µl (10 units)
[α-^{32}P]dNTP	1 µl (10 mCi/ml)
dH_2O to 30 µl	

Reactions were purified (Section 2.4.9) and the labelled DNA was eluted into EB buffer and stored at –20˚C until required. Variations in purification methods are stated where differences occurred.

2.7.2 Phenol extraction and ethanol precipitation

Phenol extraction was used to remove protein contaminants from DNA samples. An equal volume of phenol (pH 7-8) was added to samples, mixed thoroughly then centrifuged to separate the aqueous and phenolic phases. The aqueous phase was recovered and used for ethanol precipitation.

Sodium acetate (0.1 volume; 3 M, pH 5.2) was added to the DNA sample, followed by glycogen (1 µl; 20 mg/ml) and 2 volumes of 100% ethanol at -20°C. This was then centrifuged at 16060 x*g* for 30 minutes at 4°C. The supernatant was carefully removed and the resulting pellet washed with 70% ethanol before further centrifugation for 10 minutes. The supernatant was again removed and the pellet dried under vacuum in a Hetovac for ~30 minutes. The DNA was then resuspended as required.

2.7.3 Electromobility shift assays

Electromobility shift assays (EMSAs) were carried out with WhiB1 and Rv1675c. DNA fragments to be examined were restriction digested and radiolabelled (Sections 2.4.4 and 2.7.1). Labelled fragments (~3 ng) were incubated with varying concentrations of

the DNA-binding protein for 10 minutes on ice (WhiB1) or 10 minutes at room temperature (Rv1675c) in a total reaction volume of 10 µl. Reactions also contained 100 mM NaCl, 40 mM Tris (pH 8), 10 mM $MgCl_2$, 0.1 mM EDTA, 1 mM DTT, 0.25 mg/ml BSA, and ~1 µg calf thymus DNA. Reactions with WhiB1 also contained a further 1 mM EDTA.

Loading buffer (2 µl of 50% glycerol, bromophenol blue) was added to the samples immediately prior to loading onto a 6% polyacrylamide gel. EMSAs for WhiB1 were carried out using TBE gels and 0.5X TBE running buffer. EMSAs for Rv1675c were carried out using Tris-glycine gels with corresponding running buffer. Electrophoresis was at 30 mA for ~30 minutes. Gels were dried and visualised by autoradiography (Section 2.7.6).

6% TBE gel		6% Tris gel	
30% (w/v) Acrylamide	1.5 ml	30% (w/v) Acrylamide	1.5 ml
10X TBE buffer	0.375 ml	3 M Tris (pH 8.3)	0.95 ml
dH_2O	5.625 ml	dH_2O	5 ml
10% (w/v) APS	75 µl	10% (w/v) APS	75 µl
TEMED	7.5 µl	TEMED	7.5 µl

10X TBE		Running Buffer	
Tris	108 g	Tris	3 g
Boric acid	55 g	Glycine	14.4 g
0.5 M EDTA (pH 8)	40 ml	dH_2O to 1 litre	
dH_2O to 1 litre			

2.7.4 DNaseI Footprinting

The promoter DNA fragments of interest were restriction digested and one strand was labelled (Section 2.7.1). DNA was purified using phenol extraction and ethanol precipitation (Section 2.7.2). Approximately ~50 ng of DNA and 5-20 µM apo-WhiB1 were incubated in the presence of 40 mM Tris (pH 8), 75 mM KCl, 10 mM $MgCl_2$, 0.5 mM EDTA, 5 % (v/v) glycerol, 1 mM DTT and 250 µg/ml BSA.

Complexes were then digested with one unit of DNaseI for 7-60 seconds at 25°C. Reactions were stopped with 50 mM EDTA (pH 8), followed by phenol extraction and the DNA was ethanol precipitated (Section 2.7.2). The resulting DNA pellet was resuspended in 10 µl footprinting loading buffer and heated to 90°C for 30 seconds prior to electrophoretic fractionation on a polyacrylamide-urea gel in 1X TBE running buffer. Electrophoresis was carried out at 50 W for 2 hours before drying and visualisation using autoradiography (Section 2.7.6).

Polyacrylamide-urea gel

Gel solution (6% acrylamide, 7M urea, 1X TBE; Severn Biotech Limited)	60 ml
10% (w/v) APS	600 µl
TEMED	60 µl

Footprinting Loading Dye

Formamide	80% (v/v)
SDS	0.1% (w/v)
Glycerol	10% (v/v)
EDTA (pH 8)	8 mM
Bromophenol blue	0.1% (w/v)
Xylene cyanol	0.1% (w/v)

2.7.5 DMS methylation

Dimethylsulphate (DMS) methylation was used to prepare Maxam and Gilbert G tracks of DNA fragments, to provide a calibration for DNase I footprints (Maxam and Gilbert, 1980). Approximately ~50 ng radiolabelled DNA was incubated with 0.2% (v/v) fresh DMS (from BDH) at 25°C for 2-10 minutes. The reaction was stopped by adding 0.5 volume of DMS stop solution, followed by ethanol precipitation (Section 2.7.2) and then dried under vacuum. The resulting pellet was resuspended in 20 µl piperidine-EDTA and incubated at 90°C for 30 minutes. The sample was dried under vacuum and the resulting pellets resuspended in 10 µl footprinting loading buffer and heated to 90°C for 30 seconds before loading onto the gel (Section 2.7.4).

DMS Stop Solution		Piperidine-EDTA	
Sodium acetate (pH 7)	1.5 M	Piperidine (BDH)	10 % (v/v)
EDTA (pH 8)	15 mM	EDTA (pH 8)	10 mM
Calf thymus DNA	100 µg/ml		
2-Mercaptoethanol	1 M		

2.7.6 Autoradiography

After electrophoresis, EMSA and footprinting gels were transferred to Whatman® 3MM filter paper and dried at 80°C under vacuum. The dried gels were then exposed to Kodak medical X-ray film at -70°C. After the required exposure time, the autoradiographs were developed in Kodak Industrex developer (~2 minutes), fixed in Kodak Industrex fixer (~2 minutes) and washed in water before air-drying.

3.0 Isolation, biochemical and biophysical characterisation of WhiB1

3.1 Introduction

Members of the Wbl family of proteins, with few exceptions, are small proteins varying in length from 81-122 amino acids residues (den Hengst and Buttner, 2009). They have four highly conserved cysteine residues with a central CXXC motif which suggests that they act as ligands for a metal cofactor, and indeed a number of members of the Wbl family have been shown to bind iron-sulphur clusters (Alam *et al*., 2007; 2009; Jakimowicz *et al*., 2005; Rybniker *et al*., 2010; Singh *et al*., 2007; Smith *et al*., 2010). The seven Wbl proteins from *Mycobacterium tuberculosis* were shown to bind [2Fe-2S] clusters when aerobically expressed and purified, but following anaerobic reconstitution bound [4Fe-4S] clusters (Alam *et al*., 2009). Similar observations were made for WhiD from *Streptomyces coelicolor* (Jakimowicz *et al*., 2005). This chapter aims to characterise WhiB1 from *M. tuberculosis* and understand the nature of its iron-sulphur cluster.

3.2 Overproduction and purification of WhiB1

3.2.1 Optimisation of WhiB1 overproduction

Electrically competent *Escherichia coli* BL21 λ(DE3) cells were transformed with pGS2164, encoding recombinant His-WhiB1.

Trials to discover the best conditions for overproduction of His-WhiB1 were completed in 10 ml cultures. To first determine the optimum time for induction, 100 µl of an overnight culture was added to a 10 ml volume of LB containing kanamycin. The culture was grown at 37°C with shaking (250 rpm) until an OD_{600} of ~0.8 was reached. IPTG was added to a final concentration of 30 µg/ml and the culture was incubated at 37°C with shaking. Whole cell samples were taken before induction and at 60, 90, 120,

150, 180 and 210 minutes post induction for analysis by SDS-PAGE as described in section 2.5.2 (Figure 3.1A). There was an obvious polypeptide at ~13 kDa in all post-induction fractions, corresponding to His-WhiB1 (12.876 kDa). There was little difference in the relative abundance of His-WhiB1 as judged by SDS-PAGE, and a 2 hour induction period was chosen as it offered a good level of overproduction. Secondly, the ideal concentration of IPTG to use was determined. Growth was carried out as above and cultures were then induced with 30, 60, 120, 240 and 480 µg/ml of IPTG for 2 hours. Whole cell samples were taken for SDS-PAGE analysis (Figure 3.1B). The final concentration of 120 µg/ml of IPTG was chosen as it offered good overproduction, but all IPTG concentrations were effective. The use of different induction temperatures was the final condition tested in optimising His-WhiB1 overproduction. Growth was again carried out as described above and cultures were then induced with 120 µg/ml IPTG and moved to 25, 30 or 37°C for 2 hours. Whole cell samples were taken and analysed using SDS-PAGE (Figure 3.1C). There was good overproduction of WhiB1 at 25°C, which was chosen as it was hoped that the lower temperature would assist protein folding and solubility.

Upon finding the optimum overproduction conditions (induction with 120 µg/ml IPTG for 2 hours at 25 °C), WhiB1 was purified by affinity chromatography.

3.2.2 Purification of His-WhiB1

Cell pellets from the overproduction of WhiB1 (1-5 litres of culture) (Section 2.5.3) were resuspended in binding buffer (10 ml) and lysed in a French pressure cell according to the method detailed in Section 2.5.4. Figure 3.2B shows an SDS-PAGE gel with a clear species corresponding to His-WhiB1 at ~13 kDa in the whole cell pellet (lane 2) as well as in the soluble (lane 3) and insoluble (lane 4) fractions after lysis. It was judged that there was sufficient WhiB1 in the soluble fraction, which was therefore subsequently used for affinity purification as described in Section 2.5.5. Figure 3.2A shows the elution profile from the HiTrap chelating column. Proteins containing high levels of histidine and the protein of interest only, should bind to the column. Once the elution buffer was applied, the imidazole competes with the His-tag for the nickel column and the bound proteins are released. The first peak after the imidazole gradient usually corresponds to proteins with high histidine content, and the second peak is the

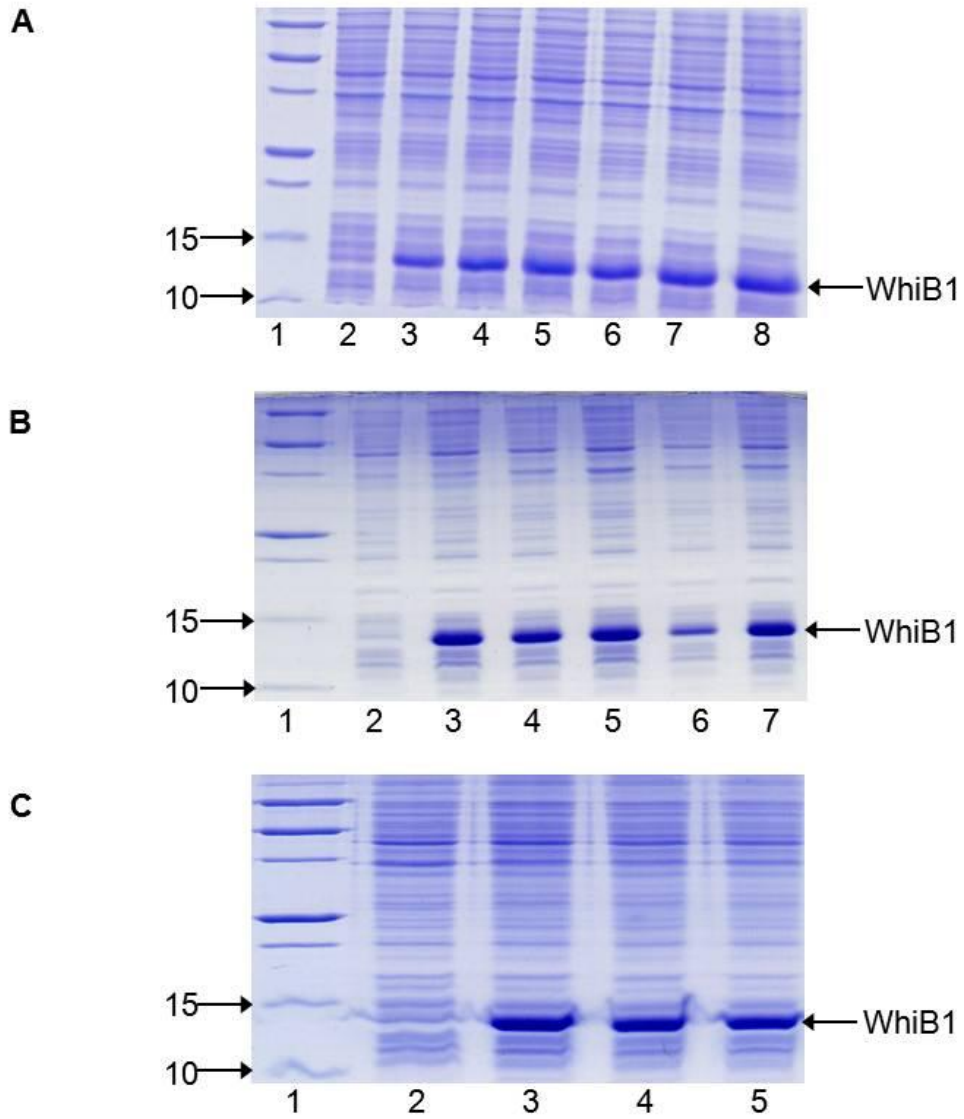

Figure 3.1: Optimisation of overexpression of recombinant WhiB1 in BL21 λ(DE3). (A) Comparison of different induction times. Lane 1, Precision plus protein standards (molecular weights indicated in kDa); Lane 2, Whole cell extract before IPTG induction; Lanes 3-8, Cell extracts with 30 μg/ml IPTG induction for 60, 90, 120, 150, 180 or 210 minutes. **(B) Comparison of different IPTG concentrations**. Lane 1, Precision plus protein standards (molecular weights indicated in kDa); Lane 2, Whole cell extract before IPTG induction; Lanes 3-7, Cell extracts after 2 hours induction with 30, 60, 120, 240 or 480 μg/ml IPTG. **(C) Comparison of different induction temperatures**. Lane 1, Precision plus protein standards (molecular weights indicated in kDa); Lane 2, Whole cell extract before IPTG induction; Lanes 3-5, Whole cell extracts after 120 μg/ml IPTG induction for 2 hours at 25, 30 and 37°C. The location of the WhiB1 polypeptide is indicated.

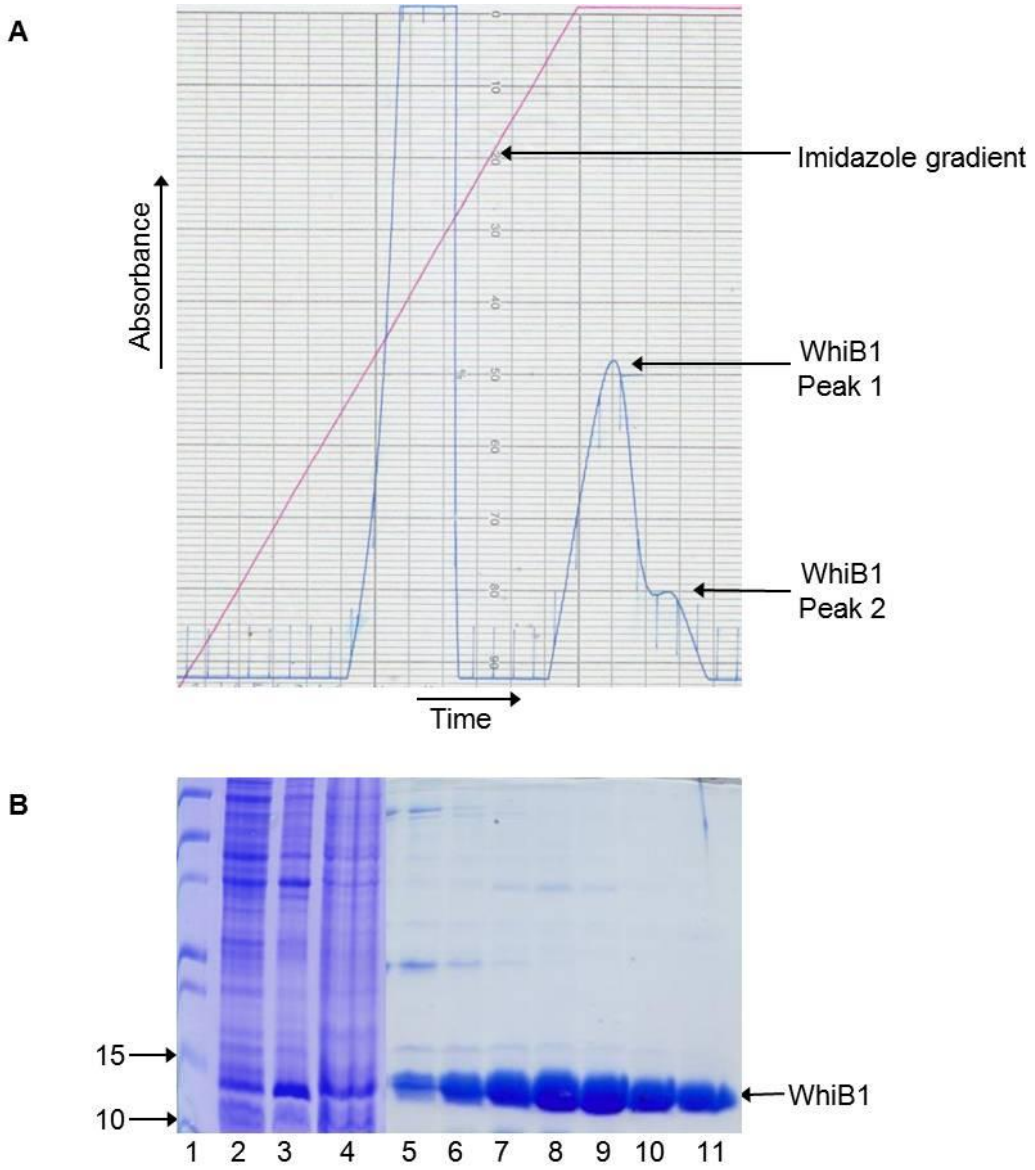

Figure 3.2: (**A) Elution profile from HiTrap chelating chromatography of cell-free extract containing His-WhiB1.** Supernatant (20 ml) was applied to a Hi-Trap chelating column (5 ml) and fractionated with a linear gradient of imidazole (0-0.5 M). The traces show protein (A_{280}: blue line) and imidazole gradient (red line). The expected location of the WhiB1 is indicated (Peaks 1 and 2). **(B) Histidine-tagged purification of His-WhiB1.** Coomassie Blue-stained SDS-PAGE gel: Lane 1, Precision plus protein standards (molecular weights indicated in kDa); Lane 2, Cell extract after induction (120 μg/ml IPTG for 2 hours at 25°C); Lane 3, Cell pellet after clarification of French pressure cell extract; Lane 4, Cell-free extract after clarification of French pressure cell extract. Lanes 5-11, Fractions collected after application of the imidazole gradient corresponding to the peak indicated in Figure 3.2A.

protein of interest. These peaks were clearly visible on the elution profile and the fractions corresponding to the second peak were analysed by SDS-PAGE. This confirmed the presence of WhiB1 at ~13 kDa (Figure 3.2B). The purification shown in Figure 3.2 was completed using a 5 ml nickel affinity column. This provided a very good level of WhiB1 from the soluble fraction (~20 mg from 5 litres of culture). The conditions described in Section 3.2.1 for overproduction, and this method of purification, have thus provided a successful way of purifying WhiB1 using the engineered histidine tag.

3.2.3 Amino acid analysis

To determine the concentration of purified WhiB1, the Bradford assay was used as described in Section 2.5.1 (Bradford, 1976). This assay can overestimate or underestimate the concentration of some proteins, which can have downstream effects on analytical experiments for which an accurate measure of WhiB1 concentration is important. Amino acid analysis gives a much more accurate measure of the protein concentration and can provide a correction factor which can be applied to all Bradford assay results for future experiments. Samples of WhiB1 were used in a Bradford assay to determine the protein concentration. They were then sent to Alta Bioscience for total amino acid analysis. Results showed that the Bradford assay was overestimating WhiB1 concentration and a correction factor of 0.86 was calculated and applied to protein concentration determination throughout the project. Furthermore this analysis confirmed the integrity of the WhiB1 protein, yielding the expected relative amounts of each amino acid.

3.3 Characterisation of the iron-sulphur cluster of WhiB1

3.3.1 Reconstitution of the cluster

Purification of large quantities of His-WhiB1 yielded some protein fractions which were colourless, some red-brown in colour and a high proportion which were straw-yellow in colour, indicating the possible presence of iron-sulphur clusters. Colour was lost upon

prolonged exposure to air. Figure 3.3 shows the UV-visible spectroscopic analysis (Section 2.6.4) of two coloured fractions from the purification depicted in Figure 3.2. The fractions corresponding to Peak 1 were straw-yellow in colour and those from Peak 2 were red-brown. These observations, along with the spectroscopy indicate the presence of a [4Fe-4S] cluster for Peak 1 (strong feature at 420 nm) and a [2Fe-2S] cluster for Peak 2 (shoulders at 420, 460 and 550 nm) (Reviewed in Orme-Johnson, 1973; Sweeney, 1980). To fully determine whether WhiB1 could incorporate an iron-sulphur cluster and what form it took, reconstitution reactions were carried out (Section 2.6.1). The concentration of the protein sample was measured and then moved to an anaerobic cabinet, where it was incubated with a source of iron, sulphur and the enzyme NifS. All samples were allowed to become anaerobic before setting up the reaction. As it proceeded, the reaction turned straw-yellow in colour which suggests the incorporation of a [4Fe-4S] cluster. To confirm this observation, spectroscopy was carried out as described in the following sections.

3.3.2 Purification of holo-WhiB1 using heparin

Heparin has a very high negative charge and can be used in the purification of DNA-binding proteins. As WhiB1 is a predicted transcription factor, it was hoped that using a HiTrap Heparin HP column (GE healthcare) would help purify the holo-WhiB1 from unincorporated components after the reconstitution reaction. Figure 3.4 shows the purification of apo-WhiB1 using heparin. A 1 ml fraction was diluted 1 in 2 with 25 mM Tris buffer (pH 7.4) to reduce the salt concentration (0.5 to 0.25 M). The diluted fraction was loaded onto the heparin column which was then washed with 25 mM Tris (pH 7.4) to remove any unbound contaminants. WhiB1 was eluted by application of 25 mM Tris buffer (pH 7.4) containing 0.5 M salt. Fractions (1 ml) were collected throughout the procedure. Samples were analysed using the Bradford assay and SDS-PAGE. Figure 3.3 shows that the protein bound to the column and was eluted by the increased salt concentration. The low molecular weight species below WhiB1 (~13 kDa) did not bind to the column. In this example 1.44 mg of apo-WhiB1 was applied to the heparin column (2 ml of sample shown in Figure 3.4, lane 3). This yielded 1.2 mg apo-WhiB1 in a 1 ml fraction after elution with the high salt buffer (Figure 3.4, lane 10), equivalent to a yield of 83%. Therefore, heparin chromatography offers a convenient method of concentrating the WhiB1 protein.

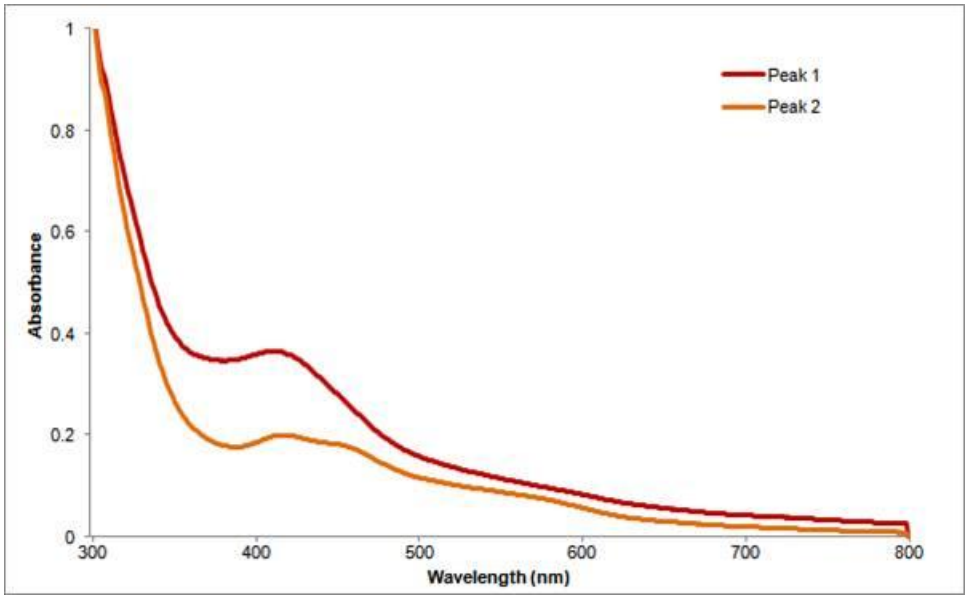

Figure 3.3: UV-visible Spectroscopy of WhiB1 fractions after His-tagged purification. Fractions corresponding to the WhiB1 main peak (Peak 1) and the shoulder (Peak 2) seen in Figure 3.2A were analysed using UV-Visible spectroscopy. There is a peak at 420 nm for Peak 1, indicative of a [4Fe-4S] cluster. The spectrum of Peak 2 shows shoulders at 420, 460 and 550 nm, indicative of a [2Fe-2S] cluster.

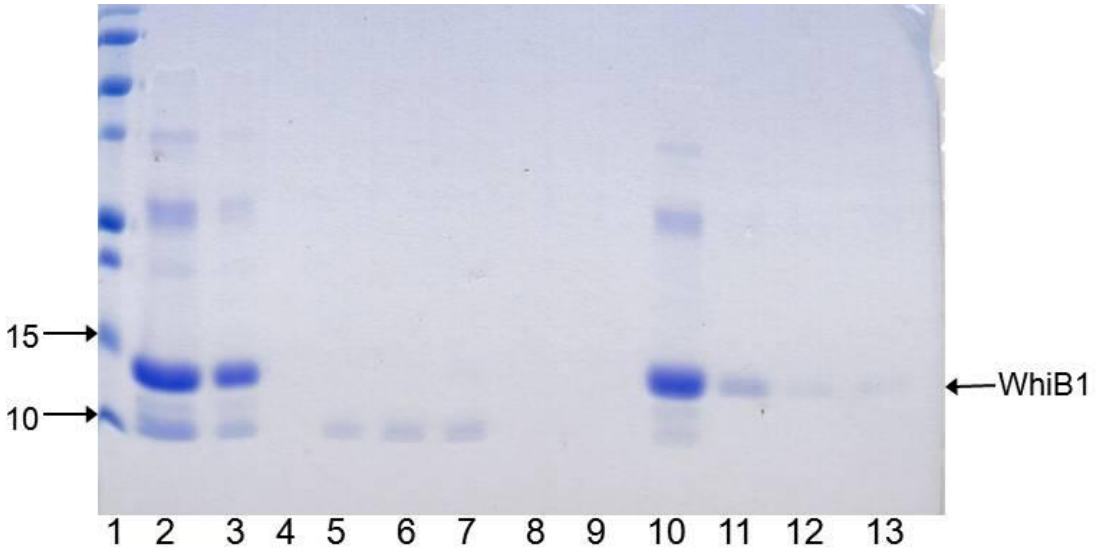

Figure 3.4: Purification of recombinant WhiB1 using a HiTrap Heparin column, following Histidine-tagged purification. Lane 1, Precision plus protein standards (molecular weights indicated in kDa); Lane 2, fraction collected after Histidine-tagged purification; Lane 3, fraction diluted with Tris buffer (25 mM, pH 7.4) before application to the heparin column; Lanes 4-6, fractions collected after protein addition (wash through); Lanes 7-9, fractions collected after column was washed with Tris buffer (25 mM, pH 7.4); Lanes 10-13, fractions collected after elution of protein with 25 mM Tris buffer (pH 7.4) containing 0.5 M salt.

This method was adopted to purify holo-WhiB1 post reconstitution, therefore allowing WhiB1 to be used for further assays with no contaminating unincorporated iron, sulphur and NifS. It also allows buffer exchange, removing imidazole which interferes with some spectroscopic analyses.

3.3.3 Characterisation of WhiB1 iron-sulphur clusters by UV-visible spectroscopy

As described (Section 3.3.1), WhiB1 was reconstituted under anaerobic conditions and the resulting sample was straw-yellow in colour. This suggested the presence of a [4Fe-4S] cluster; iron-sulphur clusters of this type have a characteristic absorbance peak at 420 nm in UV-visible spectroscopy. Accordingly, reconstitution of the iron-sulphur cluster was accompanied by an increase in absorbance at ~420 nm (Figure 3.5A). Reconstituted WhiB1 was exposed to the reductant sodium dithionite (0.2 mM for 15 minutes at 20ºC). This caused the absorbance peak at 420 nm to be partially bleached (Figure 3.5B). This suggests the [4Fe-4S] cluster can be reduced, by this strong reductant, probably from the 2+ to the 1+ state. Thus UV-visible spectroscopy has confirmed the presence of a [4Fe-4S] iron-sulphur cluster in holo-WhiB1.

3.3.4 Characterisation of the WhiB1 cluster using EPR

Electron paramagnetic spectroscopy was carried out on both apo-WhiB1 and holo-WhiB1 as described in Section 2.6.6 by Dr Jason Crack. Apo-WhiB1 was diluted with 25 mM Tris buffer (pH 7.4) containing 1 mM DTT to a final concentration of ~17 µM. Holo-WhiB1 was purified from the reconstitution reaction components using heparin chromatography and diluted with 25 mM Tris buffer (pH 7.4) containing 1 mM DTT to a final concentration of ~17 µM. Samples (200 µl) were frozen in liquid nitrogen in EPR tubes before analysis. Apo-WhiB1 was EPR silent, as was holo-WhiB1. This is consistent with the presence of a diamagnetic $[4Fe\text{-}4S]^{2+}$ cluster in holo-WhiB1 (Sweeney, 1980).

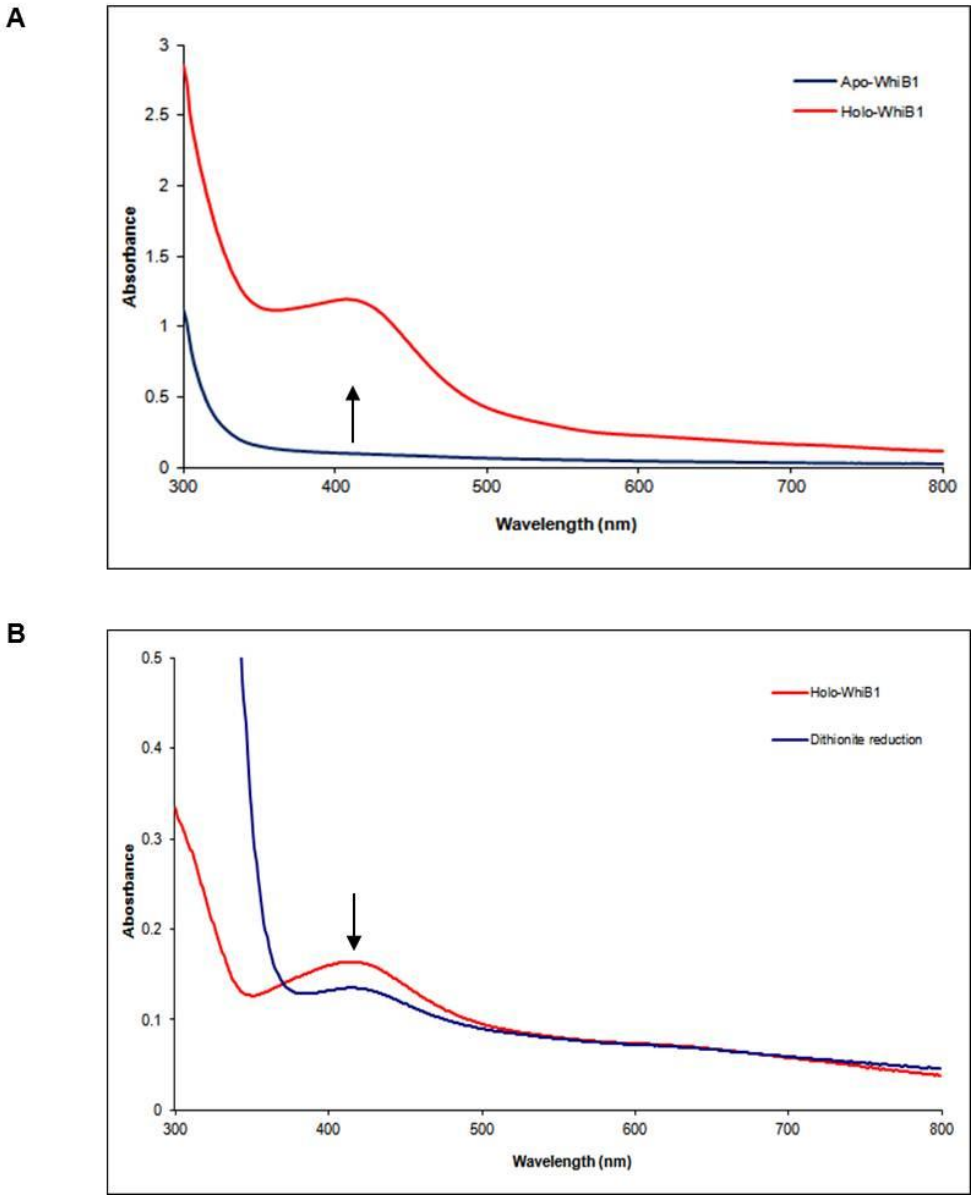

Figure 3.5: UV-visible spectroscopic analysis of reconstituted WhiB1. (A) WhiB1 (250 µM) reconstitution reaction under anaerobic conditions. The spectra shown are before (blue line) and after (red line) reconstitution. The arrow indicates the increase in absorbance at 420 nm with time. **(B) Dithionite reduction of WhiB1 (25 µM cluster).** The spectra shown are before (red line) and after (blue line) treatment with sodium dithionite (0.2 mM for 15 minutes at 20ºC). The arrow indicates the decrease in absorbance at 420 nm. (Smith *et al*., 2010).

3.3.5 Confirmation of WhiB1 cluster stoichiometry

Reconstitution of WhiB1 yields a protein sample straw-yellow in colour, and UV-visible and EPR spectroscopy indicate that it contains a $[4Fe\text{-}4S]^{2+}$ cluster. To confirm these observations, an iron assay was carried out as described in Section 2.6.8 to determine the ratio of iron atoms to WhiB1 monomers. A standard curve was created using a standard iron solution (Figure 3.6A). Protein samples were then prepared in triplicate by reconstituting WhiB1 and then purifying the holo-protein from the unincorporated reagents using heparin chromatography (Section 3.3.2). The protein concentration was measured using the Bradford assay and adjusted using the correction factor calculated from amino acid analysis (Section 3.2.3). The molar ratio of protein to iron was then calculated and the results are shown in Figure 3.6B. The average of the three repeats was 3.57 moles of iron to each WhiB1 monomer. This result is consistent with spectroscopic observations that WhiB1 binds a $[4Fe\text{-}4S]^{2+}$ cluster.

3.3.6 CD spectroscopy

Circular dichroism (CD) spectroscopy was carried out on holo-WhiB1 (196 µM) to further characterise the structure of WhiB1 as described in Section 2.6.7, in collaboration with Dr Jason Crack. The spectrum showed positive features at 427 nm and 509 nm (Figure 3.7A), similar to that of WhiD from *S. coelicolor* (Figure 3.7A) (Crack *et al.*, 2009). The spectrum was different however, to that of the oxygen sensor FNR from *E. coli*, which lacked these positive features (Figure 3.7B), highlighting a difference in iron-sulphur cluster environment of the Wbl proteins compared to FNR.

3.4 Characterisation of the oligomeric state of WhiB1

3.4.1 Analysis by SDS-PAGE

Large scale purification of His-WhiB1 yielded ~20 mg WhiB1 from 5 litres culture. Analysis of concentrated samples by SDS-PAGE often showed the presence of species of higher and lower molecular weights, than expected of a WhiB1 monomer

A

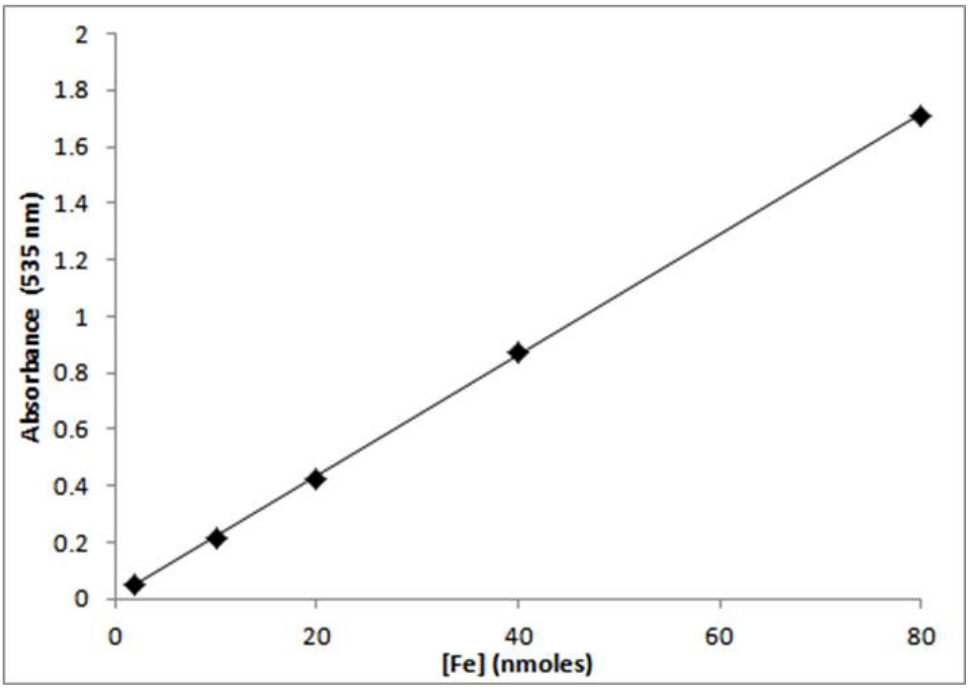

B

WhiB1 (nmoles)	Fe (nmoles)	Ratio
8.01	29	3.62
12.8	45	3.51
11.22	40	3.57

Figure 3.6: Determination of iron content in holo-WhiB1. (A) Standardisation of iron assay. Different concentrations of iron (Iron standard solution, BDH) were assayed (Section 2.6.8). **(B) Ratio of iron atoms to WhiB1.** The absorbance measured for each protein sample was used to determine the concentration of iron in the sample and the ratio subsequently calculated.

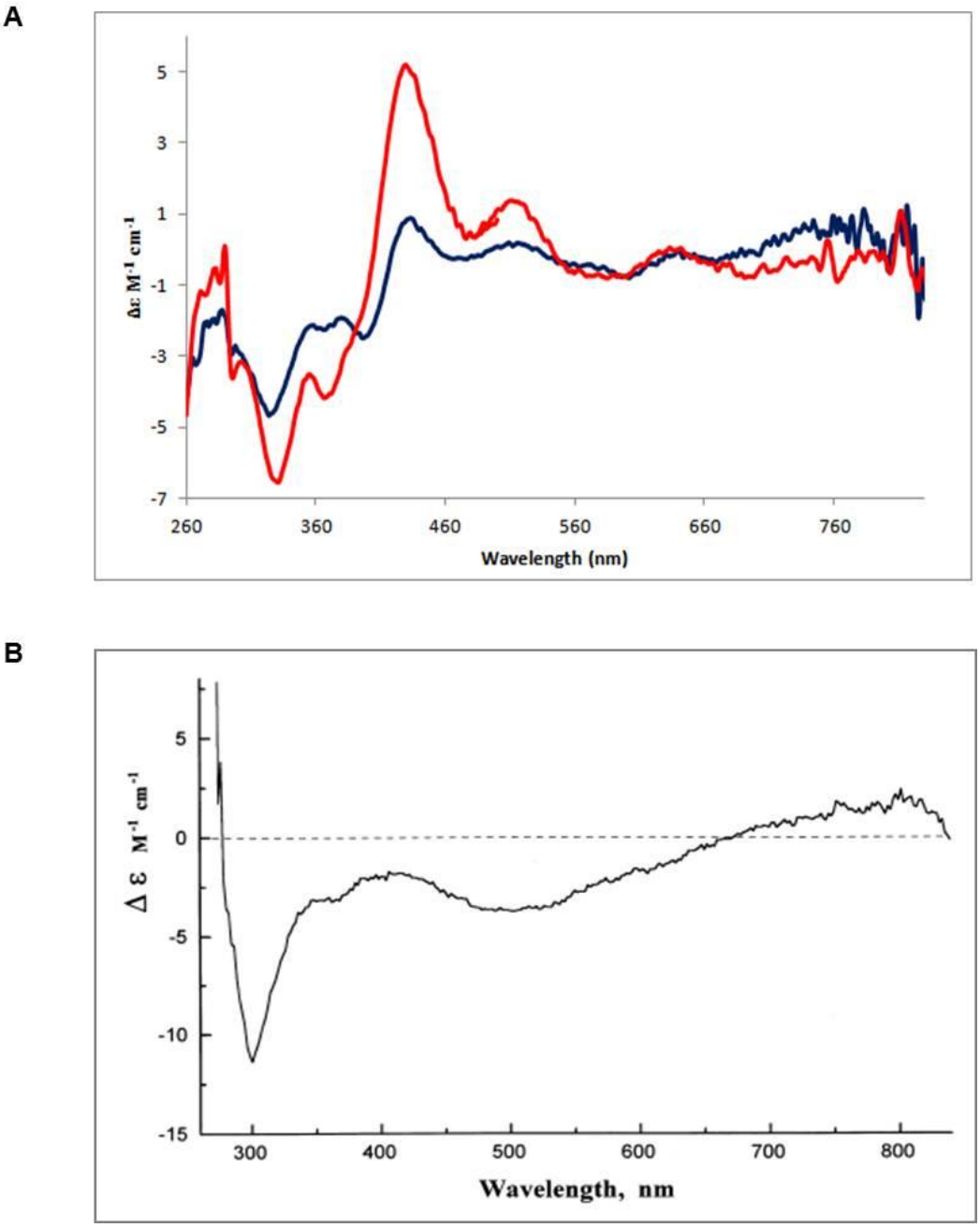

Figure 3.7: CD Spectroscopic analysis of WhiB1. (A) CD spectrum of WhiB1. Reconstituted WhiB1 (196 µM) was scanned and the spectrum (red line) is compared to that of another Wbl protein, WhiD (396 µM cluster; blue line). **(B) CD spectrum of FNR.** FNR (24 µM cluster) spectrum from Green *et al*. (1996), showing different features to the Wbl proteins.

(Figure 3.8A). To identify these species, N-terminal amino acid sequencing was carried out by Dr A.J.G. Moir (Sections 2.5.7 and 2.5.8). The four species indicated on the gel in Figure 3.8A were sequenced and the results are shown in Figure 3.8B. As shown, all four species had the same sequence, which corresponded to that of His-WhiB1. Due to the higher concentration of protein in the fractions, the cysteine residues appear to be forming inter- and intramolecular disulphide bonds, despite the presence of 100 mM β-mercaptoethanol. Addition of further fresh reducing agent to the loading dye and storage of fractions in buffer containing 1 mM DTT at -20°C prevented formation of disulphide linked oligomers. Furthermore, addition of the components of the reconstitution reaction to the protein fractions converted WhiB1 to a monomer containing a [4Fe-4S] cluster. The formation of oligomers appears to be a consequence of high concentrations of WhiB1 and the absence of the [4Fe-4S] cluster.

3.4.2 Determination of sulphydryl groups in WhiB1

The presence of disulphide bonds in apo-WhiB1, suggested by the N-terminal amino acid sequencing and SDS-PAGE analysis, was confirmed by measuring the amount of reactive thiol using DTNB as described by Thelander (1973). Assays were carried out in the absence of reducing agents under native conditions and denaturing conditions (treatment with 1% SDS). WhiB1 samples were prepared at 3.88 µM and the assay was as described in Section 2.5.11. Results revealed the presence of two (1.88 ± 0.27, n = 9) reactive thiols in the native soluble apo-protein, implying the presence, on average, of one disulphide bridge per apo-WhiB1 because WhiB1 has four cysteine residues. The number of reactive thiols per apo-WhiB1 decreased to 1.15 ± 0.15 (n = 9) after treatment with SDS, implying that unfolding the protein promoted additional disulphide bridge formation (on average 1.5 per monomer) (Smith *et al*., 2010). This propensity to form disulphide bonds accounts for the protein pattern seen on the SDS-PAGE gel and the N-terminal amino acid sequencing results.

3.4.3 Analysis by gel filtration

The oligomeric state of native WhiB1 was assessed by gel filtration chromatography (Section 2.5.10). A standard curve was produced using a set of proteins of known

A

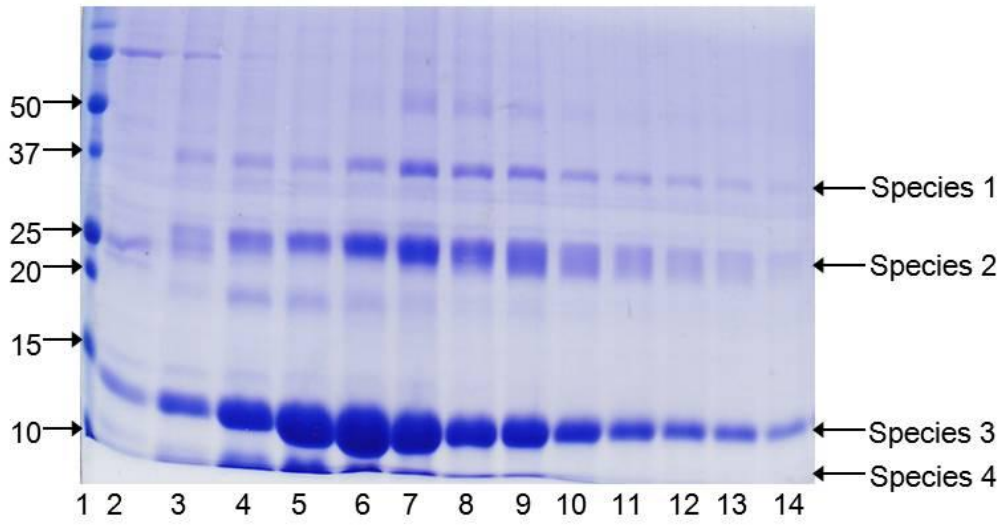

B

Species	Sequence	Predicted Protein
1	GSSHHHH	WhiB1 trimer
2	GSSHHHH	WhiB1 dimer
3	GSSHHHH	WhiB1 monomer
4	GSSHHHH	WhiB1 monomer

Figure 3.8: WhiB1 can form disulphide linked oligomers. A) SDS-PAGE analysis of His-WhiB1. Lane 1, Precision plus protein standards (molecular weights indicated in kDa); Lanes 2-15, fractions collected after imidazole elution of WhiB1 from a 5 ml Hi-trap chelating column. The SDS-PAGE was blotted and used for N-terminal amino acid sequencing to identify the four species indicated. **B) Results from N-terminal amino acid sequencing.** Table shows the sequence of the four species analysed. The six amino acids given correspond to the histidine tag on the WhiB1 protein. The predicted proteins corresponding to the species are shown.

molecular weights (Figure 3.9). As shown earlier (Section 3.4.1), apo-WhiB1 has a tendency to form oligomers in high concentrations or under insufficiently reducing conditions. Apo-WhiB1 (50 µM) was purified using heparin chromatography and eluted in 20 mM sodium phosphate buffer, pH 7.4 with 0.5 M NaCl, treated with 1 mM DTT (for reducing conditions) or 1 mM diamide (for oxidising conditions) and applied to the calibrated Shodex KW805 column. Due to the aggregation of apo-WhiB1 (as has been shown previously on SDS-PAGE gels, Section 3.4.1), the elution profile was difficult to interpret due to the formation of many large oligomers (data not shown). Holo-WhiB1 (50 µM) was reconstituted and the reaction purified using heparin chromatography. Holo-WhiB1 samples were treated with 1 mM DTT and 1 mM diamide also, where indicated. The results for Holo-WhiB1 are shown in Figure 3.10. The trace shows a peak at ~715 seconds (Figure 3.10). When used to determine the molecular weight using the standard curve (Figure 3.9B), a value of ~12.5 kDa was obtained. This corresponds to a WhiB1 monomer (actual molecular weight 12.876 kDa). There was no effect of adding diamide or DTT to these samples. These data indicate that holo-WhiB1 is a monomer with a [4Fe-4S] cluster, but in high concentrations the apo- form has a tendency to form oligomers through the formation of disulphide bridges.

3.5 Discussion

Work undertaken in this chapter has characterised the apo-form of WhiB1 and the nature of the iron-sulphur cluster in the holo-form of WhiB1. As suggested in the literature, the presence of four highly conserved cysteine residues in the Wbl proteins are expected to bind iron-sulphur clusters (den Hengst and Buttner, 2008). Here we show that WhiB1 can incorporate both a [2Fe-2S] and a [4Fe-4S] cluster. Aerobic overproduction and purification of WhiB1 yielded protein in its apo-form, containing no cluster, as well as holo- protein containing either a [2Fe-2S] or a [4Fe-4S] cluster (Section 3.3.1 and Figure 3.3). The observation that aerobically purified WhiB1 could contain a [2Fe-2S] cluster is consistent with findings for the other WhiB proteins of *M. tuberculosis* and WhiD from *S. coelicolor* (Alam *et al*., 2007; 2009; Jakimowicz *et al*., 2005; Singh *et al*., 2007). *Streptomyces coelicolor* WhiD, after overexpression, was found in coloured inclusion bodies and following solubilisation the resulting protein was red-brown in colour. UV-visible spectroscopic analysis showed features at 420, 450 and 550 nm indicating the presence of a [2Fe-2S] cluster (Jakimowicz *et al*., 2005).

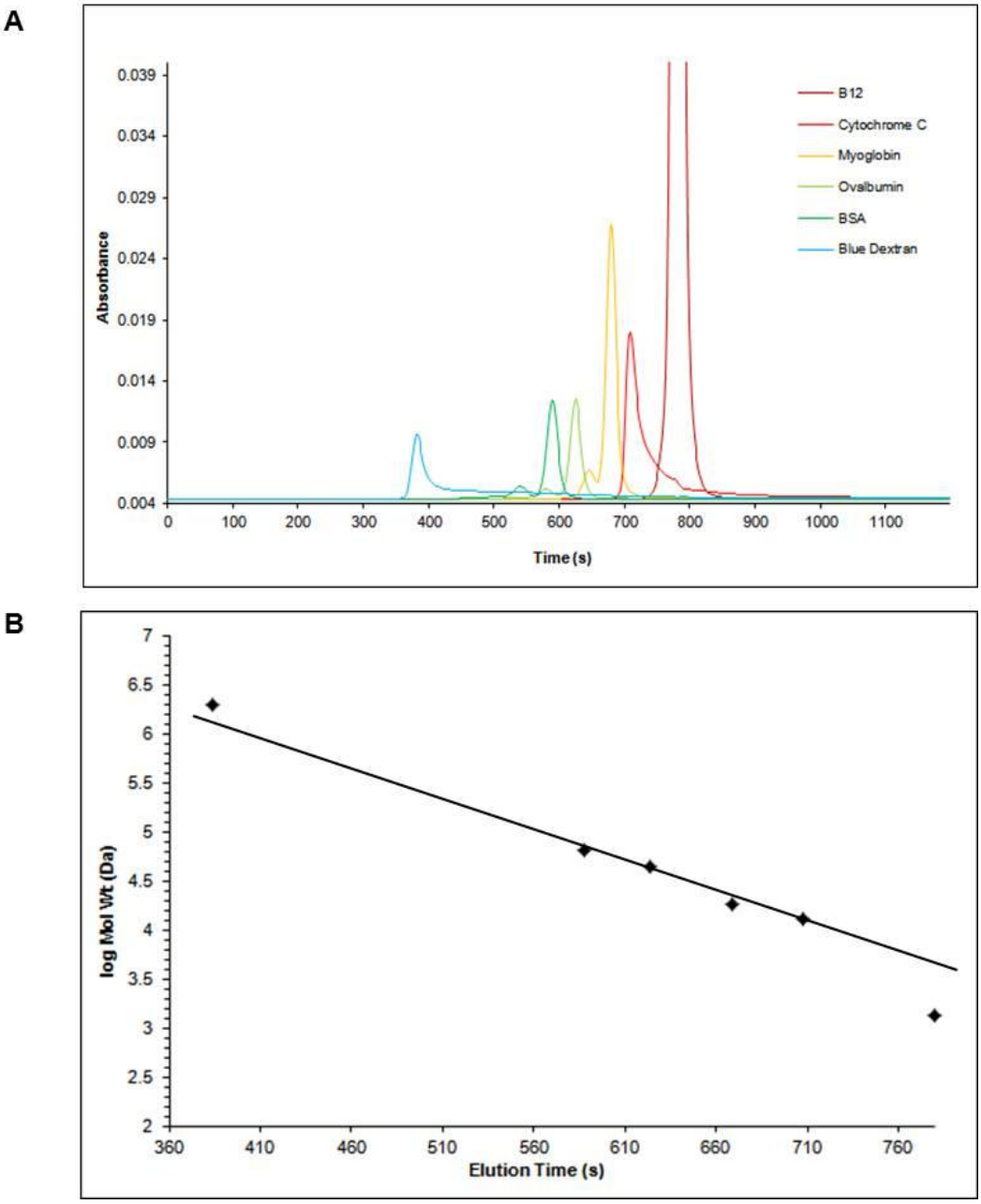

Figure 3.9: Molecular weight standard curve for gel filtration. (A) Peaks of the molecular weight standards. Standards were prepared (5 mg/ml of vitamin B12, 1.38 kDa; cytochrome C, 12.385 kDa; myoglobin, 18.8 kDa; ovalbumin, 47.2 kDa; BSA, 66kDa and 132 kDa; blue dextran, 2000 kDa) in 20 mM sodium phosphate pH 7.4 with 0.5 M NaCl and run on a Shodex KW805 column. **(B) Calibration graph.** The elution time of each protein was plotted against the log of its molecular weight and a standard curve produced.

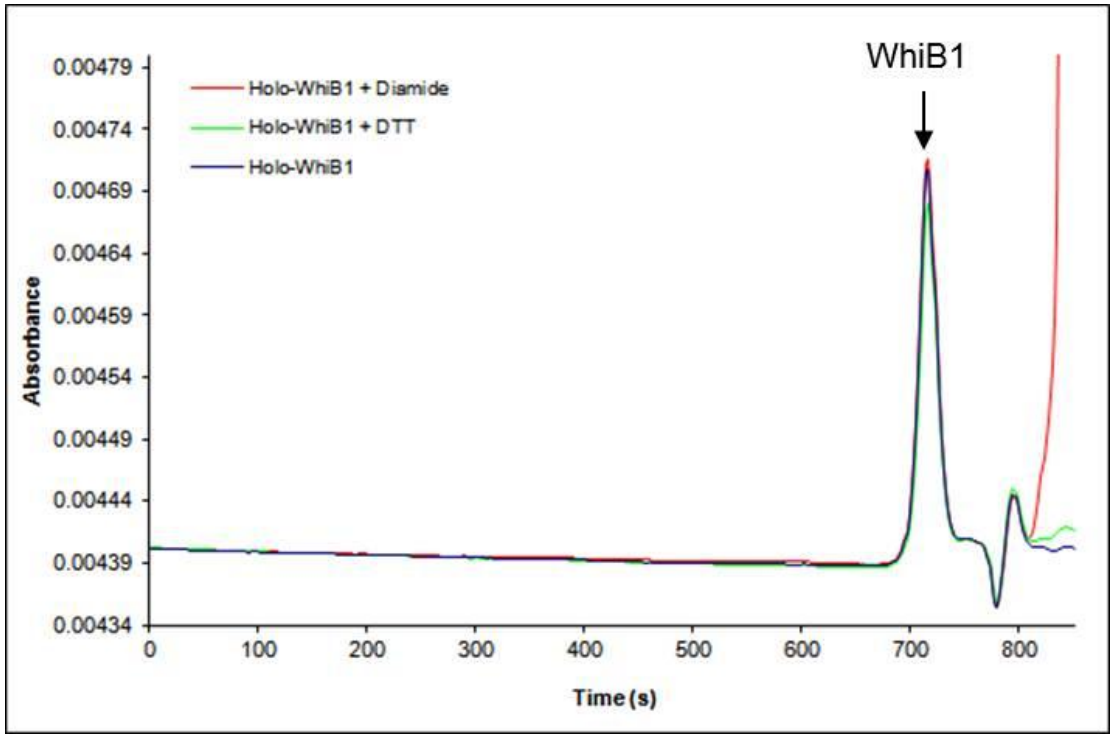

Figure 3.10: Gel filtration analysis of holo-WhiB1. Holo-WhiB1 (50 µM initial concentration) was analysed in normal conditions (no pre-treatment of holo-WhiB1), reducing conditions (holo-WhiB1 pre-treated with 1 mM DTT) and oxidising conditions (holo-WhiB1 treated with 1 mM diamide). The peak corresponding to the WhiB1 monomer is indicated.

A similar spectrum with features at 420, 460 and 550 nm was seen for WhiB1 (Figure 3.3). Calculations showed that there was a 15-37 % occupation of WhiD with a [2Fe-2S] cluster, and it was expected that the presence of a [2Fe-2S] cluster was a result of aerobic purification (Jakimowicz *et al*., 2005). Similar findings were seen for the seven WhiB proteins of *M. tuberculosis* (Alam *et al*., 2007; 2009; Singh *et al*., 2007). To determine the true nature of the iron-sulphur cluster of WhiB1, the cluster was reconstituted under anaerobic conditions (Section 3.3.1). The resulting protein sample was straw yellow in colour and UV-visible spectroscopic analysis showed a spectrum with a strong peak at 420 nm, indicative of a [4Fe-4S] cluster (Figure 3.5A). This was confirmed by analysis of the stoichiometry providing 3.57 Fe: 1 WhiB1 (Section 3.3.5). The [4Fe-4S] cluster underwent reduction with dithionite (Figure 3.5B) and combined with the presence of a silent species in EPR analysis (Section 3.3.4), it was concluded that WhiB1 incorporates a $[4Fe\text{-}4S]^{2+}$ cluster which can undergo one electron reduction. Reconstitution under anaerobic conditions for WhiD of *S. coelicolor* and the other Wbl proteins of *M. tuberculosis* also showed them to bind [4Fe-4S] clusters with UV-visible spectroscopy showing strong features at 420 nm and EPR showing silent species (Alam *et al*., 2007; 2009; Jakimowicz *et al*., 2005; Singh *et al*., 2007).

CD analysis of holo-WhiB1 showed positive features at 427 nm and 509 nm, similar to those of WhiD (430 nm and 515 nm), and negative features at 335, 375 and 600 nm (325, 395 and 600 nm in WhiD) (Section 3.3.6 and Figure 3.7A; Crack *et al*., 2009). In contrast, the well characterised oxygen-sensing transcription factor FNR from *E. coli* has a very different CD spectrum (compare Figure 3.7A to 3.7B) with negative features at 300 nm and 500 nm, and a positive feature at 800 nm (Green *et al*., 1996). This suggests that the environment surrounding the [4Fe-4S] clusters of these two Wbl proteins is different to that surrounding the [4Fe-4S] cluster of FNR, and the sensitivity and function of the cluster of WhiB1 will be analysed in Chapter 4.

As discussed, WhiB1 binds a [4Fe-4S] and this holo-form of WhiB1 is a monomer, shown by gel filtration analysis (Section 3.4.3 and Figure 3.10). The iron-sulphur cluster-containing form of WhiD from *S. coelicolor* is also found as a monomer as shown by analytical gel filtration (Crack *et al*., 2009; Jakimowicz *et al*., 2005). The apo-form of WhiB1 however, has a tendency to form oligomers especially in the absence of reducing conditions or when at high concentrations. Gel filtration analysis of apo-WhiB1 showed no distinct peak corresponding to a monomer but a heterogeneous

spectrum which could not be interpreted due to aggregation forming oligomers (Section 3.4.3). Similar observations were made for partially iron-loaded WhiD purified from inclusion bodies (Jakimowicz *et al*., 2005). Garg and co-workers, suggested that WhiB1 forms a homo-dimer under reducing conditions (Garg *et al*., 2007), with similar reports for WhiB3 (Alam and Agrawal, 2008) and WhiB4 (Alam *et al*., 2007). For WhiB3 however, the size of the homo-dimer was 26 kDa instead of the expected 32 kDa, which was attributed to the globular form of the dimer forming a compact complex (Alam and Agrawal, 2008). Interestingly, these groups showed that WhiB1, WhiB3 and WhiB4 were found as monomers in reducing SDS-PAGE (Alam *et al*., 2007; Alam and Agrawal, 2008; Garg *et al*., 2007). These findings correspond to our findings for WhiB1, whereby in reducing conditions the main species was seen as a monomer (Section 3.4.1). In insufficient reducing conditions, oligomers of apo-WhiB1 were seen due to the formation of disulphide bonds between monomers (Section 3.4.1 and Figure 3.8). These observations corroborate the findings of Crack *et al*. with WhiD, whereby dimeric species were lost under reducing conditions (Crack *et al*., 2009). It was concluded that WhiB1 is a monomeric protein when in the holo-form, but the apo-form has a tendency to oligomerise through the formation of intermolecular disulphide bonds. As well as the formation of intermolecular disulphide bonds, intramolecular disulphide bonds are formed in apo-WhiB1, as can be seen by a species on SDS-PAGE which migrated faster than the monomer (Figure 3.8). This has also been seen for WhiB2, WhiB3, WhiB4 and WhiB5 (Alam *et al*., 2007; 2009; Alam and Agrawal, 2008; Garg *et al*., 2007). Interestingly, the inability of the intramolecular disulphide form of WhiB1 to bind heparin (Figure 3.4) suggested that this is a distinct conformational form of the protein that could fulfil a specific biological role. The presence of disulphide bonds was further confirmed by the reactive thiol assay (Section 3.4.2). This showed the presence of 1 disulphide bond in each apo-WhiB1 monomer, which increased to 1.5 in unfolded WhiB1 (Smith *et al*., 2010). Mass spectroscopy of WhiB1, WhiB3 and WhiB4 indicated the presence of 2 disulphide bonds per monomer in apo-WhiB1 (Alam *et al*., 2007; Alam and Agrawal, 2008; Garg *et al*., 2007).

Work in this chapter has begun to characterise the biochemical and biophysical properties of WhiB1. It can incorporate a $[4Fe\text{-}4S]^{2+}$ cluster and in this form is seen as a monomer. Apo-WhiB1 is also found as a monomer in reducing conditions but has a tendency to oligomerise in the absence of reductant, due to the formation of both

intermolecular and intramolecular disulphide bonds. Work will now focus on the role of the iron-sulphur cluster and function of WhiB1.

4.0 Functional characterisation of WhiB1

4.1 Introduction

As shown in Chapter 3, *Mycobacterium tuberculosis* WhiB1 can be overproduced in both its apo- and holo- form (with a [2Fe-2S] or [4Fe-4S] cluster) and upon reconstitution incorporates a [4Fe-4S] cluster. Proteins containing iron-sulphur clusters can act as sensors of environmental changes, including the presence or absence of oxygen and nitric oxide, and relay this information by altering gene expression. This process occurs through changes in protein conformation and thus changes in DNA-binding affinity (Crack *et al*., 2012). This chapter aims to characterise the sensitivity of the WhiB1 iron-sulphur cluster to oxygen and nitric oxide to determine whether holo-WhiB1 may act as a sensor for either of these physiologically significant gases. The [4Fe-4S] cluster of WhiB3 from *M. tuberculosis*, is slowly degraded in the presence of oxygen and also reacts with nitric oxide forming dinitrosyl-iron thiol complexes (DNICs) (Singh *et al*., 2007). The presence of a predicted helix-turn-helix, as well as phenotypic studies of mutants, led to the suggestion that Wbl proteins function as DNA-binding transcription factors (den Hengst and Buttner, 2009). This function has been attributed to WhiB3 whereby interaction to promoter DNA of genes known to be differentially regulated in a *whiB3* mutant, and with the essential sigma factor SigA, has been seen (Guo *et al*., 2009; Singh *et al*., 2009; Steyn *et al*., 2002). It has also been suggested that Wbl proteins, including WhiB1, function as protein disulphide reductases (Alam *et al*., 2007; 2009; Garg *et al*., 2007), although WhiD from *Streptomyces coelicolor* was shown to lack such activity (Crack *et al*., 2009). Here, the role of the iron-sulphur cluster on any DNA-binding ability or protein disulphide reductase activity will be analysed to determine WhiB1 function.

4.2 Insensitivity of the iron-sulphur cluster of WhiB1 to oxygen

As previously discussed in Chapter 3, WhiB1 can be purified in its holo-form containing either a [2Fe-2S] or [4Fe-4S] cluster (Figure 3.3). Upon prolonged exposure to air, the cluster of WhiB1 disassembles to give apo-WhiB1. These observations

indicate that the iron-sulphur cluster of WhiB1 is relatively stable in air. Upon reconstitution, WhiB1 ligates a [4Fe-4S] cluster. To determine how stable this cluster is, and whether upon oxygen exposure the cluster disassembles into a [2Fe-2S] form then to apo-WhiB1, or [4Fe-4S] to apo-WhiB1, UV-visible spectroscopy was carried out (Section 2.6.4). WhiB1 was reconstituted and purified using heparin chromatography as described previously (Sections 2.6.1 and 2.6.2). The resulting holo-protein contained 10 μM of [4Fe-4S] cluster and was exposed to oxygen by the addition of air-saturated buffer (25 mM Tris, pH 7.4 containing 0.5 M NaCl, 10% glycerol and 1 mM DTT) equivalent to a final concentration of 110 μM oxygen. Spectra were taken at 0 and 120 minutes (Figure 4.1). There was a minor decrease in absorbance at 420 nm over the two hours incubation with oxygen (Figure 4.1). This shows that the [4Fe-4S] cluster of WhiB1 is very stable in the presence of oxygen. After prolonged exposure for 24-72 hours, the cluster disassembled to give apo-WhiB1. There were no signs in the spectroscopy to indicate the formation of an intermediate [2Fe-2S] cluster.

4.3 Sensitivity of the iron-sulphur cluster of WhiB1 to nitric oxide

After concluding that the iron-sulphur cluster of WhiB1 was relatively stable in oxygen, its stability to nitric oxide was then tested. Proli NONOate (Alexis Biochemicals and Cayman Chemicals) was the chosen nitric oxide donor as it reacts immediately, releasing two molecules of nitric oxide per molecule (half-life of 1.8 seconds at pH 7.4 and 37°C). This was used in all the following experiments to determine the sensitivity of holo-WhiB1 to nitric oxide.

4.3.1 UV-visible spectroscopic analysis

To test whether the iron-sulphur cluster of WhiB1 is sensitive to nitric oxide, UV-visible spectroscopy was carried out as described in Section 2.6.4 with holo-WhiB1 and Proli NONOate. Reconstituted and heparin purified WhiB1 (22 μM cluster) in 25 mM Tris (pH 7.4) containing 0.5 M NaCl was analysed before exposure to Proli NONOate (570 μM) for three hours to allow any reaction to run to completion under anaerobic conditions. This gave a ratio of 52 nitric oxide: [4Fe-4S]. After exposure for three hours

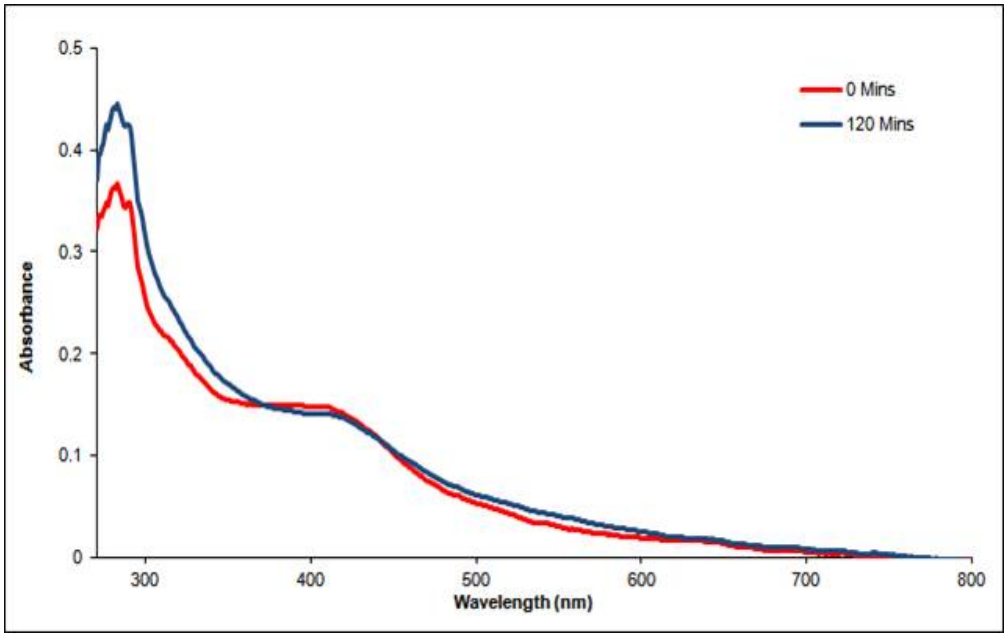

Figure 4.1: UV-visible spectroscopy of the reaction of WhiB1 and oxygen. Spectra showing WhiB1 (10 μM cluster) in air-saturated buffer containing 1 mM DTT, equivalent to a final concentration of 110 μM oxygen at 0 minutes (red line) and 120 minutes (blue line).

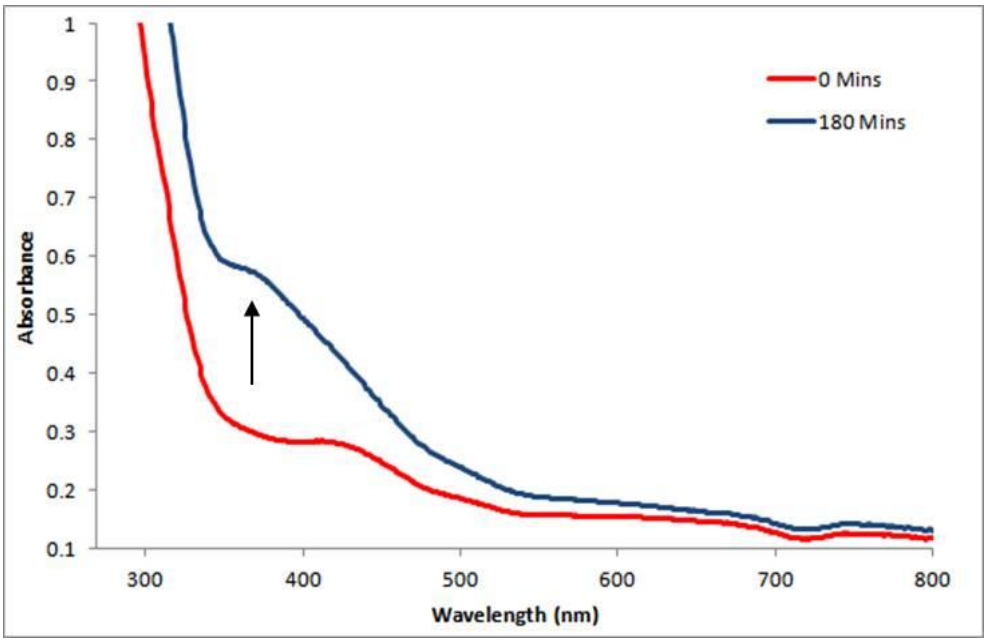

Figure 4.2: UV-visible spectroscopic analysis of the reaction of WhiB1 and nitric oxide. The spectra of holo-WhiB1 (22 μM cluster) before (red line) and after (blue line) the addition of 570 μM Proli NONOate for 3 hours were measured. This gave a ratio of 52 nitric oxide:1 [4Fe-4S]. The increase in absorbance at 350-360 nm due to the formation of nitrosylated clusters is indicated.

the UV-visible spectrum was obtained (Figure 4.2). The absorbance peak at 420 nm, indicative of a [4Fe-4S] cluster, was lost after exposure to nitric oxide. A shoulder was formed at 350-360 nm as shown in Figure 4.2. This feature is typical of nitrosylated iron complexes, which are formed in the reaction of iron-sulphur clusters and nitric oxide. These complexes can be found as both dinitrosylated iron complexes (DNICs) and tetranitrosylated iron complexes (Roussin's red esters - RREs), which both contribute to the absorbance profile (Figure 4.3; Cruz-Ramos *et al*., 2002). The reaction of holo-WhiB1 and nitric oxide was then subjected to further study, as the iron-sulphur cluster is more sensitive to nitric oxide than oxygen.

4.3.2 EPR spectroscopic analysis

As described previously (Section 3.3.4), WhiB1 was analysed using EPR spectroscopy to determine the nature of the iron-sulphur cluster. Both apo-WhiB1 and holo-WhiB1 were EPR silent (Figure 4.4A). This indicated the presence of a $[4Fe\text{-}4S]^{2+}$ cluster in holo-WhiB1 (Section 3.3.4). Holo-WhiB1 (17 μM), post reconstitution and heparin purification was then exposed to a 27-fold molar excess of Proli NONOate under anaerobic conditions for ten minutes and then two hours. These reactions were in 25 mM Tris (pH 7.4) containing 1 mM DTT. Samples (200 μl) were frozen in liquid nitrogen in EPR tubes before analysis by Dr Jason Crack at the University of East Anglia (Section 2.6.6). As shown in Figure 4.3, the nitrosylation of iron-sulphur clusters can result in di- and tetra-nitrosylated iron complexes. Dinitrosylated iron complexes (DNICs) have characteristic EPR spectra, whereas tetranitrosylated iron complexes are EPR silent. After treatment of holo-WhiB1 with Proli NONOate for ten minutes, an axial EPR spectrum (g = 2.048, 2.03 and 2.022) was detected (Figure 4.4A and B). This indicated the presence of 6 μM DNIC from 17 μM iron-sulphur cluster, i.e. ~10% of the total iron was present as an EPR-detectable DNIC. Due to the presence of DTT in the reaction buffer, some of this intensity may have arisen from a DTT co-ordinated DNIC species. The intensity of the signal at 2.03 decreased upon longer incubation of holo-WhiB1 and Proli NONOate for two hours (Figure 4.4A and B). This decrease was equivalent to 2.8 μM DNIC, i.e. ~4% of the total iron (Smith *et al*., 2010). The EPR analysis of the reaction of holo-WhiB1 with nitric oxide combined with the UV-visible spectroscopy suggests a formation of a mixture of EPR active DNICs and EPR silent

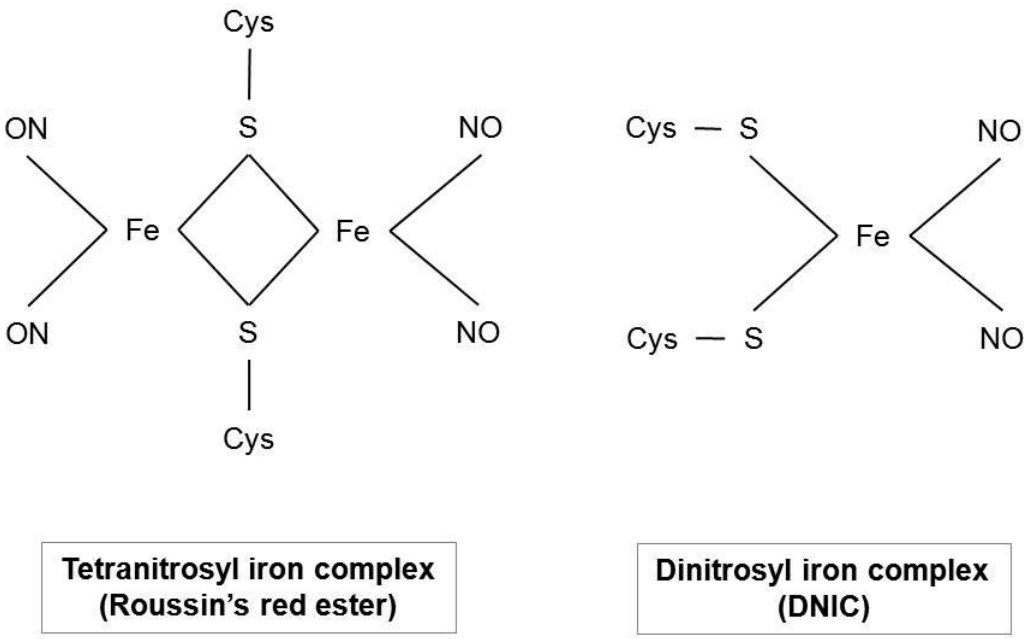

Figure 4.3: Diagram showing two forms of nitrosylated iron-sulphur clusters. Upon reaction of iron-sulphur clusters with nitric oxide, dinitrosyl iron complexes (DNICs) and tetranitosyl iron complexes (also known as Roussin's red esters – RREs) can form.

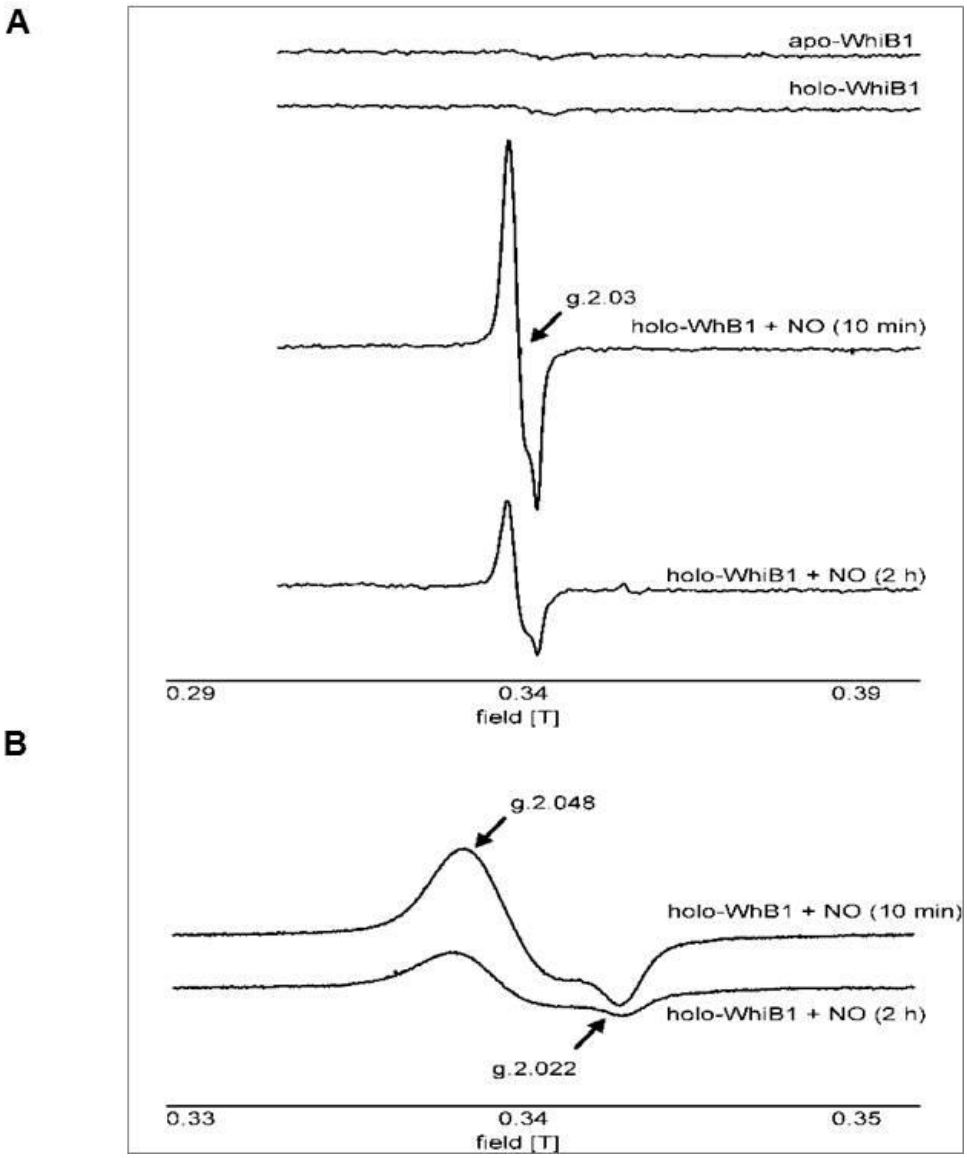

Figure 4.4: EPR analysis of WhiB1 and its response to nitric oxide. (A) From top to bottom: apo-WhiB1; anaerobically reconstituted holo-WhiB1; holo-WhiB1 treated with a 27-fold molar excess of Proli NONOate for ten minutes under anaerobic conditions; holo-WhiB1 treated with a 27-fold molar excess of Proli NONOate for two hours. Spectra were recorded at 20 K. **(B)** EPR spectra (g = ~2 region) of the nitric oxide treated samples in **(A)** measured at 77 K for quantification. For all samples, WhiB1 concentration was 17 µM. The spectra were obtained using a continuous-wave EPR spectrometer with a microwave frequency of 9.68 GHz operating at a 100 kHz magnetic field modulation.

nitrosylated iron complexes, presumably tetranitrosylated iron complexes, with the EPR-silent form as the major species (Smith *et al*., 2010).

4.3.3 Stoichiometry of the reaction of WhiB1 with nitric oxide

To determine the stoichiometry of the reaction of WhiB1 with nitric oxide, holo-WhiB1 was titrated against Proli NONOate under anaerobic conditions and the changes in absorbance monitored using UV-visible spectroscopy. Reconstituted WhiB1 (19 µM cluster) was analysed in a cuvette maintaining anaerobic conditions as described in Section 2.6.4. The reaction buffer used was 100 mM Tris (pH 7.4) containing 0.5 M NaCl and 10% glycerol to reduce the effect of the additions of Proli NONOate which is stored in sodium hydroxide. Proli NONOate was injected through the silicone seal, to maintain anaerobic conditions, in increasing amounts (0-90 µM). UV-visible spectra were obtained 10 minutes after each addition (Figure 4.5A), and a decrease in absorbance at 420 nm and an increase at 350-360 nm was seen, along with an isosbestic point at 480 nm. These features are indicative of the formation of nitrosylated iron sulphur clusters (Cruz-Ramos *et al*., 2002). The cumulative change in absorbance at 355 nm (corresponding to nitrosylation) was calculated for each addition of Proli NONOate, accounting for the dilution factor, and plotted against the ratio of nitric oxide:WhiB1. Eight nitric oxide molecules reacted per iron-sulphur cluster of WhiB1 (Figure 4.5B), suggesting the formation of an octa-nitrosylated iron-sulphur centre.

4.3.4 Stopped-flow kinetics of the reaction of holo-WhiB1 and nitric oxide

Stopped-flow rapid rate kinetic analysis of the reaction of the [4Fe-4S] cluster of WhiB1 with nitric oxide was carried out as described in Section 2.6.5 and in Crack *et al*. (2011). Holo-WhiB1 (7 µM cluster) was exposed to 300 µM or 643 µM nitric oxide giving a nitric oxide:[4Fe-4S] ratio of ~43 and ~92 respectively. The absorbance at 364 nm (formation of nitrosylated clusters) and 420 nm (disassembly of the [4Fe-4S] cluster) was measured over time and the resulting absorbance spectra are shown in Figure 4.6. The spectra shown are averages of at least seven runs per wavelength and nitric oxide concentration. The reaction of WhiB1 with nitric oxide was extremely rapid

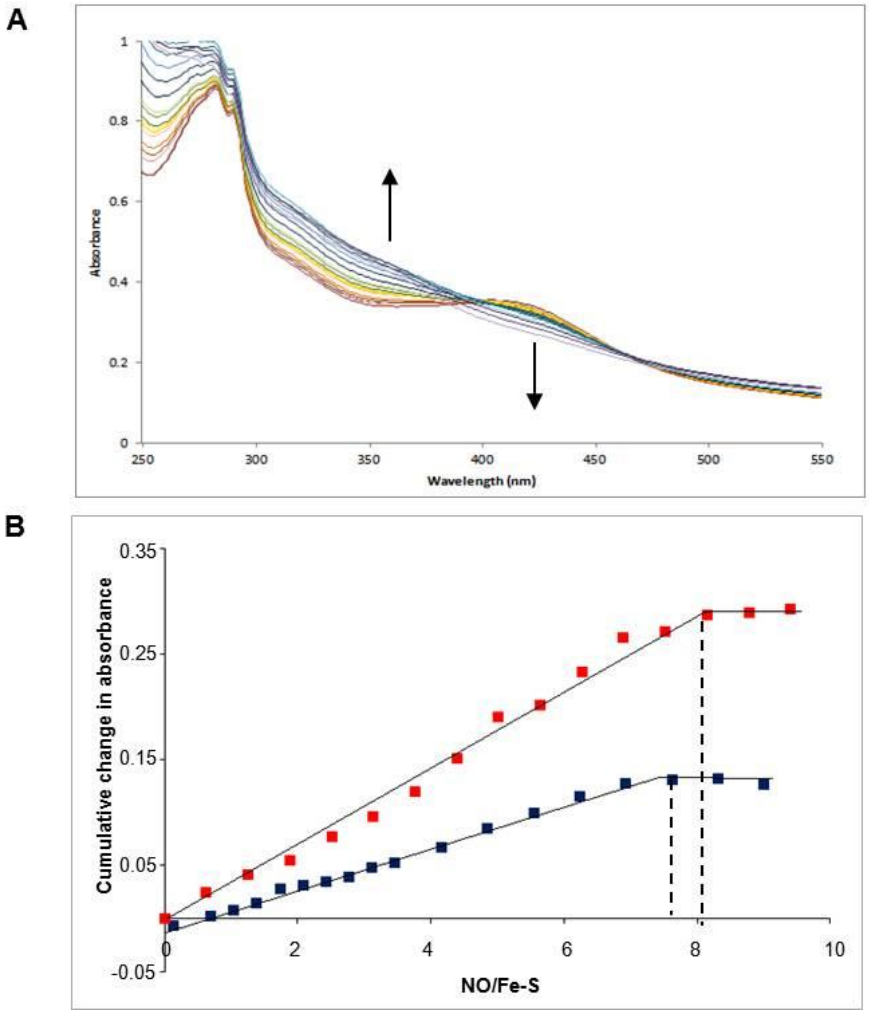

Figure 4.5: Stoichiometry of the reaction of Holo-WhiB1 with nitric oxide. (A) Reconstituted WhiB1 (19 µM cluster) was exposed to increasing amounts of Proli NONOate (0-90 µM in 10 µM increments) under anaerobic conditions. UV-visible spectra were obtained 10 minutes after each addition. The arrows indicate the decrease in absorbance at 420 nm and the increase in absorbance at 355 nm as the concentration of nitric oxide increased. **(B)** The cumulative changes in absorbance at 355 nm (corresponding to the formation of nitrosylated WhiB1) from two representative titrations. The dilution associated with each addition of Proli NONOate was taken into account. These values were plotted against the total nitric oxide added (µM; correction factor applied) divided by the initial concentration of iron-sulphur cluster (µM). The dashed vertical lines indicate the points at which further addition of NONOate failed to change the absorbance at 355 nm.

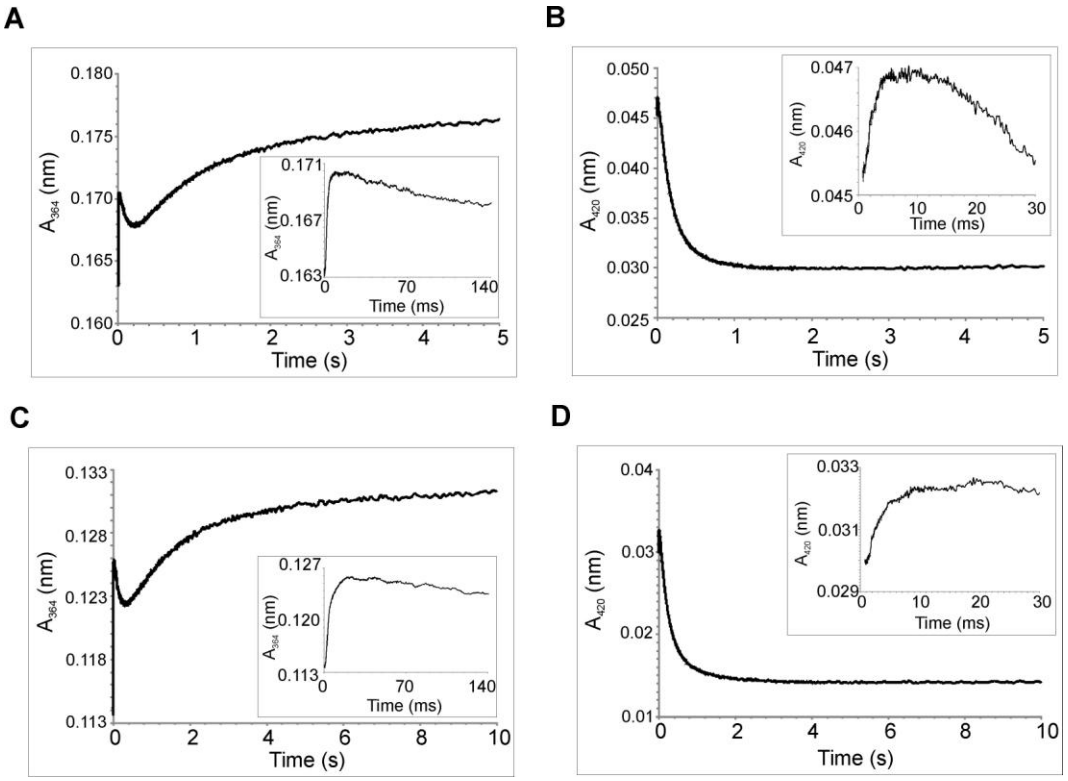

Figure 4.6: Stopped-flow kinetics of holo-WhiB1 nitrosylation. Holo-WhiB1 (7 μM [4Fe-4S]) in the presence of 643 μM nitric oxide, giving a [nitric oxide]:[4Fe-4S] ratio of ~92, was measured at 364 nm **(A)** and 420 nm **(B)**. Holo-WhiB1 (7 μM [4Fe-4S]) in the presence of 300 μM nitric oxide, giving a [nitric oxide]:[4Fe-4S] ratio of ~43, was measured at 364 nm **(C)** and 420 nm **(D)**. Inserts show early events in the reaction time course. Crack *et al*. (2011).

and multiphasic, with reaction completion in 5 seconds for the addition of 643 µM nitric oxide and 10 seconds for the addition of 300 µM (Figure 4.6).

4.3.5 Kinetic analysis

The reaction of the [4Fe-4S] cluster of WhiB1 with nitric oxide was modelled using the reaction below, based on that of Sutton *et al*., (2004) for FNR and oxygen.

$$\text{nitric oxide} + \text{WhiB1} \underset{k_{-1}}{\overset{k_1}{\rightleftarrows}} \text{nitric oxide.WhiB1} \xrightarrow{k_2} \text{Product}$$

Three distinct phases were observed at both wavelengths (364 and 420 nm), suggesting a three step reaction A→B→C→D. The data were fitted separately, and together, under pseudo-first order conditions to exponential function: $y = y_0 + (y_{max} - y_0)(1 - e^{[-kobs \,.\, x]})$, by computing fits for the parameters y_0, k_{obs} and y_{max} (Sutton *et al*., 2004). Curve fitting was carried out by Dr Jason Crack and described in Crack *et al*. (2011). Each absorbance data set (364 nm and 420 nm) gave similar rate constants for the initial, rapid phase and final, slower phase of the reaction of holo-WhiB1 with nitric oxide. The intermediate phase however, had different characteristics at 364 nm compared to 420 nm, indicating that these two wavelengths report different processes in the intermediate part of the reaction. Thus the overall reaction was modelled as a four-step reaction: A→B→C→D→E, where the initial and final steps (A→B and D→E) are detected at both wavelengths, and steps B→C and C→D are detected at 364 nm and 420 nm respectively (Crack *et al*., 2011).

Similar observations were made with WhiD from *S. coelicolor* as reported in Crack *et al*. (2011). Plots of the observed pseudo-first order rate constants (k_{obs}) against nitric oxide concentration for the reaction with WhiD were linear for each step, indicating a first order dependence on nitric oxide (Figure 4.7, blue lines; Crack *et al*., 2011). Using this information, the data for WhiB1 at the two nitric oxide concentrations also suggests a linear relationship between k_{obs} and nitric oxide concentration (Figure 4.7, red lines; Crack *et al*., 2011). The rate constants (from the linear fits in Figure 4.7) for the reaction of holo-WhiB1 with nitric oxide are summarised below.

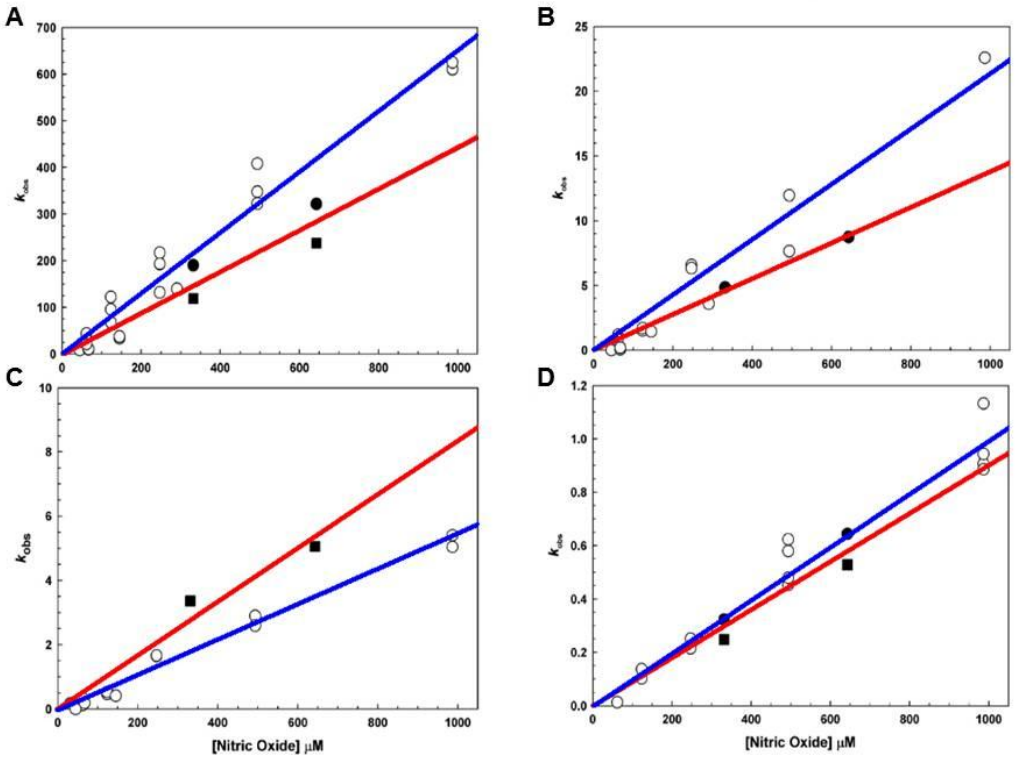

Figure 4.7: Kinetic dependencies of the nitrosylation reaction on nitric oxide concentration. Multiphase kinetics were observed for the reactions of both holo-WhiB1 and holo-WhiD with NO over a range of concentrations (under pseudofirst-order conditions) at both $A_{364\ nm}$ and $A_{420\ nm}$. The observed rate constants (k_{obs}) are plotted as a function of NO concentration. Panels A-D correspond to steps 1-4, respectively, of the four-step mechanism. k_{obs} corresponds to $A_{364\ nm}$ (●) and $A_{420\ nm}$ (■) for WhiB1. Least-square linear fits of the data are shown (red lines), the gradient of which corresponds to the apparent second-order rate constant. Data for WhiD (○) are plotted for comparison with least-square linear fits (blue lines). Figure and legend adapted from Crack *et al*. (2011).

Reaction Step	Rate constant ($M^{-1}s^{-1}$)
A→B	(4.40 ± 0.44) X 10^5
B→C	(1.38 ± 0.04) X 10^4
C→D	(8.34 ± 0.93) X 10^3
D→E	(0.90 ± 0.06) X 10^3

4.3.6 Conformational changes in WhiB1 upon exposure to nitric oxide

The oligomeric state of both apo- and holo-WhiB1 was analysed using gel filtration as described in Section 3.4.3. Holo-WhiB1 (50 μM) after treatment with 1 mM Proli NONOate was also analysed as described in Section 2.5.10. Holo-WhiB1 was seen as a monomer with a symmetrical peak (Figure 3.10) corresponding to a molecular weight of ~12.5 kDa, when compared to a standard curve (Figure 3.9B). Holo-WhiB1 after treatment with Proli NONOate eluted as an asymmetrical peak, with a shoulder (Figure 4.8). The peak corresponded to ~715 seconds and the shoulder to ~700 seconds elution time. When used to determine the molecular weights using the standard curve (Figure 3.9B), the peak gave a molecular weight of ~12.5 kDa as for holo-WhiB1 (actual molecular weight 12.876 kDa) and the shoulder ~15.8 kDa. This data shows that reaction of the iron-sulphur cluster of WhiB1 with nitric oxide causes a conformational change in the protein structure with a subsequent change in its gel filtration elution profile.

4.3.7 Stability of the nitrosylated form of WhiB1

The reaction of holo-WhiB1 with nitric oxide leads to the formation of a nitrosylated iron-sulphur cluster. To determine whether this form of WhiB1 is stable or dissociates quickly to yield apo-WhiB1, UV-visible spectroscopy was carried out. Under anaerobic conditions holo-WhiB1 (4.2 μM cluster), in 25 mM Tris buffer (pH 7.4) containing 0.5 M NaCl, 10% glycerol and 1 mM DTT, was analysed by UV-visible spectroscopy (Figure 4.9, red trace). It was then exposed to Proli NONOate (400 μM), yielding ~10 μM nitrosylated form which was unchanged after 2 hours (Figure 4.9, orange trace). The cuvette was then uncapped and the reaction exposed to air. Spectra were

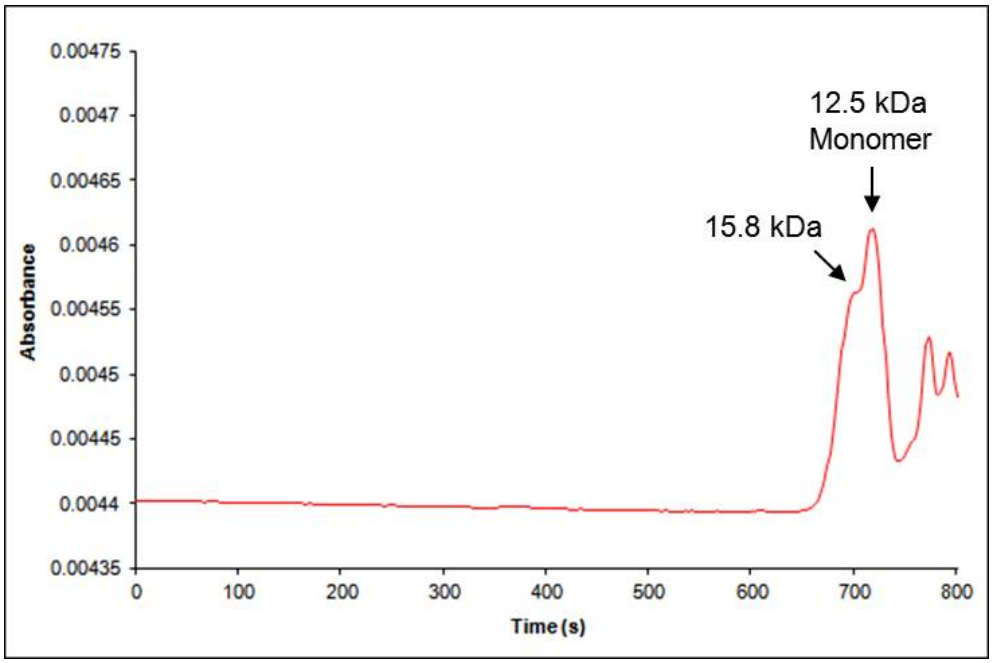

Figure 4.8: Gel filtration analysis of holo-WhiB1 and Proli NONOate. Holo-WhiB1 (50 µM) was exposed to 1 mM Proli NONOate. The peak corresponding to the WhiB1 monomer is indicated, along with the shoulder formed as a result of the conformational change in WhiB1 after reaction of its iron-sulphur cluster with nitric oxide.

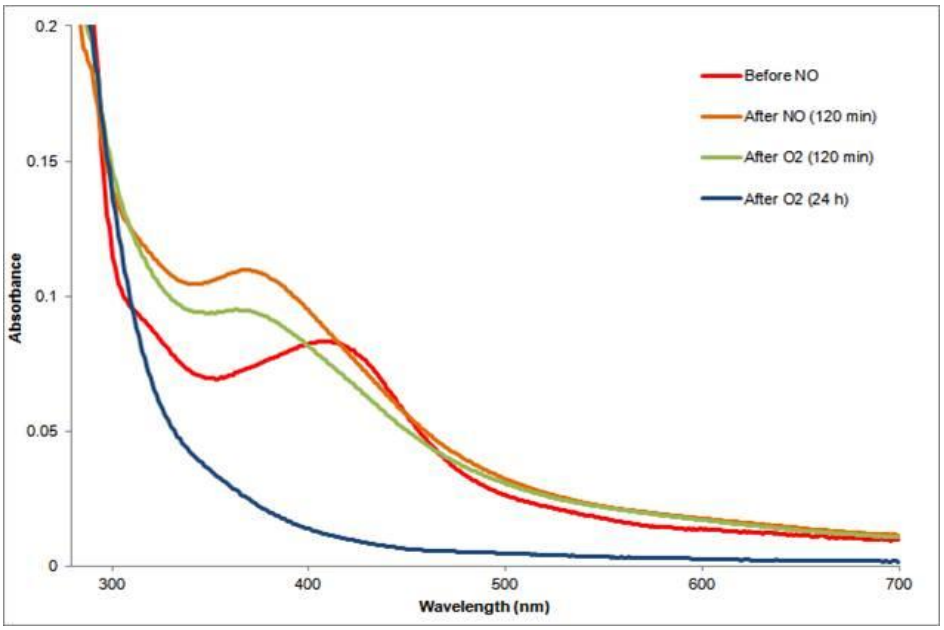

Figure 4.9: Stability of the nitrosylated form of WhiB1. UV-visible spectra were obtained for holo-WhiB1 (4.2 µM cluster) before and after exposure to 400 µM Proli NONOate in anaerobic conditions and in the presence of 1 mM DTT for 2 hours. This provided ~10 µM nitrosylated cluster which was unchanged in this time. The reaction was then exposed to air and spectra obtained after 2 and 24 hours.

taken after 2 hours (green line) and 24 hours (blue line). Introduction of oxygen caused the absorbance at 355 nm to decrease by ~20% after 2 hours and only after 24 hours was the nitrosylated form of WhiB1 fully degraded to apo-WhiB1. Thus the nitrosylated WhiB1 is a relatively stable form of the protein.

4.4 Protein disulphide reductase activity of WhiB1

To determine whether WhiB1 has general protein disulphide reductase activity, an insulin reduction assay was carried out as described in Section 2.5.12. The table below shows the results of the assays with increasing concentrations of apo-WhiB1, as well as holo-WhiB1 and nitric oxide-treated WhiB1 (exposed to 100 μM Proli NONOate) compared to *Escherichia coli* thioredoxin, a *bone fide* general protein disulphide reductase.

Protein	**Concentration (μM)**	**Rate (ΔA_{600} min^{-2})(x 10^{-3})**
None	-	0.07
Thioredoxin	2.5	1.30
Apo-WhiB1	5	0.10
Apo-WhiB1	10	0.43
Apo-WhiB1	20	0.45
Holo-WhiB1	5	0.07
Nitric oxide-treated apo-WhiB1	5	0.07
Nitric oxide-treated holo-WhiB1	5	0.02

Although increased insulin reduction was observed as the concentration of apo-WhiB1 increased, with 5 μM WhiB1 the rate of reaction was slow compared to that of a lower concentration of thioredoxin and were similar to that of the rate obtained where no protein was assayed. There was no significant reduction for holo-WhiB1 or nitric oxide-treated samples.

4.5 The DNA-binding properties of WhiB1

4.5.1 Apo-WhiB1 binds at its own promoter

Electromobility shift assays were carried out to determine whether WhiB1 was capable of binding to its own promoter DNA (P*whiB1*) as described in Section 2.7.3. Increasing concentrations of apo-WhiB1 and holo-WhiB1 (0, 5, 10, 20 and 50 μM) were incubated separately with ~2 nM radiolabelled P*whiB1* (Section 2.7.1) before separation of protein-DNA complexes from free P*whiB1* DNA. Figure 4.10 shows how apo-WhiB1, in the presence of a reducing agent, binds P*whiB1* (lanes 2-5). The smeared appearance of the EMSA at lower protein concentrations suggests that the complex is relatively unstable and dissociates during electrophoresis (Figure 4.10, lane 3). DNA-binding was inhibited by the presence of the [4Fe-4S] cluster in holo-WhiB1 (Figure 4.10, lanes 6-9). EMSAs were carried out by Dr M. Stapleton and are reported in Smith *et al*. (2010).

4.5.2 DNA-binding of holo-WhiB1 is restored by treatment with nitric oxide

Holo-WhiB1 does not bind to the *whiB1* promoter (Figure 4.10), indicating that the presence of the [4Fe-4S] cluster inhibits DNA-binding. Electromobility shift assays (Section 2.7.3) were carried out on nitric oxide-treated holo-WhiB1 with P*whiB1* to determine whether nitrosylation of the cluster would allow DNA-binding. Increasing concentrations of holo-WhiB1 (0, 5, 10, 20 and 50 μM) were treated with a 20-fold molar excess of Proli NONOate for 1 minute at room temperature before incubation with ~2 nM radiolabelled P*whiB1* (Section 2.7.1). Protein-DNA complexes were then separated from free P*whiB1* DNA by electrophoresis. Figure 4.11A shows how nitric oxide-treated holo-WhiB1 binds to the *whiB1* promoter (lanes 2-5 and 7-10). In the absence of additional reducing agent (30 mM DTT), nitric oxide-treated holo-WhiB1 formed a second retarded species of lower mobility (Figure 4.11A, lane 5). This species was absent in the presence of increased reducing agent (Figure 4.11A, lanes 9 and 10). Reconstitution of the cluster following nitric oxide-treatment then abolished DNA-binding (not shown). EMSAs were performed by Dr M. Stapleton and are reported in Smith *et al*. (2010).

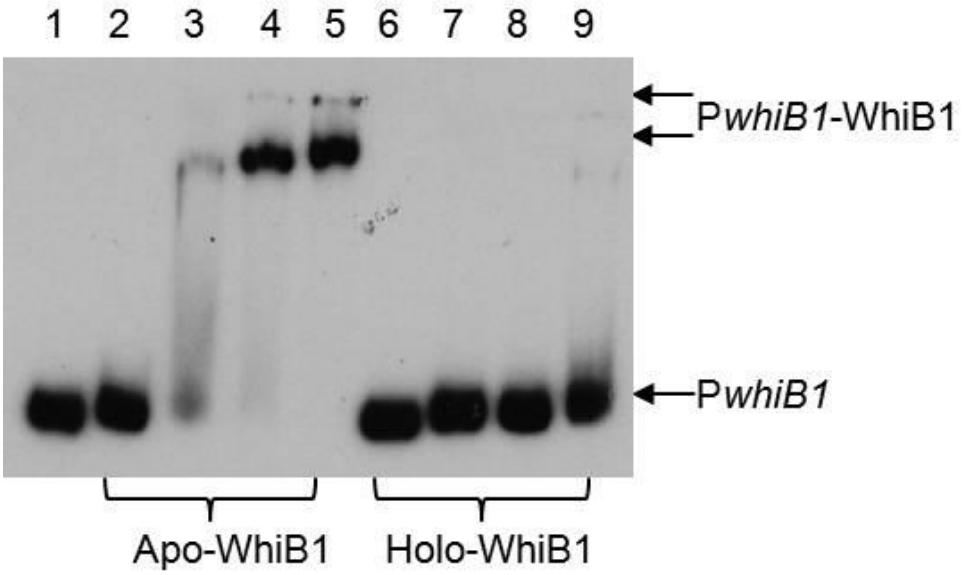

Figure 4.10: Binding of WhiB1 at the *whiB1* promoter (P*whiB1*) region. Radiolabelled P*whiB1* was incubated with increasing concentrations of apo- or holo-WhiB1 as indicated before separation of protein-DNA complexes (P*whiB1*-WhiB1) from free DNA (P*whiB1*) by electrophoresis. Lane 1, no protein; lanes 2-5 and 6-9 contain, 5, 10, 20 and 50 μM WhiB1 respectively. The locations of P*whiB1* and P*whiB1*-WhiB1 are indicated. EMSAs were carried out by Dr M. Stapleton (Smith *et al*., 2010).

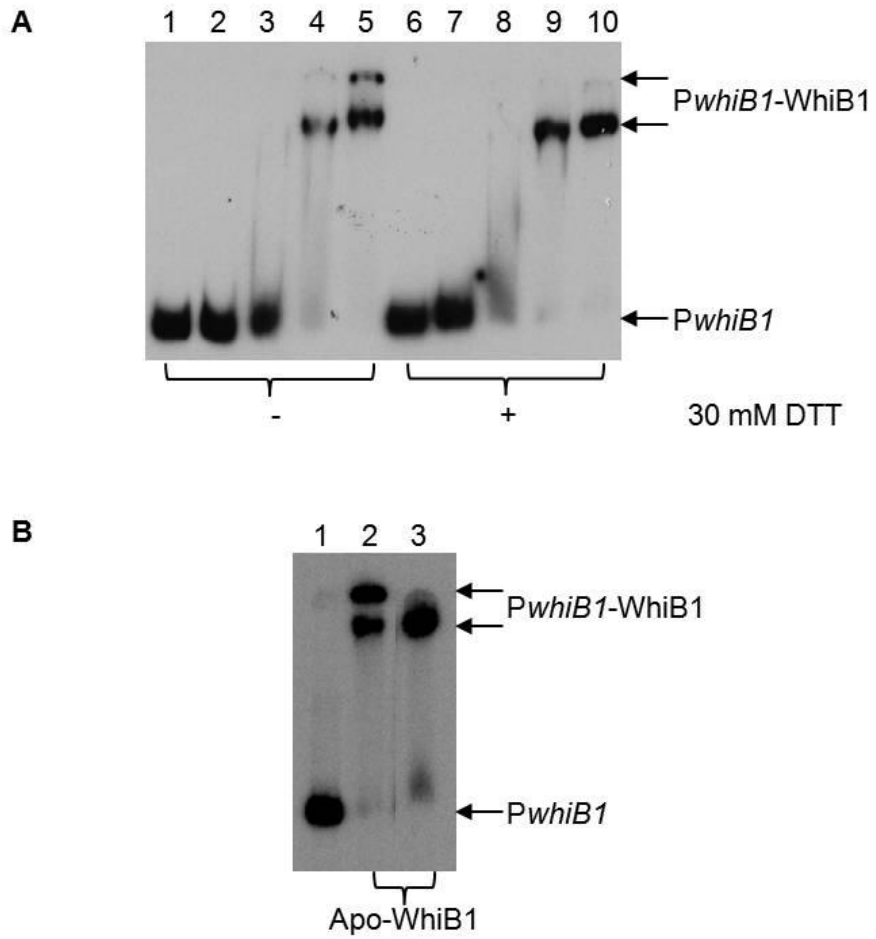

Figure 4.11: Effect of nitric oxide treatment and oxidation state on DNA-binding by WhiB1. (A) Treatment of holo-WhiB1 with nitric oxide permits binding to P*whiB1*. A 10-fold molar excess of Proli NONOate was added to increasing concentrations of holo-WhiB1. After incubation for 1 minute at room temperature, an aliquot was removed and DTT added to a final concentration of 30 mM. After further incubation for 3 minutes at room temperature, P*whiB1*-WhiB1 complexes were separated from P*whiB1* by electrophoresis. Lanes 1 and 6, no protein; lanes 2-5 and 7-10 contain, 5, 10, 20 and 50 μM WhiB1 respectively. The locations of P*whiB1* and P*whiB1*-WhiB1 complexes are indicated. **(B) Oxidation of WhiB1 results in formation of a second retarded species.** Radiolabelled P*whiB1* was incubated with apo-WhiB1 before separation of protein-DNA complexes (P*whiB1*-WhiB1) from free DNA (P*whiB1*) by electrophoresis. Lane 1, no protein; lane 2, 20 μM apo-WhiB1 pre-treated with 5 mM diamide, lane 3, 20 μM apo-WhiB1 pre-treated with 1 mM DTT. The locations of P*whiB1* and P*whiB1*-WhiB1 are indicated. EMSAs were carried out by Dr M. Stapleton (Smith *et al*., 2010).

4.5.3 DNA-binding is affected by the oxidation state of WhiB1

As discussed in Section 4.5.2, in the absence of additional reducing agent a second retarded species of lower mobility was seen upon binding of nitric oxide-treated holo-WhiB1 to P*whiB1* (Figure 4.11A, lane 5). Apo-WhiB1 was therefore also analysed to determine whether a similar species would be seen in its oxidised state. Apo-WhiB1 (20 μM) was pre-treated with either the oxidising agent diamide (5 mM) or the reducing agent DTT (1 mM) and incubated with ~2 nM radiolabelled P*whiB1* (Section 2.7.1). Protein-DNA complexes were then separated from free P*whiB1* DNA by electrophoresis (Section 2.7.3). Figure 4.11B shows how oxidised apo-WhiB1 showed two retarded species compared to one for reduced apo-WhiB1 (compare lanes 2 and 3). EMSAs were carried out by Dr M. Stapleton and reported in Smith *et al*. (2010).

4.5.4 DNA-binding of WhiB1 is specific

The specificity of DNA-binding of WhiB1 was determined by carrying out EMSAs with various promoters and by competition assays. Apo-WhiB1 was unable to bind to *rpfA, ahpC* and Rv*3616c* promoter DNA (Smith *et al*., 2010; Stapleton *et al*., 2012). Competition electromobility shift assays were carried out to further demonstrate the specificity of DNA-binding of WhiB1 to its own promoter. Apo-WhiB1 (20 μM) was incubated with ~2 nM radiolabelled P*whiB1* (Section 2.7.1) and a 100-fold excess of unlabelled P*whiB1* or P*rpfA* DNA. Protein-DNA complexes were then separated from free DNA by electrophoresis (Section 2.7.3). Addition of unlabelled P*whiB1* inhibited binding of both reduced (Figure 4.12A, compare lanes 2 and 3) and oxidised (Figure 4.12B, compare lanes 2 and 3) apo-WhiB1 to radiolabelled P*whiB1*. A 100-fold excess of unlabelled P*rpfA* however, did not affect binding (Figure 4.12A and B, compare lanes 2 and 4). The DNA-binding ability of apo-WhiB1 is thus specific to its promoter (P*whiB1*) in both its oxidised and reduced forms. EMSAs were carried out by Dr M. Stapleton and reported in Smith *et al*. (2010).

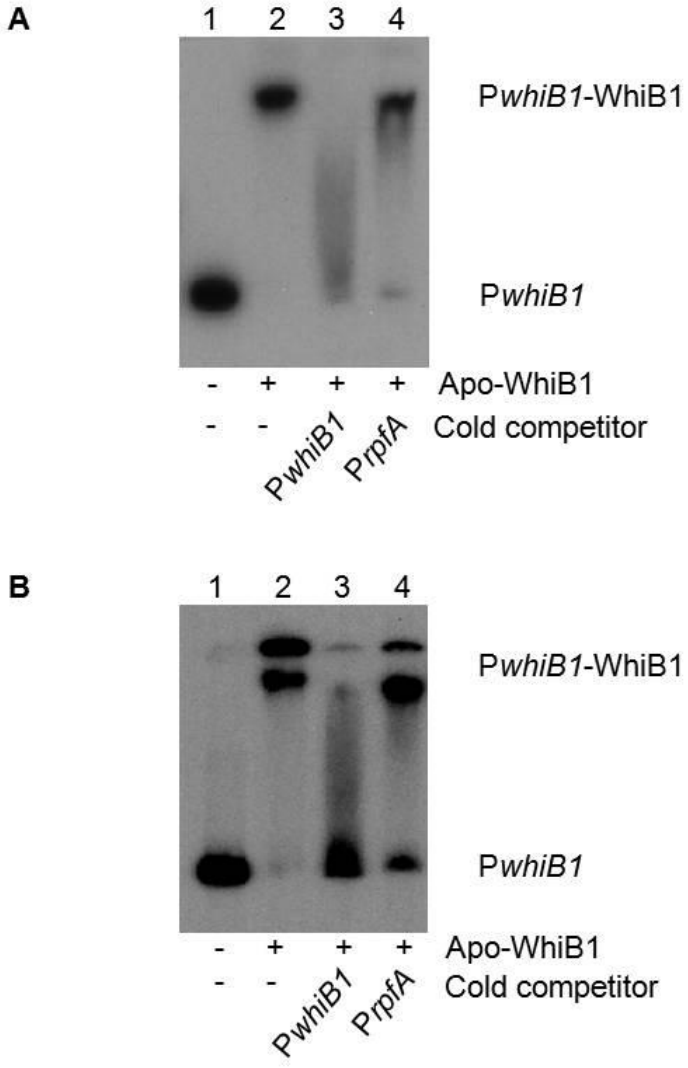

Figure 4.12: DNA-binding by WhiB1 is specific. (A) DNA-binding of apo-WhiB1 in reducing conditions is specific to the *whiB1* promoter. Binding of 20 μM apo-WhiB1 in the presence of 1 mM DTT to radiolabelled P*whiB1* (lane 2) was challenged by the presence of a 100-fold excess of unlabelled P*whiB1* DNA (lane 3) or a 100-fold excess of unlabelled P*rpfA* DNA (lane 4). Lane 1 contains no protein. The locations of P*whiB1* and P*whiB1*-WhiB1 complexes are indicated **(B) DNA-binding of apo-WhiB1 in oxidising conditions is also specific to the *whiB1* promoter.** Binding of oxidised apo-WhiB1 (20 μM, pre-treated with 5 mM diamide) to radiolabelled P*whiB1* (lane 2) was challenged by the presence of a 100-fold excess of unlabelled P*whiB1* DNA (lane 3) or a 100-fold excess of unlabelled P*rpfA* DNA (lane 4). Lane 1 contains no protein. The locations of P*whiB1* and P*whiB1*-WhiB1 complexes are indicated. EMSAs were carried out by Dr M. Stapleton (Smith *et al*., 2010).

4.5.5 DNase footprinting of WhiB1 at P*whiB1*

Apo-WhiB1 binds to its own promoter (P*whiB1*). To identify the binding site, DNase I footprinting was carried out as described in Section 2.7.4. Increasing concentrations of apo-WhiB1 (0, 5, 10, 20 μM) were incubated with radiolabelled P*whiB1* before digestion with DNase I and separation of fragments by electrophoresis. A Maxam and Gilbert G track was prepared as described in Section 2.7.5 and run alongside the samples to allow sequence analysis. A distinctive DNAse I cleavage pattern was seen, showing a protected region located at -40 to -3 relative to the transcript start site (Figure 4.13, region labelled W). The footprint also exhibited several hypersensitive sites, suggesting that apo-WhiB1 causes significant distortion of P*whiB1* upon binding (Figure 4.13). DNase footprinting was carried out by Dr M. Stapleton and is reported in Smith *et al*. (2010).

4.6 Discussion

As previously shown in Chapter 3, WhiB1 incorporates a [4Fe-4S] cluster. Iron-sulphur clusters are intrinsically sensitive to oxygen, and thus holo-WhiB1 was exposed to oxygen to determine whether the cluster reacts to form apo-WhiB1. Purification of WhiB1 produces protein containing either a [4Fe-4S] or [2Fe-2S] cluster or protein in its apo-form (Figure 3.3). Upon prolonged exposure to oxygen after purification, the clusters disassemble forming apo-WhiB1. This indicates that the cluster of WhiB1 is relatively stable. Reconstituted WhiB1, containing a [4Fe-4S] cluster (10 μM), was exposed to an 11-fold molar excess of oxygen and the absorbance measured in the presence of 1 mM DTT (Figure 4.1). After 120 minutes, there was very little change in absorbance at 420 nm, indicating the [4Fe-4S] cluster was still present and not sensitive to oxygen in this time. After ~24 hours plus, the cluster disassembled to apo-WhiB1. There was no sign of changes in the absorbance spectrum indicating the formation of an intermediate [2Fe-2S] cluster in the reaction with oxygen. It is therefore thought that the [2Fe-2S] cluster containing WhiB1 seen in purification is due to partial iron-incorporation, and not a degradation product of the reaction of the [4Fe-4S] cluster of WhiB1 with oxygen. The slow rate of the reaction shows that the iron-sulphur cluster of WhiB1 is relatively stable in the presence of oxygen, in comparison to the rapid reaction of the iron-sulphur cluster of the known oxygen sensor, FNR of *Escherichia coli* (Crack

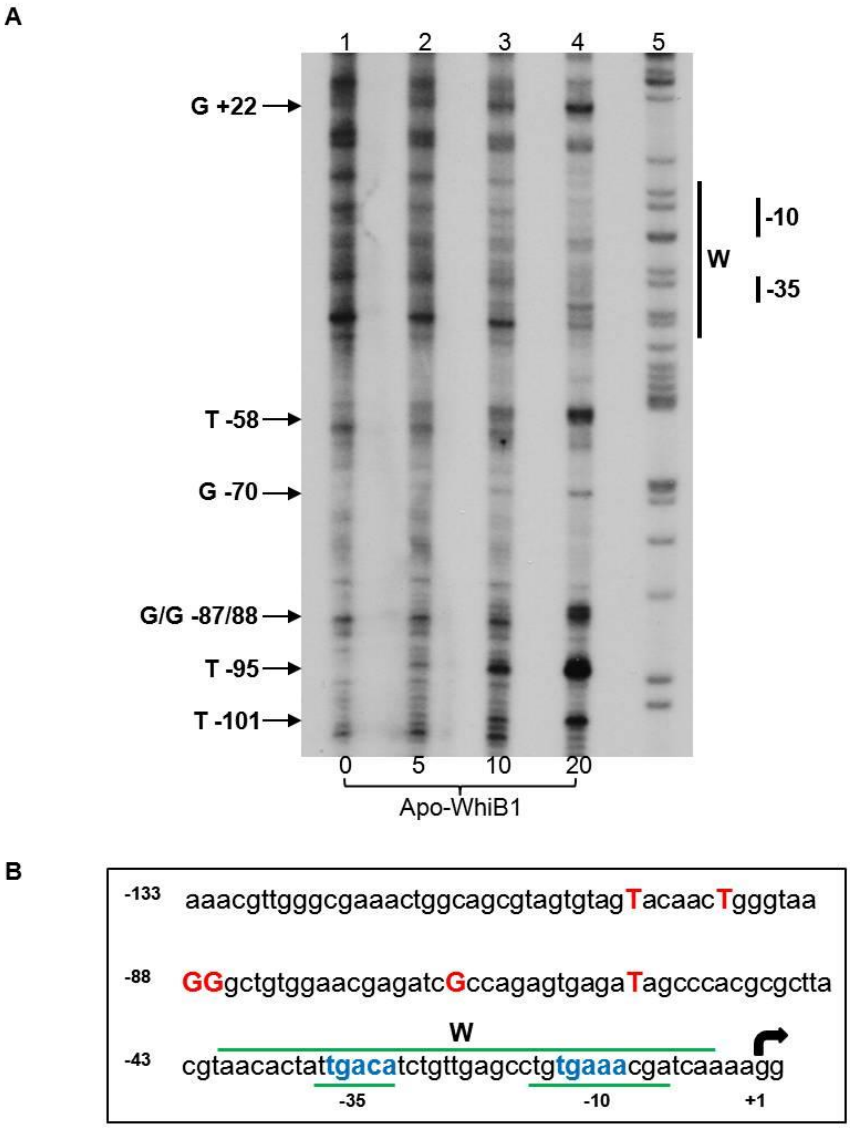

Figure 4.13: Binding of apo-WhiB1 at the *whiB1* promoter region. (A) DNase I footprint of apo-WhiB1 at P*whiB1*. Apo-WhiB1 was incubated with P*whiB1* before DNase I digestion. Hypersensitive sites associated with interaction with apo-WhiB1 are indicated with arrows; numbering is relative to the transcriptional start site. The location of apo-WhiB1 interaction (W) is indicated, as well as the -10 and -35 elements. Lane1 1, no protein; lanes 2-4, 5, 10 and 20 μM apo-WhiB1; lanes 5, Maxam and Gilbert G track. **(B) Nucleotide sequence of P*whiB1*.** Important features highlighted are; the transcript start site (+1, block arrow), -10 and -35 elements (underlined), the hypersensitive sites that characterise interaction with apo-WhiB1 (red), the location of the protected region (W, overlined), and two related DNA sequences within the protected region (blue). Footprinting was carried out by Dr M. Stapleton (Smith *et al*., 2010).

et al., 2004). As shown in Chapter 3 (Figure 3.7), the CD spectrum of the oxygen-insensitive iron-sulphur cluster of WhiB1 is very different to the oxygen-sensitive iron-sulphur cluster of FNR. This difference in cluster environment may contribute to the oxygen stability of the WhiB1 cluster.

The reaction of other Wbl proteins with oxygen has also been analysed. WhiD from *Streptomyces coelicolor* was refolded from inclusion bodies and the [4Fe-4S] cluster reconstituted. Upon oxygen exposure, changes in absorption spectra were consistent with formation of a [2Fe-2S] cluster after 50 minutes and an apo-protein after a subsequent 100 minutes (Jakimowicz *et al*., 2005). The rate of the reaction was dependent on the degree of oxygen exposure and the presence of DTT, whereby the first stage of the reaction, the change in [4Fe-4S] to [2Fe-2S], was faster in the absence of DTT (Jakimowicz *et al*., 2005). A similar reaction profile and rate was seen for the reaction of holo-WhiB3 from *M. tuberculosis* with oxygen, with a 75% cluster loss in 180 minutes (Singh *et al*., 2007). The reaction of holo-WhiB4 from *M. tuberculosis* and oxygen, again showed a similar reaction profile but with a slower rate of change over ~84 hours (Alam *et al*., 2007). This reaction was carried out in the presence of DTT because omission of the reducing agent led to precipitation, which is similar to our observations for WhiB1. Although the reaction of WhiD and WhiB3 with oxygen are quicker than that of WhiB1, the rates of reaction are still relatively slow. The clusters of WhiB3, WhiB4 and WhiD all react with oxygen through a [2Fe-2S] intermediate. Interestingly, similar to the reaction profile for WhiB1, WhiD purified with a [4Fe-4S] cluster (native-WhiD) reacts with oxygen to form apo-WhiD with no [2Fe-2S] intermediate (Crack *et al*., 2009). This reaction was still faster than that for WhiB1, with full cluster disassembly in 120 minutes (Crack *et al*., 2009). The difference in the reaction profiles of protein refolded from inclusion bodies (WhiB3, WhiB4 and WhiD) compared to that of protein purified in a soluble form (WhiB1 and native-WhiD) may highlight that small changes in protein fold due to refolding from inclusion bodies, affects the environment around the cluster and subsequently its interaction with molecular oxygen.

As the iron-sulphur cluster of WhiB1 was shown to be relatively oxygen stable, its sensitivity to nitric oxide was then analysed. Nitric oxide is a key component of the host response to *M. tuberculosis* infection, and to mount an effective response against it, bacteria must reprogram gene expression. This reprogramming of gene expression is

likely to involve the upregulation of nitric oxide detoxification systems. *Mycobacterium tuberculosis* is capable of detoxifying nitric oxide by its oxidation with haem-bound oxygen via the truncated haemoglobin trHbN, yielding nitrate ion (Couture *et al*., 1999; Ouellet *et al*., 2002; Pathania *et al*., 2002). This detoxification system is likely to be sufficient for detoxification of endogenous nitric oxide, produced by nitrite reduction by the Nar nitrate reductase system in *M. tuberculosis*. The Nar system is upregulated in hypoxic conditions to allow the reduction of nitrate to nitrite (Sohaskey and Wayne, 2003), however nitric oxide can be produced if nitrite is then reduced. The increase in exogenous nitric oxide experienced by *M. tuberculosis* during infection, may saturate the detoxification systems. Nitric oxide sensing transcription factors may therefore play an important role in *M. tuberculosis* survival. There are a number of bacterial nitric oxide sensing regulators that serve in this role, including a number of iron-sulphur containing proteins. FNR, Iron-regulatory protein-1 (IRP1), NsrR, SoxR and WhiB3 are all examples of nitric oxide sensitive transcription factors (Cruz-Ramos *et al*., 2002; Ding and Demple, 2007; Kennedy *et al*., 1997; Spiro, 2007; Tucker *et al*., 2008; Wardrop *et al*., 2000). The reaction of nitric oxide with the iron-sulphur clusters of these regulators causes conformational changes which then have effects on their function. The iron-sulphur cluster of FNR reacts with nitric oxide to form a dinitrosyl-iron complex (DNIC), and this form of FNR is incapable of binding DNA (Cruz-Ramos *et al*., 2002). A similar finding for the nitrosylation of the [2Fe-2S] cluster of NsrR, causing inactivation of the protein, is seen (Tucker *et al*., 2008). In contrast, reaction of nitric oxide with the [2Fe-2S] cluster of SoxR forming a DNIC, activates the protein (Ding and Demple, 2000). The apo-forms of WhiB3 and IRP1 are capable of binding DNA and mRNA respectively, both of their iron-sulphur clusters react with nitric oxide forming DNIC compounds (Kennedy *et al*., 1997; Singh *et al*., 2007). In the case of IRP1, exposure to nitric oxide activates mRNA binding by promoting cluster disassembly (Wardrop *et al*., 2000). Characterisation of the reaction of holo-WhiB1 with nitric oxide detailed here showed a rapid reaction which then had an effect on protein function.

Initial UV-visible spectroscopic tests with holo-WhiB1 and Proli NONOate, a rapid nitric oxide releaser, showed a change in the absorbance spectrum (Figure 4.2). The peak at 420 nm, corresponding to the [4Fe-4S] cluster, was replaced with a shoulder at 350-360 nm. Absorbance at this wavelength is attributed to nitrosylated iron-sulphur clusters, thus the cluster of WhiB1 reacts with nitric oxide. Nitrosylated iron-sulphur

clusters that absorb at this wavelength can be found in two forms; dinitrosyl iron complexes (DNICs) and tetranitrosylated iron complexes (also known as Roussin's red esters - RREs) (Figure 4.3). To determine which of these species is formed, electron paramagnetic spectroscopy (EPR) was carried out as the DNICs are EPR active with characteristic EPR spectra, whereas RREs are EPR silent. Results showed the presence of DNIC species after the reaction of holo-WhiB1 with nitric oxide, corresponding to 10% of the total iron content after 10 minutes, falling to 4% after 2 hours (Figure 4.4). This may indicate that the remaining iron is present as RREs. Taken with the UV-visible spectroscopic analysis, to which both dinitrosyl and tetranitrosyl iron complexes contribute, the EPR data suggests a mixture is present with the EPR silent RREs the major species. The iron-sulphur cluster of WhiB3 has been shown to be a nitric oxide sensitive also, forming DNIC compounds identified by EPR analysis (Singh *et al*., 2007).

The reaction of holo-WhiB1 with nitric oxide was further analysed to understand the reaction mechanism. Titrating increasing amounts of nitric oxide against holo-WhiB1 and monitoring the change in absorbance showed 8 nitric oxide molecules reacted with each [4Fe-4S] cluster (Figure 4.5). Similar findings were seen for WhiD from *S. coelicolor* (Crack *et al*., 2011). The spectral properties of the product and the stoichiometry are consistent with the formation of two RREs per holo-WhiB1. Accordingly, using the molar absorption coefficient of tetranitrosylated clusters, determined by Cruz-Ramos *et al*. (~8500 $M^{-1}cm^{-1}$) (Cruz-Ramos *et al*., 2002), the absorbance increase at 360 nm upon the completion of the titration was equivalent to the formation of ~2.5 RREs (Smith *et al*., 2010). As discussed in Crack *et al*. (2011), DFT (Density Functional Theory) was used to calculate the possibility of two RREs being present after reaction of nitric oxide with the iron-sulphur clusters of WhiB1 and WhiD. These calculations suggested the possibility of a novel octa-nitrosylated cluster, $[4Fe^{I}_{4}(NO)_{8}\text{-}(S\text{-}cys)_{4}]^{0}$, being formed in the protein cavity from the dimerisation of two RREs (Figure 4.14; Crack *et al*., 2011). The formation of such an octa-nitrosylated species would entail a rearrangement of the iron positions relative to cysteine thiols (Crack *et al*., 2011). This would lead to conformational changes, as indicated by gel filtration analysis for WhiB1 (Section 4.3.6), which may allow a switch in the DNA-binding properties of Wbl proteins (Singh *et al*., 2007; 2009; Smith *et al*., 2010). The nitrosylated iron-sulphur cluster was a stable product under anaerobic conditions, but

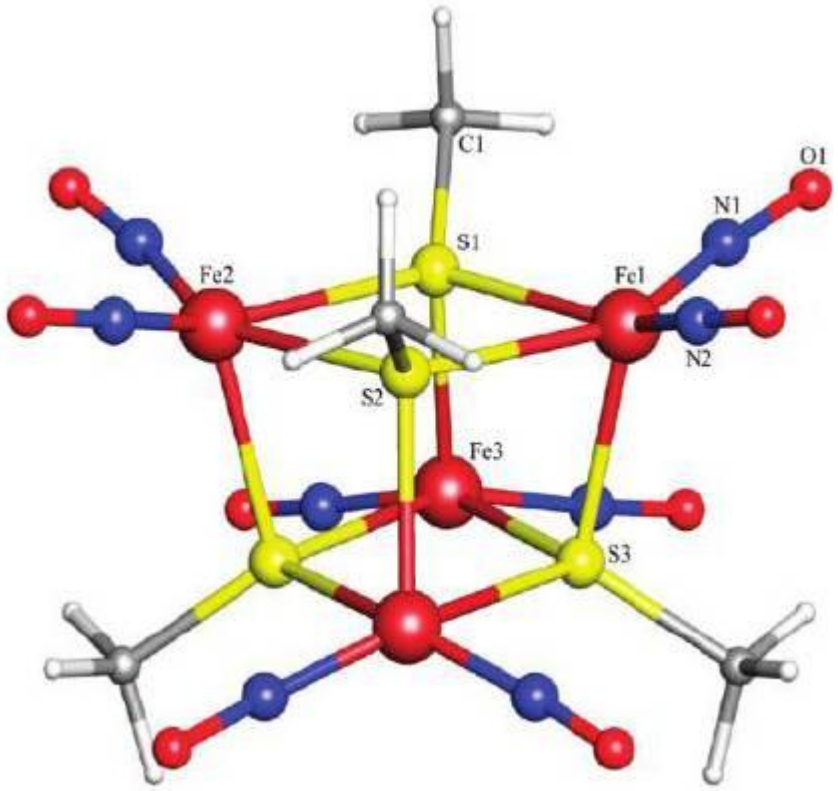

Figure 4.14: Model depicting the proposed octa-nitrosylated cluster resulting from nitrosylation of the [4Fe-4S] cluster of Wbl proteins. DFT calculations suggest the formation of this cluster from the dimerisation of two RREs for WhiB1 and WhiD. Figure is adapted from Crack *et al*. (2011).

was slowly degraded upon exposure to oxygen (Figure 4.9; Section 4.3.6). Similar findings were seen for nitrosylated WhiD (Crack *et al*., 2011).

Another interesting feature of the reaction of holo-WhiB1 with nitric oxide, is the speed of the reaction. Unlike the reaction with oxygen, the iron-sulphur cluster of WhiB1 reacts with 8 nitric oxide molecules extremely rapidly in a complex multiphasic reaction (Crack *et al*., 2011). As discussed in Section 4.3.5, the reaction of the iron-sulphur cluster with nitric oxide proceeds in a four step mechanism. There is little known about how the protein environment can regulate the relative rates of attack of nitric oxide and other diatomic molecules on the specific sites of iron-sulphur clusters. The mechanism by which nitric oxide reacts with the iron-sulphur clusters of both WhiB1 and WhiD provides new insight. The first step of the reaction (A→B) was detected at both wavelengths (420 nm; monitoring [4Fe-4S] cluster loss and 364 nm; monitoring nitrosylated cluster appearance) and is first order with respect to nitric oxide. This is the fastest step of the reaction (Section 4.3.5) and is very likely to be the binding of one nitric oxide molecule to the cluster. This increases the accessibility for further nitric oxide-binding in steps B→C (detected at 364 nm) and C→D (detected at 420 nm) (Crack *et al*., 2011). These steps are both first order with respect to nitric oxide also, and it is thought that this indicates either a single nitric oxide is involved in each step, or that nitric oxide binding to different irons of the cluster occurs independently. Fluorescence titration data of the reaction of WhiD with nitric oxide suggests the formation of a stable intermediate with a stoichiometry of 4 nitric oxide:1 [4Fe-4S] cluster (Crack *et al*., 2011). Intermediate D therefore appears to be a tetranitrosylated cluster, indicating that in steps B→C and C→D, there is binding of one or two nitric oxide molecules. The last step of the reaction, D→E (detected at both wavelengths) was again first order, leading to the formation of the octa-nitrosylated cluster (Crack *et al*., 2011).

The findings discussed here on the reaction of nitric oxide with the iron-sulphur cluster of WhiB1, and those also seen for WhiD, have provided a detailed insight into the mechanism of the reaction (Crack *et al*., 2011; Smith *et al*., 2010). The effects of nitric oxide on the function of WhiB1 were then analysed.

Wbl proteins have long been considered to function as DNA-binding transcription factors, and evidence of this has recently been obtained for WhiB1, WhiB2 and WhiB3

from *M. tuberculosis* as well as the WhiBTM4 protein from mycobacteriophage TM4 (Rybniker *et al*., 2010; Singh *et al*., 2009; Smith *et al*., 2010). WhiB2 was capable of binding to its own promoter, as seen here for WhiB1 (Rybniker *et al*., 2010). WhiBTM4 was also capable of binding to the *whiB2* promoter region, suggesting WhiB2 is capable of regulating its own expression and is inhibited by WhiBTM4 (Rybniker *et al*., 2010). WhiB3 was shown to bind to the promoter regions of two polyketide biosynthetic genes (*pks2* and *pks3*), and this was independent of the state of the iron-sulphur cluster (Singh *et al*., 2009). Recently, a number of Wbl proteins, including WhiB1, have been suggested to act as general protein disulphide reductases (Alam *et al*., 2007; 2009; Garg *et al*., 2007). Here, apo-WhiB1 was shown to have insignificant general protein disulphide reductase activity (Section 4.4). Similarly, protein disulphide reductase activity was not seen for WhiD from *S. coelicolor* (Crack *et al*., 2009). Results here indicate that WhiB1 is not a general protein disulphide reductase, although the propensity of apo-WhiB1 to form both intra- and inter-disulphide bonds (Chapter 3) suggests such redox chemistry is possible. It may require an as yet unidentified reductase and specific target proteins for reduction. In this context WhiB1 specifically interacts with and reduces disulphide bonds in the α(1,4)-glucan branching enzyme GlgB (Garg *et al*., 2009). Results presented here suggest WhiB1 to behave as a DNA-binding transcription factor, interacting with its own promoter. However, it is possible that WhiB1 is bi-functional, acting as both a gene regulator and a specific GlgB reductase.

The [4Fe-4S] cluster of WhiB1 reacts specifically and rapidly with nitric oxide to convert the protein from a non-DNA-binding protein to a form capable of binding to its own promoter. This suggests that WhiB1 may play a role in establishing *M. tuberculosis* infections by controlling gene expression in response to macrophage-generated or endogenous nitric oxide. Recent evidence has shown that *whiB1* expression was not directly affected by exogenous nitric oxide but was highly up-regulated by cAMP (Larsson *et al*., 2012). Previous studies have shown *whiB1* expression to be activated by intermediate levels (2.5 μM) of the cAMP receptor protein (CRP) Rv3676, and repressed by high levels (20 μM) of Rv3676 (Stapleton *et al*., 2010). *In vitro* transcription reactions with apo-WhiB1 and P*whiB1* in the absence of Rv3676 or in the presence of either intermediate or high concentrations of Rv3676, showed apo-WhiB1 always repressed its own transcription. This shows the inhibition is more severe than that mediated by high concentrations of Rv3676, and silences any Rv3676-dependent

activation of *whiB1* expression, at least *in vitro* (Smith *et al*., 2010). DNase I footprinting of apo-WhiB1 at the *whiB1* promoter showed a 37 bp protected region at -40 to -3, relative to the transcription start site, obscuring both the -35 and -10 elements (labelled W; Figure 4.13). This site was downstream of the Rv3676 activating site (centred at -58.5) and overlapped the repressing Rv3676 site (centred at -37.5) (Stapleton *et al*., 2010). The footprint was also characterised by hypersensitive sites which span a region too large for the binding of one apo-WhiB1 monomer, suggesting multiple apo-WhiB1 interactions (Figure 4.13). Based on the location of the protected site in the footprint, repression of transcription is likely to occur by apo-WhiB1 blocking RNA polymerase binding. As mentioned in Section 4.1, WhiB3 interacts with the sigma factor SigA (Steyn *et al*., 2002). Therefore it is also a possibility that WhiB1 interacts with SigA to repress *whiB1* transcription by inhibiting RNA polymerase activity, or by preventing RNA polymerase from accessing the promoter. What is clear is that there is a complex interplay between at least two regulators (WhiB1 and Rv3676) and their cognate signals (nitric oxide and cAMP) to control the expression of the essential *whiB1* gene. Further *in vivo* studies to establish the dynamics of WhiB1 and Rv3676 activities during infection should shed new light on this emerging regulatory partnership.

Upon infection of macrophages, mycobacterial-derived cAMP increases promoting bacterial survival by interfering with host signalling pathways (Agarwal *et al*., 2009). cAMP is also important in *M. tuberculosis* gene regulation, affecting the regulatory properties of the cAMP receptor proteins Rv3676 and Rv1675c (Gazdik and McDonough, 2005; Rickman *et al*., 2005; Stapleton *et al*., 2010). As discussed here, *whiB1* expression is under dual regulation of the cAMP-responsive Rv3676 protein and the nitric oxide-responsive WhiB1 protein. This regulation may provide a mechanism to integrate the transcriptional response to two signals, cAMP and nitric oxide, associated with infection (Figure 4.15; Smith *et al*., 2010). Although the detailed mechanism remains unknown, the data suggests that in the environment of the macrophage (high nitric oxide and cAMP levels) transcription of the essential transcription factor *whiB1* will be inhibited. This is consistent with entry of *M. tuberculosis* into the dormancy state. At low nitric oxide concentrations (related to the immunocompromised state), holo-WhiB1 is formed, de-repressing *whiB1* transcription, consistent with emergence from dormancy (Smith *et al*., 2010).

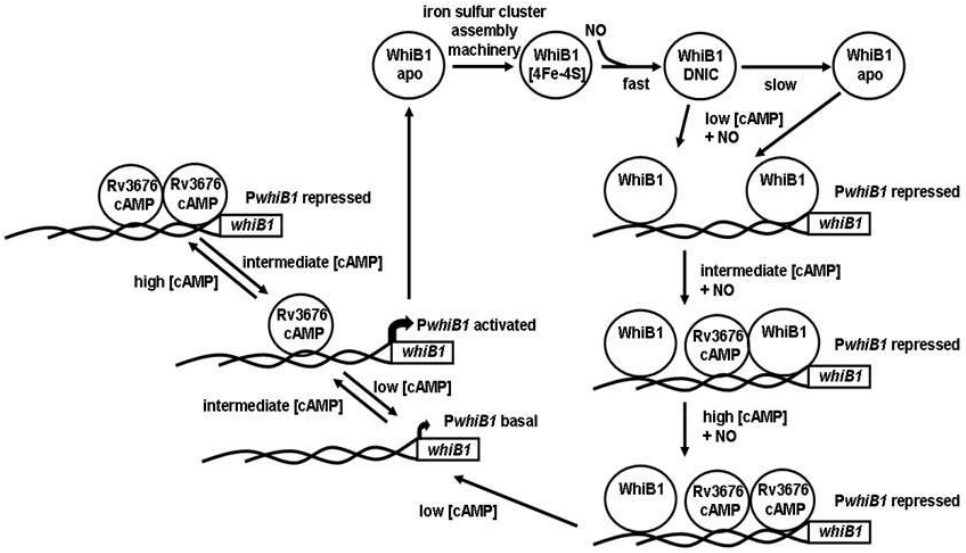

Figure 4.15: Model depicting nitric oxide- and cAMP-mediated regulation of *whiB1* expression. The forms of WhiB1 are represented by labelled circles, where no specific form is indicated this represents a mixture of oxidised and reduced apo-WhiB1 and nitrosylated-WhiB1. The *whiB1* promoter DNA (P*whiB1*), Rv3676 (labeled circles), nitric oxide and iron-sulphur cluster biosynthesis machinery are also indicated. Clockwise from bottom left, when cAMP levels are low and nitric oxide is absent, transcription of *whiB1* occurs at basal levels. At intermediate concentrations of cAMP, expression of *whiB1* is activated by the *M. tuberculosis* CRP protein (Rv3676) binding at class I site to allow increased synthesis of apo-WhiB1 (Stapleton *et al.*, 2010). At high concentrations of cAMP, Rv3676 occupies tandem sites at P*whiB1* and represses *whiB1* expression. Apo-WhiB1 protein acquires a $[4Fe\text{-}4S]^{2+}$ resulting in the non-DNA-binding form. Each WhiB1 $[4Fe\text{-}4S]^{2+}$ cluster reacts rapidly with 8 nitric oxide molecules to produce a mixture of DNIC and RRE complexes. In the presence of oxygen, the nitrosylated form of WhiB1 slowly degrades to yield apo-WhiB1 (Figure 4.9). DNA-binding activity has been demonstrated for reduced and oxidised apo-WhiB1 and nitric oxide-treated WhiB1. The DNA-binding apo-WhiB1 severely represses *whiB1* expression *in vitro* in the presence and absence of the *M. tuberculosis* CRP, Rv3676, by interactions at sites located upstream and downstream of the Rv3676 binding sites. Apo-WhiB1 can be switched off by the action of the iron-sulphur cluster assembly machinery to regenerate the non-DNA-binding holo-WhiB1 resulting in de-repression of *whiB1* expression and synthesis of apo-WhiB1 protein. Figure and legend from Smith *et al*. (2010).

A key question arising from these observations is ‘what are the roles of the various forms of WhiB1?’ WhiB1 has been shown to exist in [4Fe-4S], [2Fe-2S], nitrosylated, reduced apo-, and oxidised apo- forms. Apo-WhiB1 and nitric oxide-treated-holo-WhiB1 both bind to the *whiB1* promoter specifically, and the binding of the apo-form is affected by oxidation state with two species being formed in oxidising conditions (Sections 4.5.1 – 4.5.4; Figures 4.10 – 4.12). It is thought that the slower migrating complex (Figure 4.11B) is formed by P*whiB1* and oxidised (disulphide) apo-WhiB1, whereas the faster migrating species is formed by P*whiB1* and reduced (dithiol) apo-WhiB1 (Figure 4.11B) or P*whiB1* and nitrosylated-WhiB1 (Figure 4.11A). The DNA-binding activity of WhiB1 is therefore modulated by its nitric oxide-responsive iron-sulphur cluster and the oxidation state of the protein. Further work is now required to establish whether all the various forms have distinct functions, or whether they have overlapping activities and which of the forms present *in vitro* are physiologically relevant.

To conclude, WhiB1 from *M. tuberculosis* is an essential protein with a [4Fe-4S] cluster that acts as a specific nitric oxide-sensor converting it from a non-DNA-binding protein to a DNA-binding protein capable of repressing its own transcription. This sensing of nitric oxide and the resulting switch in DNA-binding, as well as the essential nature of WhiB1, has implications for the control of *M. tuberculosis* gene expression during the infection process (Smith *et al*., 2010).

5.0 Structure-function relationships of WhiB1

5.1 Introduction

To further our understanding of WhiB1, the structure-function relationships of the protein were analysed using site-directed mutagenesis of several amino acids. Residues involved in iron-sulphur cluster coordination, those that may be potentially involved in modulating the cluster environment, and residues in the predicted DNA-binding region were altered to discover those important for WhiB1's function as a nitric oxide-sensing transcription factor.

Like most members of the Wbl family in the Actinomycetes, WhiB1 has four conserved cysteine residues (C9, 37, 40 and 46) in its N-terminal region. They are believed to act as the ligands for the [4Fe-4S] iron sulphur cluster (Crack *et al*., 2011; Smith *et al*., 2010). Replacement of all four conserved cysteine residues at once in WhiB3 from *Mycobacterium tuberculosis* abolished cluster coordination (Singh *et al*., 2007), and the *in vivo* function of WhiD from *Streptomyces coelicolor* required all four cysteine residues (Jakimowicz *et al*., 2005). Interestingly, in the WhiB2 protein from *Mycobacterium smegmatis*, only three of the four cysteine residues were required for function *in vivo*. The cysteine 67 residue (equivalent to C9 in WhiB1) was not required for function, whereas the aspartic acid 71 residue (equivalent to D13 in WhiB1) was (Raghunand and Bishai, 2006b). The four cysteine residues of WhiB1 and the aspartic acid 13 residue were all individually altered to alanine and their role in cluster ligation analysed.

As shown in Chapter 4, the iron-sulphur cluster of WhiB1 is stable upon exposure to oxygen but reacts rapidly with nitric oxide (Crack *et al*., 2011; Smith *et al*., 2010). The stability of the iron-sulphur cluster to oxygen is unusual, and residues potentially involved in aiding this feature were identified. The transcription factor FNR of *Escherichia coli* contains an oxygen-sensitive [4Fe-4S] cluster, and residues involved in promoting this have been analysed (Bates *et al*., 2000; Jervis *et al*., 2009). The serine 24 to phenylalanine variant of FNR had increased oxygen stability, and structural models suggested that the cysteine 23 ligand is shielded by the phenylalanine side-chain thereby

protecting the cluster (Jervis *et al*., 2009). In contrast, serine at position 24 is believed to permit the interaction of the FNR [4Fe-4S] with oxygen. A proline residue (P41) in a similar position to serine 24 in WhiB1 was altered to serine to see whether this variant may have increased oxygen sensitivity and thus implicate proline in control of the cluster environment. Another residue involved in oxygen sensitivity of the iron-sulphur cluster of FNR is leucine 28 as shown by Bates *et al*. (2000). Alteration of leucine 28 to histidine produced a variant that was functional under aerobic conditions, i.e. the cluster did not undergo rapid disassembly (Bates *et al*., 2000). A glutamic acid residue (E45) in a comparable position to leucine 28 was altered to leucine to determine whether this would increase the oxygen sensitivity of the iron-sulphur cluster of WhiB1.

As discussed in Chapter 4, apo- and NO-treated-holo-WhiB1 are capable of binding to *whiB1* promoter DNA (Smith *et al*., 2010). The C-terminal region of WhiB1 is predicted to encode the DNA-binding domain. Sequence analysis and secondary structure predictions suggest the presence of a β-turn motif (^{58}GVWGG^{62}) followed by a predicted helical region (^{63}EDERRALKRRNA^{76}), forming part of an unconventional helix-turn-helix. There is very little evidence that these features of the C-terminal region are involved in DNA-binding, except in the Mycobacteriophage protein WhiBTM4. The variants L55Q, V56D, V58E (in the β-turn) and R67C (in the helix) of WhiBTM4 showed impaired DNA-binding (Rybniker *et al*., 2010). Amino acid sequence alignment of 28 Wbl proteins using ClustalW identified two regions (^{72}KRRN^{75} and ^{78}TKAR^{81}) located downstream of the β-turn that are highly conserved in the WhiB1 members. These positively-charged regions, along with the β-turn were targeted for site-directed mutagenesis to determine their role in DNA-binding, to hopefully provide new information on the importance of specific regions in the C-terminal domain.

5.2 Site-directed mutagenesis

To produce WhiB1 with the specified amino acid substitution, site-directed mutagenesis was carried out using the overexpression plasmid pGS2164 encoding His-WhiB1 as the template and primers designed to alter the amino acid in question (Sections 2.4.7 and 2.4.10). The resulting plasmids were sequenced by Source Bioscience and those with the correct substitutions were transferred to BL21 λ(DE3) and used for the analysis

described in this chapter. Tables 2.1 and 2.2 detail all of the strains and plasmids containing the required amino acid alteration respectively.

5.3 Analysis of the four cysteine residues involved in cluster-binding

5.3.1 Iron-sulphur cluster incorporation of the four cysteine variants

The four cysteine residues (C9, C37, C40 and C46) were individually altered to alanine to determine their role in cluster-binding. Each of the four proteins were overproduced and purified as described for wild-type WhiB1 (Sections 3.2.1 and 3.2.2). Wild-type WhiB1 purified with some colour, as previously shown (Figure 3.3) whereas the four variants were colourless after purification. The cysteine variant proteins (C9A, C37A, C40A and C46A) as well as wild-type WhiB1 (all 30 μM) were then anaerobically incubated overnight with the components for iron-sulphur cluster incorporation as described previously (Section 3.3.1). The wild-type WhiB1 turned straw-yellow, indicative of it binding a [4Fe-4S] cluster, whereas C9A, C37A, C40A and C46A showed little change in colour (Figure 5.1A). All proteins were then separated from unincorporated reconstitution components using heparin chromatography (Section 3.3.2). The four cysteine variants were colourless compared to wild-type WhiB1 (Figure 5.1B). This indicates their inability to incorporate an iron-sulphur cluster.

To confirm the absence of iron-sulphur clusters in the four cysteine variants, UV-visible spectroscopy was carried out on them alongside wild-type apo- and holo-WhiB1 (Section 2.6.4). Holo-WhiB1 (4.5 μM) showed an absorbance spectrum with a characteristic peak at 420 nm, indicative of a [4Fe-4S] cluster (Figure 5.2). The four cysteine variants (C9A, 2.5 μM; C37A, 3.7 μM; C40A, 3.6 μM; C46A, 3.6 μM) showed no peak at 420 nm and had spectra which resembled that of apo-WhiB1 (2.3 μM) (Figure 5.2). The $A_{420\ nm}$:$A_{280\ nm}$ ratios were 0.35, wild-type holo-WhiB1; 0.06, C9A; 0.06, C37A; 0.04, C40A; 0.09, C46A; and 0.02 wild-type apo-WhiB1. All samples were analysed in 25 mM Tris (pH 7.4) containing 0.5 M NaCl and 10 % glycerol. These data, taken together show that all four cysteine residues are required for cluster ligation.

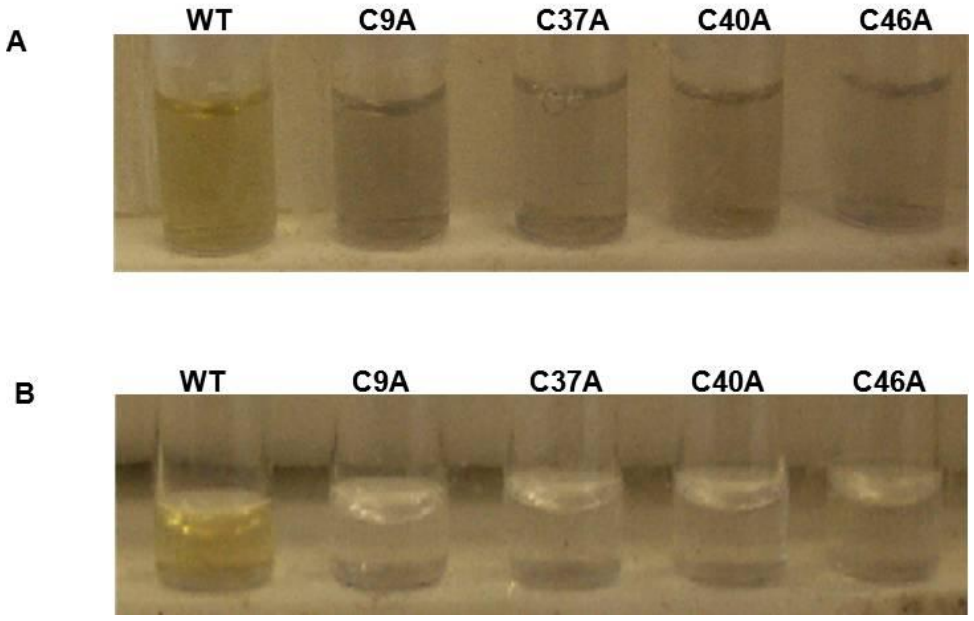

Figure 5.1: Photographs depicting the reconstitution reaction of WhiB1. The four cysteine mutants of WhiB1, alongside the wild-type, were incubated with the reconstitution components overnight under anaerobic conditions and photographed **(A)**. Each reaction was filtered and purified using heparin Sepharose to isolate the protein from un-incorporated reactants and photographed **(B)**.

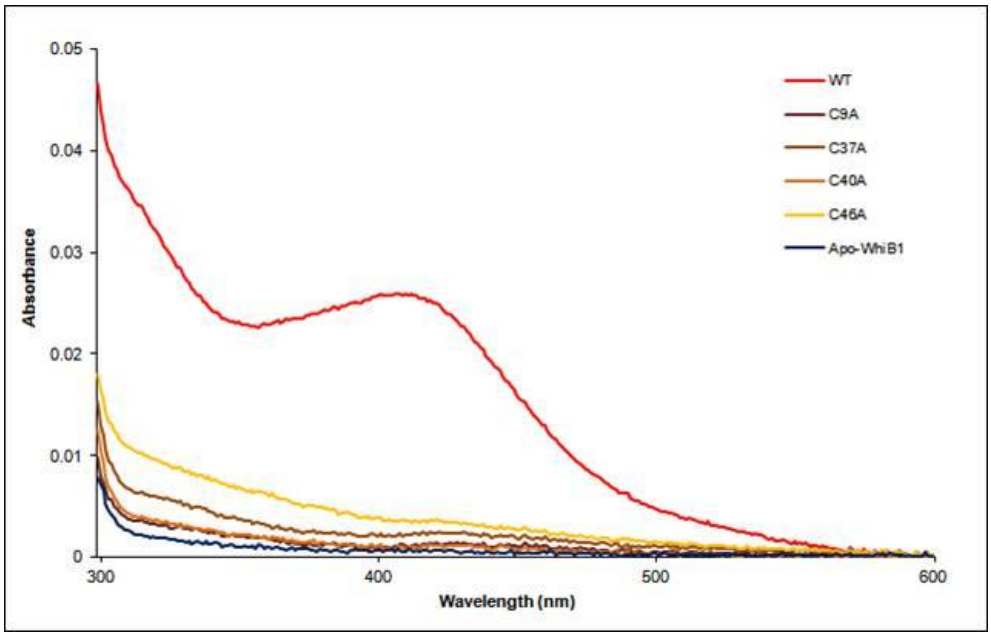

Figure 5.2 UV-visible spectroscopic analysis of wild-type WhiB1 and the four cysteine mutants. Wild-type (WT) WhiB1 and the four cysteine variants were anaerobically incubated with the components for reconstitution of the iron-sulphur clusters. The samples were purified by heparin chromatography and spectra obtained for the resulting proteins; WT (4.5 μM), C9A (2.5 μM), C37A (3.7 μM), C40A (3.6 μM), C46A (3.6 μM). Apo-WhiB1 (2.3 μM) was also shown for comparison.

5.3.2 DNA-binding properties of the four cysteine variants

As shown in Section 4.4.1 and (Smith *et al.*, 2010), the apo-form of WhiB1 is capable of binding the *whiB1* promoter DNA whereas the holo-form cannot. It was therefore expected that the cysteine variants would retain the ability to bind DNA, providing that they were correctly folded. Electromobility shift assays (Section 2.7.3) were carried out to test this hypothesis. Increasing concentrations (0, 1, 2, 5, 10 and 15 μM) of wild-type apo-WhiB1, C9A, C37A, C40A and C46A were incubated with ~3 ng of radiolabelled P*whiB1* (Section 2.7.1) before separation of protein-DNA complexes from free P*whiB1*. Figure 5.3 shows how each of the cysteine variants binds P*whiB1* in the same manner as wild type apo-WhiB1 (compare top panel to middle and bottom panels). This shows that the cysteine residues, although essential for cluster ligation, are not required for DNA-binding.

5.4 Analysis of the WhiB1-D13A variant

5.4.1 Iron-sulphur cluster characterisation of WhiB1-D13A

As mentioned above, the iron-sulphur cluster of WhiB2 from *M. smegmatis* is thought to be ligated by three cysteine residues and a conserved aspartate residue (D71) (Raghunand and Bishai, 2006b). The conserved aspartate 13 residue in WhiB1 was therefore altered to an alanine and the resulting protein analysed. The D13A variant of WhiB1 was overproduced and purified as described for wild-type WhiB1 (Sections 3.2.1 and 3.2.2). The resulting protein (72 μM) was anaerobically incubated with the components for iron-sulphur cluster reconstitution overnight (Section 3.3.1). The D13A sample was straw-yellow in colour indicating that it had acquired a [4Fe-4S] cluster. It was then purified by heparin chromatography (Section 3.3.2) before analysis using UV-visible spectroscopy. An absorbance spectrum was obtained for D13A (18.75 μM) in 25 mM Tris (pH 7.4) containing 0.5 M NaCl, 10 % glycerol and 1 mM DTT (Figure 5.4A). An absorbance peak at 420 nm, indicative of a [4Fe-4S] cluster, was observed resembling the absorbance spectrum of wild-type holo-WhiB1. Exposure to 110 μM oxygen caused little change in absorbance at 420 nm over 24 hours (Figure 5.4A). In contrast, exposure of 20 μM D13A (in 25 mM Tris (pH 7.4) containing 0.5 M NaCl,

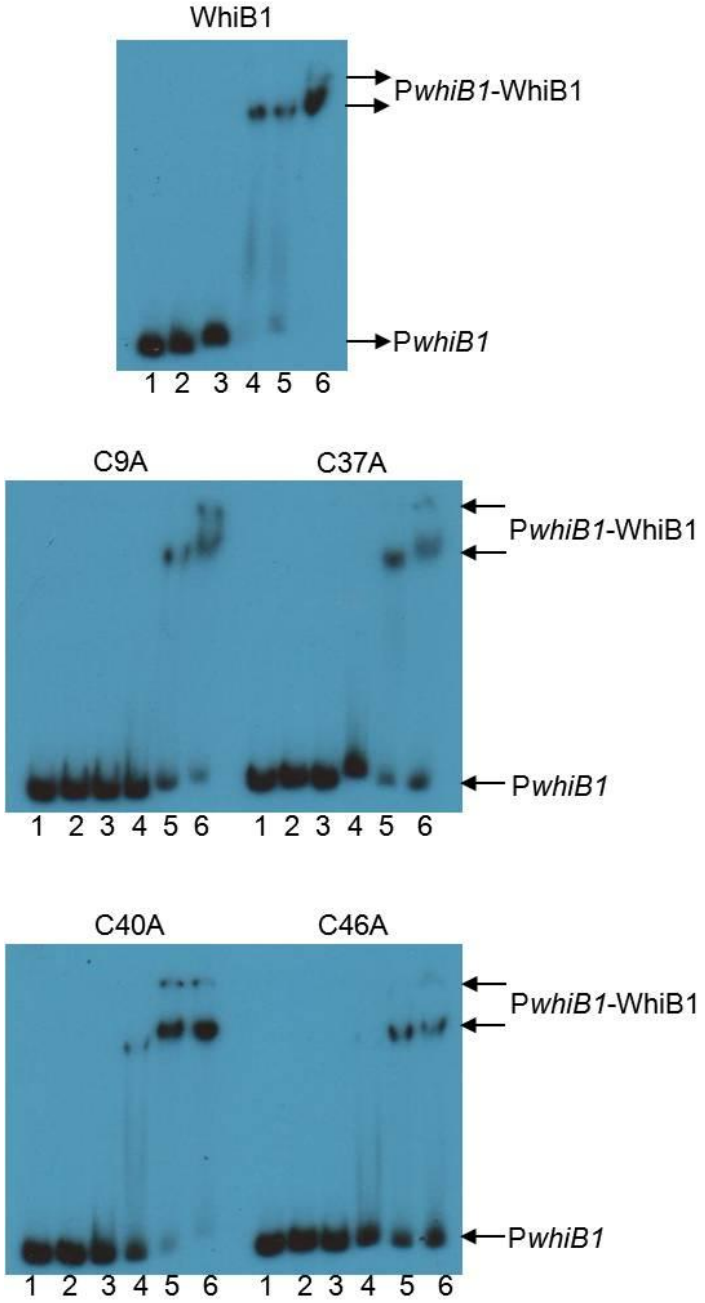

Figure 5.3: DNA-binding properties of the four cysteine mutants of WhiB1. Radiolabelled P*whiB1* was incubated with increasing concentrations of the indicated WhiB1 proteins before separation of protein-DNA complexes (P*whiB1*-WhiB1) from free DNA (P*whiB1*) by electrophoresis. Lanes 1, no protein; lanes 2-6 contain, 1, 2, 5, 10 and 15 μM WhiB1 respectively. The locations of P*whiB1* and P*whiB1*-WhiB1 complexes are indicated.

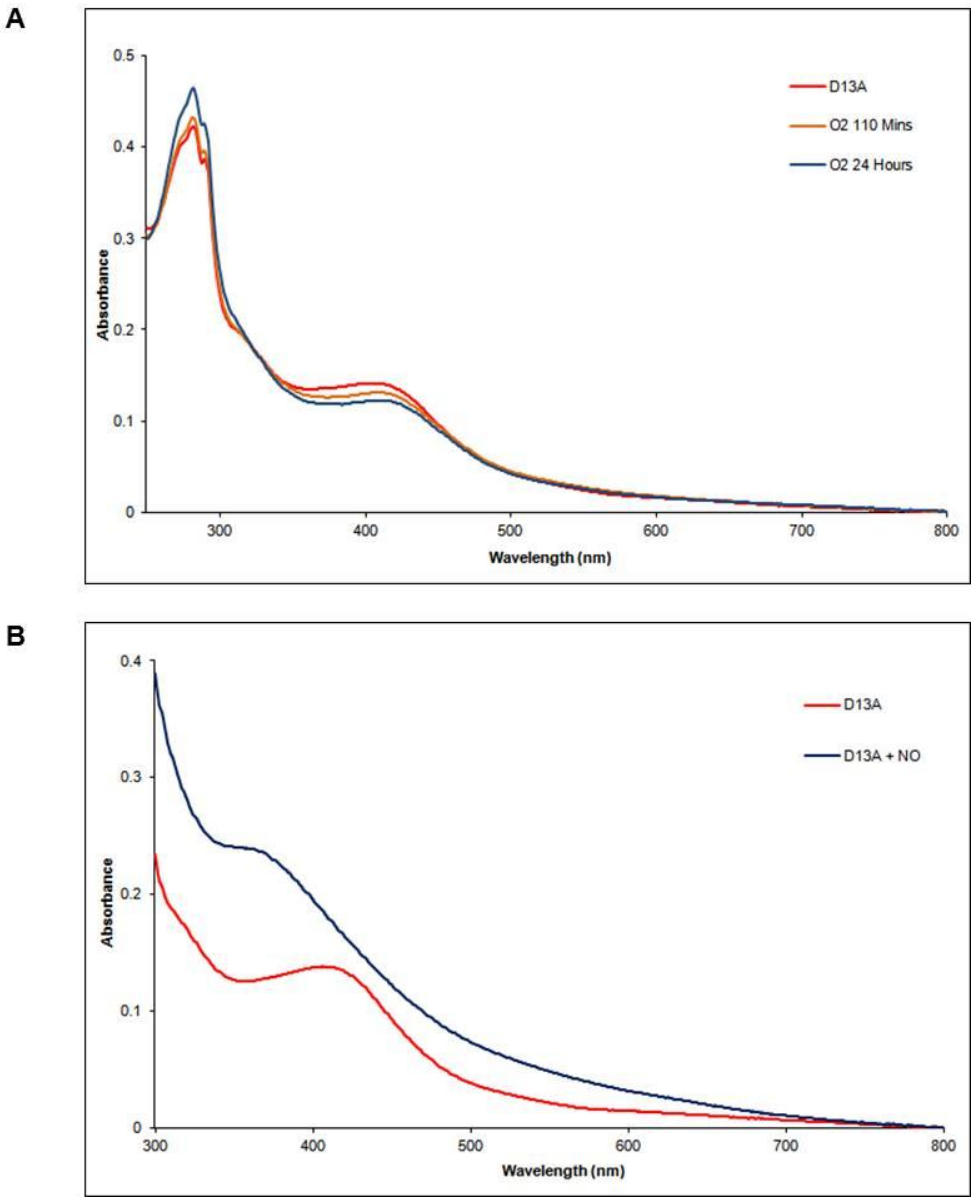

Figure 5.4: UV-Visible spectroscopy of the D13A variant of WhiB1. (A) WhiB1-D13A (18.75 μM) incorporates a [4Fe-4S] cluster (red line). The cluster was stable under 110 μM oxygen for up to 24 hours (orange and blue lines). **(B)** WhiB1-D13A reacts with nitric oxide. Reconstituted protein (20 μM; red line) was exposed to Proli NONOate (228 μM; blue line).

10 % glycerol and 1 mM DTT) to 228 μM Proli NONOate (~20 fold molar excess of nitric oxide) caused a change in the absorbance spectrum. An increase at 350-360 nm could be seen, due to the formation of nitrosylated iron-sulphur clusters (Figure 5.4B). This reaction was extremely rapid (almost complete within one minute at 25°C) and showed the same characteristics as the reaction of wild-type holo-WhiB1 to nitric oxide. It was concluded that the D13A variant therefore coordinates an oxygen-insensitive but nitric oxide-sensitive [4Fe-4S] cluster, in a similar manner to wild-type WhiB1. This shows that aspartic acid 13 does not have a role in cluster binding, and corroborates the findings that the iron-sulphur cluster of WhiB1 is ligated by the four cysteine residues.

5.4.2 DNA-binding properties of WhiB1-D13A

As shown, the D13A variant had no effect on cluster acquisition. Due to the location of this residue being in the N-terminal domain, it was not expected to have an effect on DNA-binding by the apo-form to P*whiB1*. An electromobility shift assay (Section 2.7.3) was carried out to determine whether the D13A variant could bind P*whiB1*. Increasing concentrations (0, 0.5, 1, 2, 4, 8 and 16 μM) of apo-WhiB1-D13A were incubated with ~3 ng of radiolabelled P*whiB1* (Section 2.7.1) before separation of protein-DNA complexes from free P*whiB1*. Figure 5.5 shows how the D13A variant binds the *whiB1* promoter in the same manner as wild-type apo-WhiB1 (Figure 5.3, top panel). These findings further confirm that the D13A variant of WhiB1 has properties similar to those of wild-type WhiB1.

5.5 Analysis of the P41S and E45L WhiB1 variants

The WhiB1 proline 41 residue was altered to serine to determine whether this variant would become more oxygen sensitive, based on the findings that alteration of a serine in a similar position to phenylalanine in FNR decreases its oxygen sensitivity (Jervis *et al*., 2009). The P41S variant was overproduced as described for wild-type (Section 3.2.1). Following cell breakage using the French pressure method (Section 2.5.4), the protein was found almost exclusively in the insoluble fraction. Attempts to purify WhiB1-P41S from the soluble cell-free extract using its histidine tag provided negligible amounts of protein (Section 2.5.5). The protein was then recovered from the insoluble fraction by

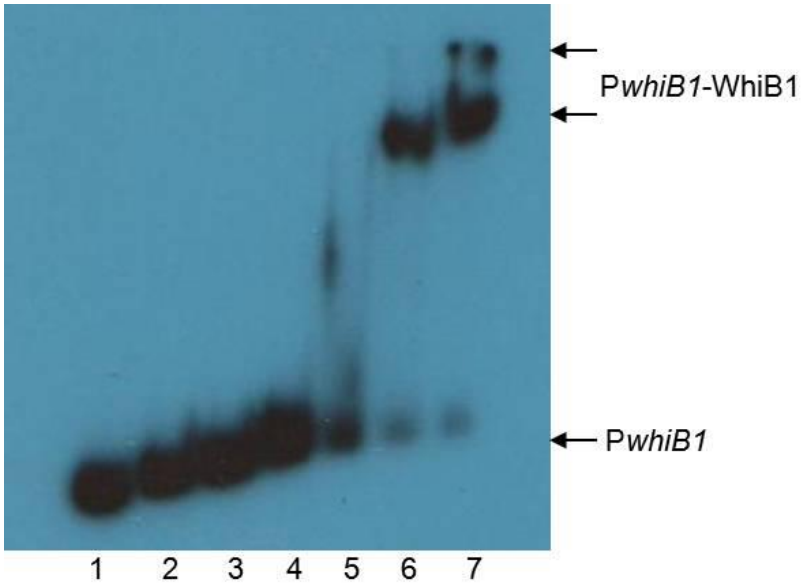

Figure 5.5: DNA-binding properties of WhiB1-D13A. Radiolabelled P*whiB1* was incubated with increasing concentrations of WhiB1-D13A before separation of protein-DNA complexes (P*whiB1*-WhiB1) from free DNA (P*whiB1*) by electrophoresis. Lane 1, no protein; lanes 2-7 contain, 0.5, 1, 2, 4, 8 and 16 μM WhiB1 respectively. The locations of P*whiB1* and P*whiB1*-WhiB1 complexes are indicated.

agitation in 6 M guanidine hydrochloride overnight at 4°C before centrifugation (Section 2.5.6). The soluble fraction, containing the P41S variant, was then applied to a HiTrap™ chelating column using the refolding programme to attempt to obtain functional protein (Section 2.5.6). Levels of pure refolded WhiB1-P41S were very low (~1 mg from 5 litres culture). Attempts to reconstitute the iron-sulphur cluster were unsuccessful, possibly due to low protein concentration, or mis-folding. It was concluded that this single amino acid residue is essential for maintaining the structural integrity of WhiB1 and further analysis was not carried out.

The glutamic acid 45 residue was altered to leucine to determine whether this change would promote oxygen sensitivity. This residue was chosen, because alteration of leucine to histidine in a similar position in FNR decreased the oxygen sensitivity of the cluster (Bates *et al*., 2000). As discussed for the P41S mutant, after overproduction and cell breakage the E45L was found almost exclusively in the insoluble fraction. Upon solubilisation with 6 M guanidine hydrochloride and refolding (Section 2.5.6), ~1.5 mg of E45L was obtained from 5 litres culture. Attempts to reconstitute the iron-sulphur cluster of this variant were also unsuccessful. It was again concluded that this single amino acid residue is essential for maintaining the structural integrity of WhiB1 and further analysis was not carried out.

Due to the inability to achieve soluble and correctly folded P41S and E45L, the protein containing a P41S:E45L double alteration was not analysed.

5.6 Analysis of the GVWGG β-turn region

5.6.1 DNA-binding properties of the β-turn variants

As discussed above, the GVWGG motif encoding a predicted β-turn is highly conserved in the Wbl family of proteins. These residues were all individually altered to glutamic acids residues as well as the serine immediately before the first glycine, as the equivalent residue in WhiBTM4 was shown to be involved in DNA-binding (Rybniker *et al*., 2010). The S57E, G58E, V59E, W60E, G61E and G62E variants were all overexpressed and purified as described for wild-type WhiB1 (Sections 3.2.1 and 3.2.2).

They were then used in electromobility shift assays to determine their DNA-binding properties (Section 2.7.3). Increasing amounts of each variant (0, 2.5, 5, 7.5 and 10 μM for all then 12.5 μM for V59E and 12.5 and 15 μM for S57E, W60E, G61E and G62E) were incubated with ~3 ng radiolabelled P*whiB1* (Section 2.7.1) before separation of protein-DNA complexes from unbound P*whiB1*. The replacement of the S57, V59 and W60 residues with glutamic acid did not significantly impair the ability of the WhiB1 to bind P*whiB1* (Figure 5.6). Replacement of the three glycine residues (G58, G61 and G62) with glutamic acid however, inhibited DNA-binding to the *whiB1* promoter. This suggests that the structural integrity of the predicted β-turn is in part due to the glycine residues and is crucial for DNA-binding.

5.6.2 Iron-sulphur cluster coordination of selected β-turn variants

To confirm that the lack of DNA-binding in the glycine variants was due to the essential nature of these residues and not due to disruption of the overall fold of the protein, the G61E and G62E variants were analysed for their ability to incorporate an iron-sulphur cluster. G61E (128 μM) and G62E (66.8 μM) were anaerobically incubated overnight with the components for iron-sulphur cluster reconstitution (Section 3.3.1). The resulting protein samples were analysed using UV-visible spectroscopy. The absorption spectra for both G61E and G62E showed a peak at 420 nm, indicative of the presence of a [4Fe-4S] cluster (Figure 5.7). This indicates that the inability of the glycine residue variants to bind DNA is not due to the overall disruption of the protein fold.

5.7 Analysis of conserved regions in the DNA-binding domain

5.7.1 DNA-binding properties of variants

As noted above, two highly conserved regions in the C-terminal domain of WhiB1 proteins were identified: ^{72}KRRN^{75} and ^{78}TKAR^{81}. The positively-charged lysine and arginine residues in the first region were individually altered to glutamic acid residues for analysis of the DNA-binding abilities of the resulting proteins. The positive lysine and arginine residues in the second region, as well as arginine 77, were also altered to

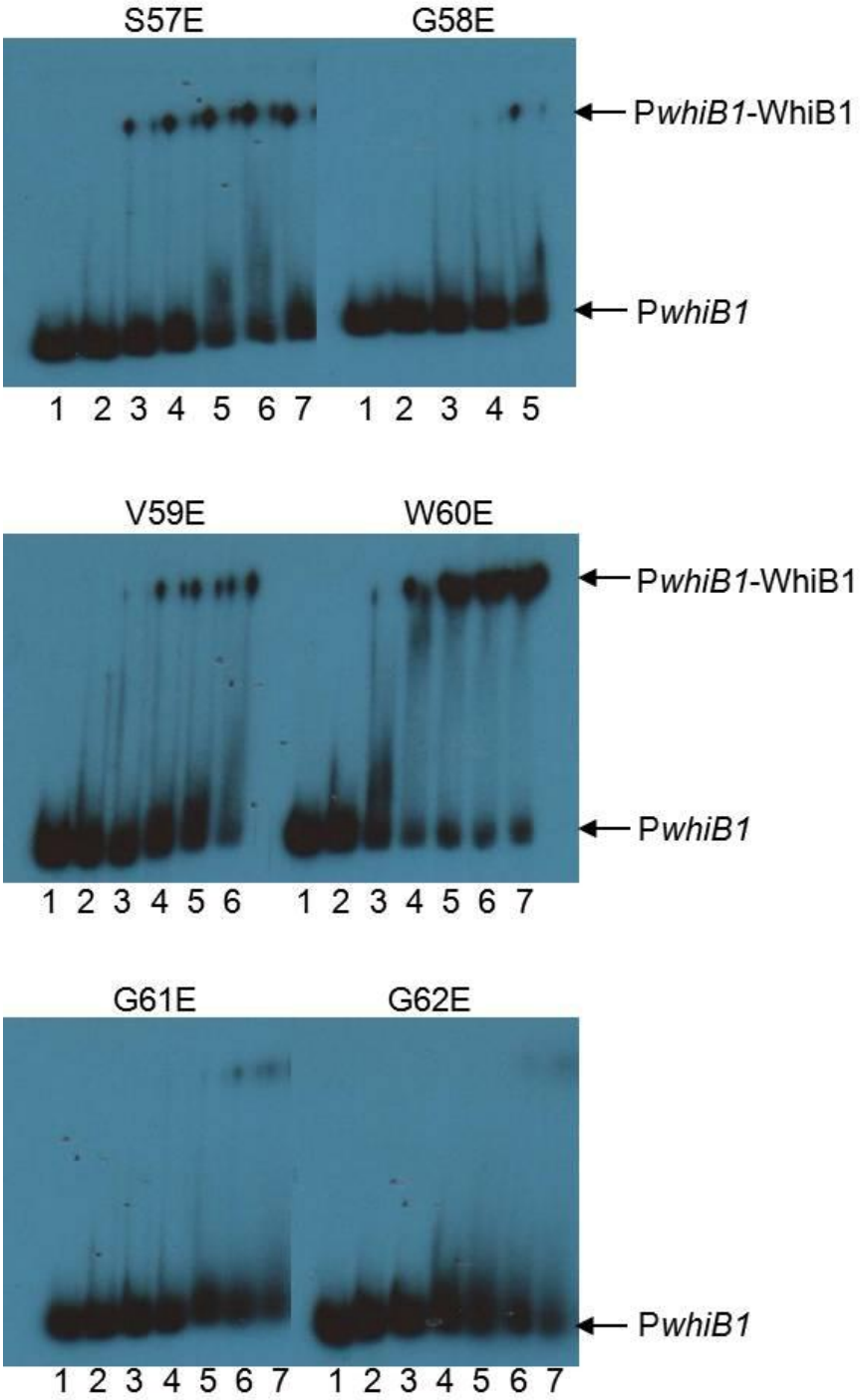

Figure 5.6: DNA-binding properties of variants in the β-turn of WhiB1. Radiolabelled P*whiB1* was incubated with increasing concentrations of the indicated WhiB1 proteins before separation of protein-DNA complexes (P*whiB1*-WhiB1) from free DNA (P*whiB1*) by electrophoresis. Lanes 1, no protein; lanes 2-7 contain, 2.5, 5, 7.5, 10, 12.5 and 15 μM WhiB1 respectively. The locations of P*whiB1* and P*whiB1*-WhiB1 complexes are indicated.

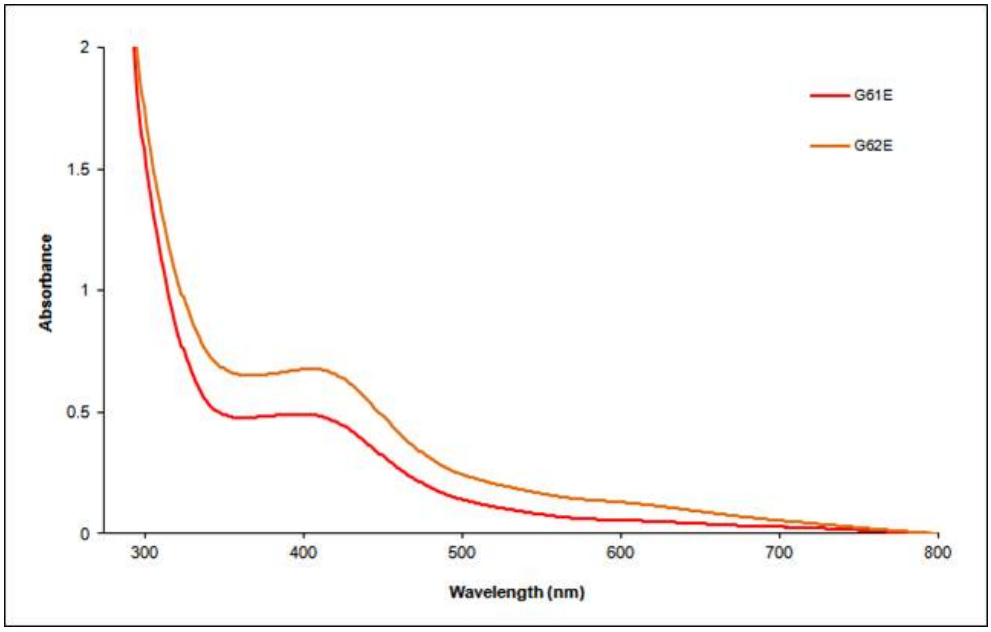

Figure 5.7: The WhiB1 G61E and G62E variants incorporate an iron-sulphur cluster. G61E (128 μM) and G62E (66.8 μM) were incubated anaerobically with the components for iron-sulphur cluster reconstitution. UV-visible spectroscopy shows a peak at 420 nm for both variants, indicating the presence of a [4Fe-4S] cluster.

glutamic acids. The latter residue is heavily conserved throughout the Wbl proteins used in the sequence alignment and thus was also analysed. Each of the variants was used in electromobility shift assays to determine their ability to bind P*whiB1* (Section 2.7.3). Increasing concentrations of protein (0, 2.5, 5, 7.5 and 10 μM for all; 12.5 and 15 μM for all apart from K72E) were incubated with ~3 ng of radiolabelled P*whiB1* (Section 2.7.1) before separation of protein-DNA complexes from unbound P*whiB1*. The alteration of all these positively-charged residues to negatively-charged glutamic acid abolished DNA-binding (Figure 5.8). This suggests that the positive nature of these conserved regions is essential for DNA-binding.

5.7.2 Iron-sulphur cluster coordination of selected variants

To confirm that the inability of the non-DNA-binding variants was due to their essential nature rather than disruption to overall protein fold, the capability of R74E, R77E and K79E to incorporate an iron-sulphur cluster was determined. These three variants were purified in the holo-form as could be seen from the characteristic straw-yellow colour of the fractions. Spectra were obtained using UV-visible spectroscopy (Figure 5.9). A peak at 420 nm can be seen for all three variants, indicative of the presence of a [4Fe-4S] cluster (13 μM R74E, 14 μM R77E and 11 μM K79E cluster concentration). This shows that these amino acids are essential for binding to the *whiB1* promoter but alteration of them does not affect the overall protein fold.

5.8 Discussion

WhiB1 is an essential iron-sulphur cluster protein. Upon exposure to nitric oxide, it switches from a non-DNA-binding holo-from to a DNA-binding nitrosylated transcription factor with the apo-form also capable of binding DNA (Crack *et al*., 2011; Smith *et al*., 2010; Stapleton *et al*., 2012). Other members of the Wbl family of the Actinomycetes have also been recognised as transcription factors with functions determined by nitric oxide (Rybniker *et al*., 2010; Singh *et al*., 2007). There has been little published on the structure-function relationships of this family of proteins, and this site-directed mutagenesis study has provided new insights into WhiB1 (Smith *et al*., 2012).

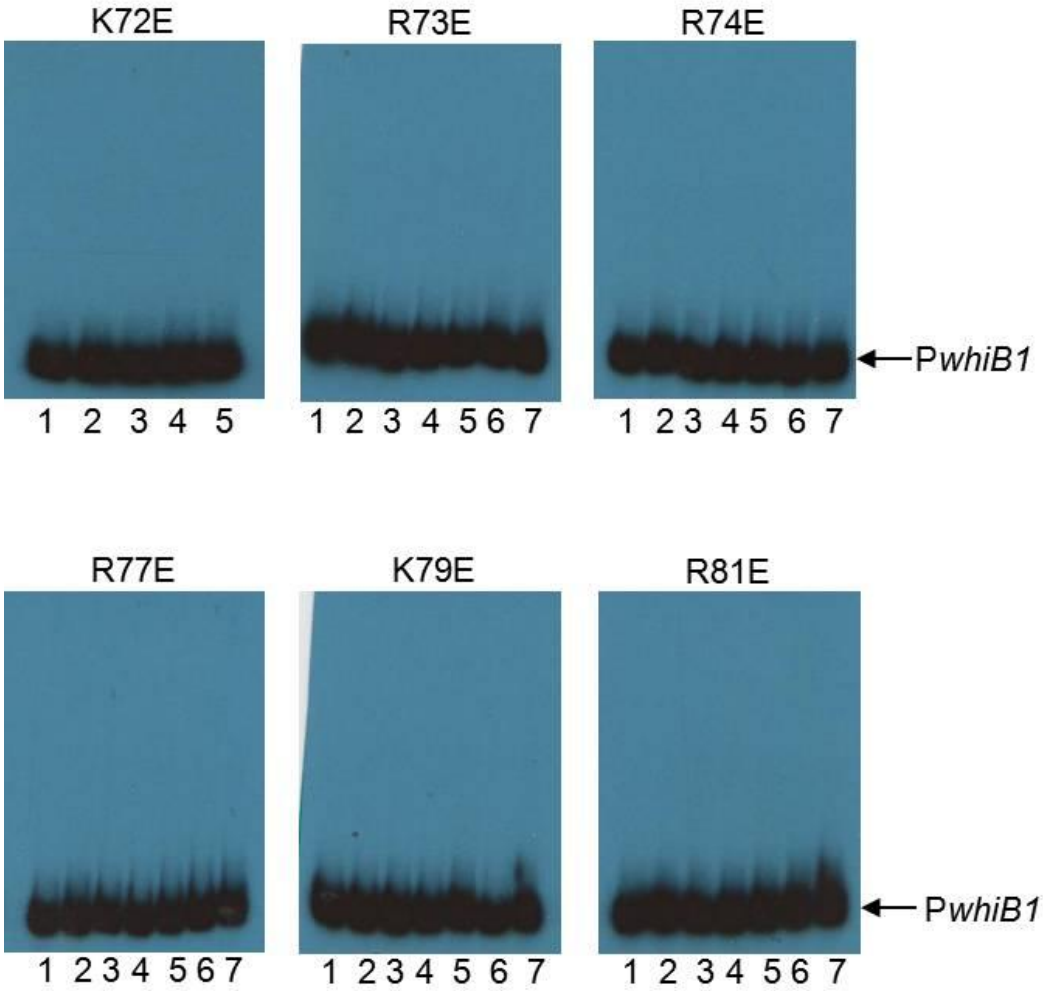

Figure 5.8: DNA-binding properties of variants in the C-terminal region of WhiB1. Radiolabelled P*whiB1* was incubated with increasing concentrations of the indicated WhiB1 proteins before separation of protein-DNA complexes (P*whiB1*-WhiB1) from free DNA (P*whiB1*) by electrophoresis. Lanes 1, no protein; lanes 2-7 contain, 2.5, 5, 7.5, 10, 12.5 and 15 μM WhiB1 respectively. The location of P*whiB1* is indicated.

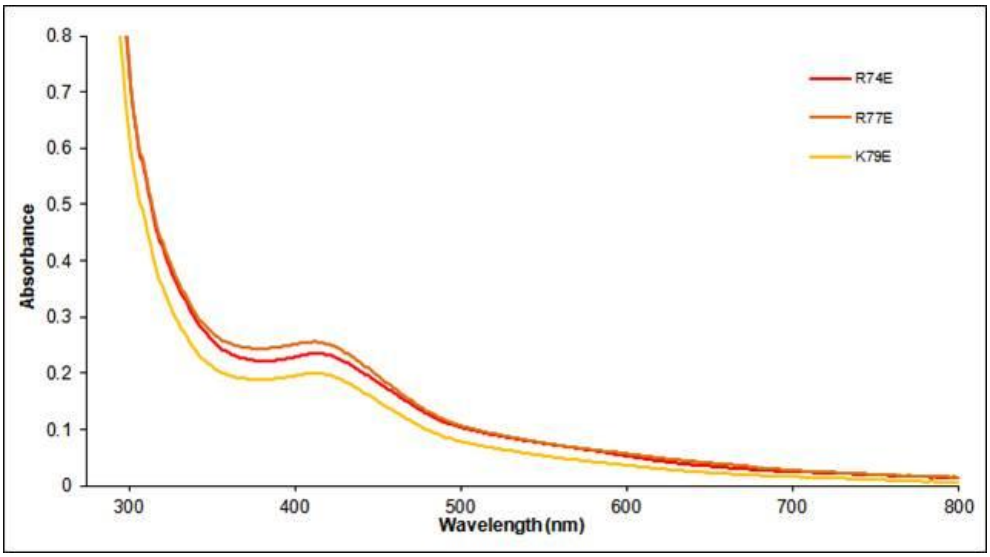

Figure 5.9: The WhiB1 R74E, R77E and K79E variants incorporate an iron-sulphur cluster. The three variants shown were purified from the cell-free extract with a characteristic straw-yellow colour. UV-visible spectroscopy showed a peak at 420 nm, indicating the presence of a [4Fe-4S] cluster.

WhiB1 has four highly conserved cysteine residues, which are common ligands for iron-sulphur cluster coordination. The alteration of each residue individually rendered WhiB1 incapable of incorporating an iron-sulphur cluster, showing the essential nature of each (Figures 5.1 and 5.2). This corresponds to similar information on WhiD from *S. coelicolor*, whereby individual alteration of the four cysteine residues to alanine prevented *in vivo* activity (Jakimowicz *et al*., 2005). Singh *et al*. also showed that simultaneous mutation of all cysteine residues in *M. tuberculosis* WhiB3 led to the inability to coordinate an iron-sulphur cluster (Singh *et al*., 2003). In contrast, the C36S and C45S variants of the Mycobacteriophage WhiBTM4 protein had some ability to bind an iron-sulphur cluster, although they had increased oxygen sensitivity (Rybniker *et al*., 2010). The cysteine residues of WhiB4 from *M. tuberculosis* have all been implicated in iron-sulphur cluster binding, although each variant protein retained some ability to coordinate a cluster albeit with reduced capacity in comparison to wild-type (Alam *et al*., 2007). The two cysteine residues in the CXXC motif (C59 and C62) showed the biggest reduction in cluster binding (Alam *et al*., 2007). This information shows the importance of the cysteine residues of WhiB1 is similar to that of WhiD from *S. coelicolor*. The aspartic acid residue (D13) was not important in cluster ligation for WhiB1 (Figure 5.4), unlike the corresponding aspartic acid 71 residue of WhiB2 in *M. smegmatis*. The D71 residue was shown to act as the fourth ligand for the iron-sulphur cluster of WhiB2, with replacement of cysteine 67 having no effect on protein function (Raghunand and Bishai, 2006b). Similarly, the [4Fe-4S] cluster of FNR from *Bacillus subtilis* is ligated by three of its six cysteine residues (C227, C230 and C235) and the aspartic acid 141 residue (Gruner *et al*., 2011; Reents *et al*., 2006). The WhiB1 iron-sulphur cluster is stable in the presence of oxygen but reacts rapidly with nitric oxide, and these properties were not affected by replacement of the conserved aspartic acid (D13) residue with alanine (Figure 5.4). The environment surrounding the iron-sulphur cluster, modulated by the amino-acid side chains, is likely to be responsible for controlling the cluster's sensitivity. The two residues targeted to determine this, proline 41 and glutamic acid 45, are likely to be essential for general protein fold as soluble correctly folded protein was unobtainable. Further targeted mutagenesis of surrounding amino acids is necessary to try to understand the cluster's environment. The four cysteine variants, and the aspartic acid variant, showed DNA-binding capabilities similar to that of wild type (Figures 5.3 and 5.5). This was expected as it is the C-terminal domain of Wbl proteins that is believed to be involved in DNA-binding, as opposed to the N-terminal domain.

The C-terminal domain of the Wbl proteins has long been considered to be responsible for DNA-binding (den Hengst and Buttner, 2008). There have however been few attempts to define the molecular requirements for DNA-binding by Wbl proteins. Three proteins with C-terminal truncations of the *M. smegmatis* protein WhiB2 were produced with differing activities (Raghunand and Bishai, 2006b). A truncation lacking twelve amino acids (corresponding to the second helix of the helix-turn-helix motif) showed similar activity to wild-type. Truncations lacking the turn-helix and the helix-turn-helix showed partial activity and no activity respectively (Raghunand and Bishai, 2006b). This shows the importance of the predicted C-terminal helix-turn-helix in function, but does not show specific residues involved in DNA-binding. Electromobility shift assays carried out on loss of function mutants in WhiBTM4 indicated that amino acid substitutions directly before and in the C-terminal β-turn (L55Q, V56D and V58E) inhibited DNA-binding (Rybniker *et al*., 2010). As shown for WhiB1, replacement of the three glycine residues (G58E, G61E and G62E) in the GVWGG β-turn motif inhibited DNA-binding (Figure 5.6). These two independent studies indicate that the structural integrity of the β-turn is necessary for DNA-binding in WhiB1 and WhiB4TM4. A fourth WhiBTM4 variant encoding a replacement of arginine 67 in the predicted helix with cysteine also caused impaired DNA-binding (Rybniker *et al*., 2010). Therefore two conserved positively-charged motifs (KRRN and TKAR) found in WhiB1 proteins in the helix downstream of the β-turn, as well as a conserved arginine residue found in other Wbl proteins, were targeted for mutagenesis. The positively charged residues were altered to glutamic acid and all the resulting proteins were incapable of binding to the *whiB1* promoter (Figure 5.8). This mutagenesis analysis, as well as that carried out on WhiBTM4, highlights the essential nature of the structural integrity of the β-turn and the positive charge of the helical region in DNA-binding. It is worth noting that these findings specifically affect DNA-binding and are not due to problems in overall protein fold as the variants were capable of incorporating an iron-sulphur cluster (Figures 5.7 and 5.9).

To conclude, the experiments described in this chapter to understand the structure-function relationships of WhiB1 have shown at least three C-terminal motifs are essential for DNA-binding and that the interaction with DNA is inhibited by the presence of a [4Fe-4S] cluster ligated by cysteine residues 9, 37, 40 and 46.

6.0 Interaction of WhiB1 and Rv1675c with other promoters

6.1 Introduction

As shown in Chapter 4, apo-WhiB1 can bind at its own promoter (P*whiB1*). This binding is specific and modulated by the presence and state of the iron-sulphur cluster, whereby holo-WhiB1 is incapable of DNA-binding but apo- and nitrosylated-WhiB1 are. Here, work has been carried out to determine whether WhiB1 can interact with other promoters, namely that for the essential chaperonin gene *groEL2* (Sassetti *et al*., 2003).

Expression of *whiB1* is regulated by Rv3676c, a cAMP receptor protein (Rickman *et al*., 2005). *Mycobacterium tuberculosis* possesses a second cAMP receptor protein, Rv1675c (Cmr – cAMP and macrophage regulator) (McCue *et al*., 2000). Rv1675c has not been fully characterised, and was therefore the subject of further study here. Rv1675c has been identified as a cAMP-responsive transcription factor, regulating four cAMP-induced genes (Gazdik and McDonough, 2005; Gazdik *et al*., 2009). Of these four genes, Rv1675c bound the promoters of *mdh* (encoding a malate dehydrogenase), *groEL2* and *Rv1265* (a gene of unknown function) suggesting direct regulation (Gazdik *et al*., 2009). Here, we aim to confirm its ability to bind the *groEL2* promoter, and to characterise the DNA-binding properties of Rv1675c with a selection of other promoters. A number of genes were identified to be potentially regulated by Rv1675c by DNA microarrays (Debbie Hunt, unpublished data). Four genes were selected for analysis here; *Rv2007c*, *fdxA* encoding a ferredoxin; *Rv2032*, an acr-coregulated gene of unknown function; *Rv3133c*, *dosR* encoding the regulator of the 2-component DosRS system; *Rv3134c*, encoding a gene of unknown function that may play a role in the phosphorelay of the DosRS system. All of the genes are predicted to be in the DosRS regulon and by completing DNA-binding experiments with the promoters for these four genes, it was hoped to determine whether Rv1675c can interact with them all individually or whether the regulatory effect is through interaction with *dosR*. Thus, the work presented in this chapter aims to understand the larger regulatory role of WhiB1 in response to the important signalling molecules, nitric oxide and cAMP.

6.2 Interaction of WhiB1 with the groEL2 promoter region

Electromobility shift assays were carried out to determine whether WhiB1 could bind to the promoter of *groEL2* as described in Section 2.7.3. Increasing concentrations of apo-WhiB1 (0, 0.25, 5, 10, 20 and 40 µM) were incubated separately with ~1.6 nm radiolabelled P*groEL2* (Section 2.7.1) before separation of protein-DNA complexes from free DNA by electrophoresis. Figure 6.1A shows how apo-WhiB1 binds P*groEL2* (lanes 4-6). As discussed in Chapter 4, holo-WhiB1 is incapable of binding to *whiB1* promoter DNA (Figure 4.10). This observation can also be seen for holo-WhiB1 and P*groEL2* (Figure 6.1B). The binding of apo-WhiB1 to the *groEL2* promoter is specific, as shown for binding to P*whiB1*, as addition of unlabelled P*rpfA* in competition EMSAs did not affect binding (Stapleton *et al.*, 2012). As previously discussed in Chapter 4, WhiB1 was unable to bind to the *rpfA*, *ahpC* and *Rv3616c* promoters, further indicating that DNA-binding of WhiB1 is specific to P*whiB1* and P*groEL2* (Smith *et al*., 2010; Stapleton *et al*., 2012). EMSAs were carried out by Dr Melanie Stapleton (Stapleton *et al*., 2012).

6.3 Characterisation of Rv1675c

6.3.1 Optimisation of Rv1675c overproduction

Electrically competent cells of *Escherichia coli* BL21 λ(DE3) were transformed with pGS2103, encoding recombinant His-Rv1675c.

Trials to discover the best conditions for overproduction of His-Rv1675c were completed in 10 ml cultures. To first determine the optimum time for induction, 100 µl of an overnight culture was added to a 10 ml volume of LB containing kanamycin. The culture was grown at 37 °C with shaking (250 rpm) until an OD_{600} of ~0.8 was reached. IPTG was added to a final concentration of 30 µg/ml and the culture returned to 37 °C with shaking. Whole cell samples were taken before induction and at 60, 90, 120, 150, 180 and 210 minutes post induction for analysis by SDS-PAGE as described in Section 2.5.2 (Figure 6.2A). There was a prominent polypeptide at ~30.5 kDa in all post-

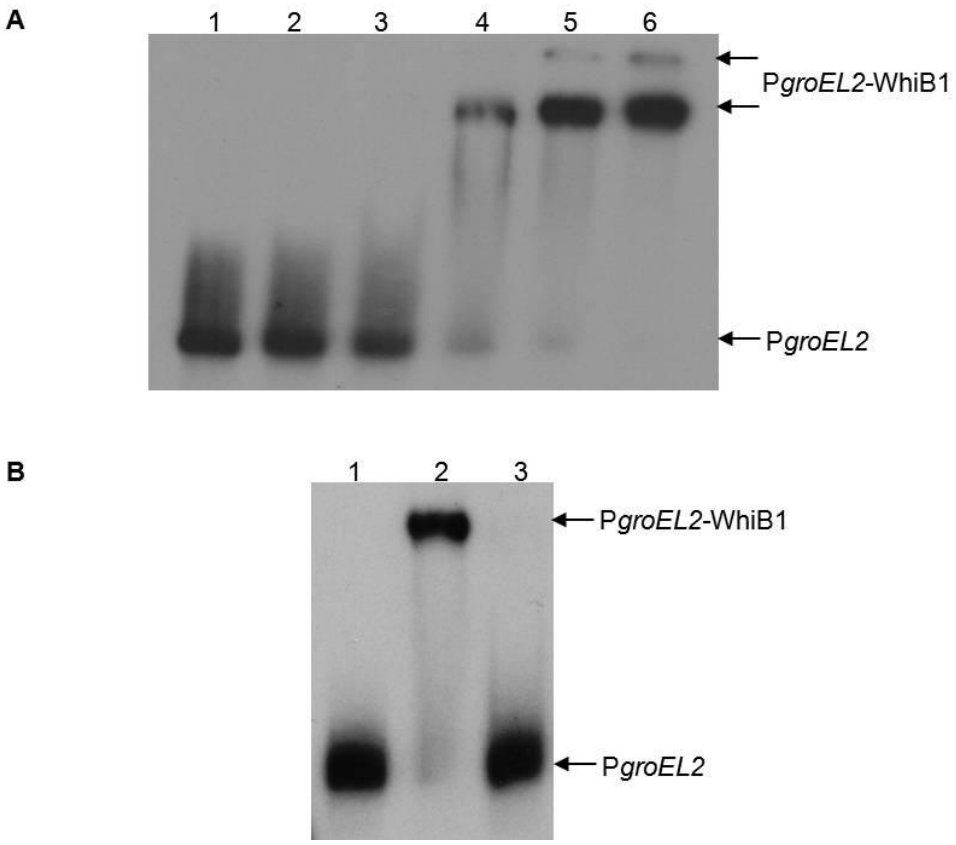

Figure 6.1: DNA-binding properties of WhiB1 at the *groEL2* promoter region (P*groEL2*). (A) WhiB1 binds P*groEL2*. Radiolabelled P*groEL2* was incubated with increasing concentrations of WhiB1 before separation of protein-DNA complexes (P*groEL2*-WhiB1) from free DNA (P*groEL2*) by electrophoresis. Lanes 1, no protein; lanes 2-6 contain 2.5, 5, 10, 20 and 40 μM apo-WhiB1 respectively. The locations of P*groEL2*-WhiB1 and P*groEL2* are indicated. **(B) Holo-WhiB1 does not bind P*groEL2*.** Radiolabelled P*groEL2* was incubated with apo-WhiB1 or holo-WhiB1 before separation of protein-DNA complexes (P*groEL2*-WhiB1) from free DNA (P*groEL2*) by electrophoresis. Lane 1, no protein; lane 2, 20 μM apo-WhiB1; lane 3, 20 μM holo-WhiB1. The locations of P*groEL2* and P*groEL2*-Rv1675c are indicated. EMSAs were carried out by Dr Melanie Stapleton and are reported in Stapleton *et al*., 2012.

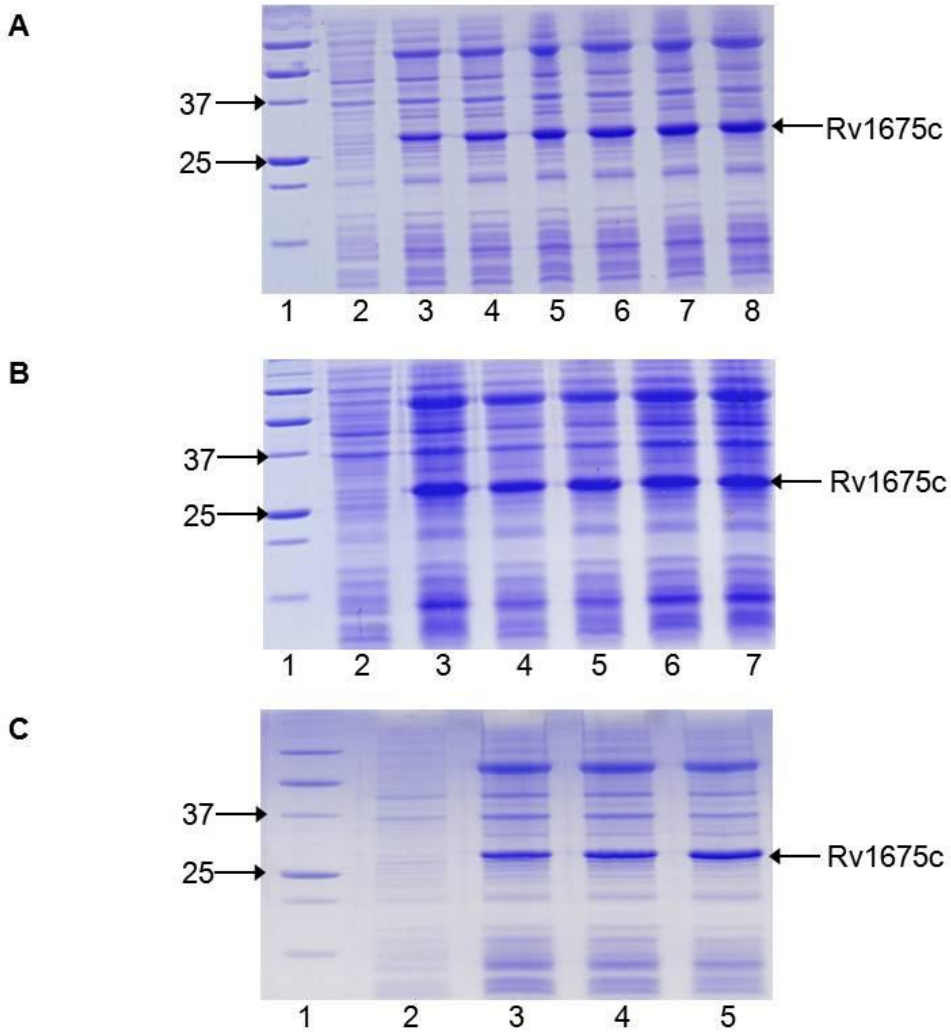

Figure 6.2: Optimisation of overexpression of recombinant Rv1675c in BL21 λ(DE3). (A) Comparison of different induction times. Lane 1, Precision plus protein standards (molecular weights indicated in kDa); Lane 2, Cell extract before IPTG induction; Lanes 3-8, Cell extracts with 30 μg/ml IPTG induction for 60, 90, 120, 150, 180 and 210 minutes. **(B) Comparison of different IPTG concentrations**. Lane 1, Precision plus protein standards (molecular weights indicated in kDa); Lane 2, Cell extract before IPTG induction; Lanes 3-7, Cell extracts after 120 minutes induction with 30, 60, 120, 240 and 480 μg/ml IPTG. **(C) Comparison of different induction temperatures**. Lane 1, Precision plus protein standards (molecular weights indicated in kDa); Lane 2, Cell extract before IPTG induction; Lanes 3-5, Cell extracts after 120 μg/ml IPTG induction for 2 hours at 25, 30 and 37°C. The location of the Rv1675c polypeptide is indicated.

induction fractions, corresponding to His-Rv1675c. There was little difference in relative abundance of His-Rv1675c as judged by SDS-PAGE, and 2 hours was chosen as it offered a good level of overproduction. Secondly, the ideal concentration of IPTG to use was determined. Growth was carried out as above and cultures were then induced with 30, 60, 120, 240 and 480 µg/ml of IPTG for 2 hours. Whole cell samples were taken for SDS-PAGE analysis (Figure 6.2B). The final concentration of 120 µg/ml of IPTG was chosen as it offered good overproduction, but all IPTG concentrations were effective. The use of different induction temperatures was the final condition tested in optimising His-RV1675c overproduction. Growth was again carried out as described above and cultures were then induced with 120 µg/ml IPTG and moved to 25, 30 or 37 °C for 2 hours. Whole cell samples were taken and analysed using SDS-PAGE (Figure 6.2C). There was good overproduction of Rv1675c at 25 °C, which was chosen as it was hoped that the lower temperature would assist protein folding and solubility.

Upon finding the optimum overproduction conditions (induction with 120 µg/ml IPTG for 2 hours at 25 °C), Rv1675c was purified by affinity chromatography.

6.3.2 Purification of His-Rv1675c overproduction

Cell pellets from the overproduction of Rv1675c (1-5 litres of culture) (Section 2.5.3) were resuspended in binding buffer (10 ml) and lysed in a French pressure cell according to the method detailed in Section 2.5.4. After clarification of the cell-free pellet from the insoluble pellet, SDS-PAGE analysis showed Rv1675c to be in the soluble fraction (data not shown). This was subsequently used for affinity purification as described in Section 2.5.5. Figure 6.3A shows the elution profile from the HiTrap chelating column. Three peaks were seen on the elution profile for Rv1675c purification, and fractions corresponding to the peaks were analysed by SDS-PAGE (Figure 6.2B). The first two contained off-target proteins, but the third corresponded to Rv1675c, confirmed by the presence of a species on SDS-PAGE at ~30.5 kDa (Figure 6.3B). The purification shown in Figure 6.3 was achieved using a 1 ml nickel affinity column. This provided a good level of Rv1675c from the soluble fraction (~11 mg from 1 litre of culture). The conditions described in Section 6.3.1 for overproduction, and this method of purification, have thus provided a successful way of purifying Rv1675c using its histidine tag to be used in DNA-binding experiments.

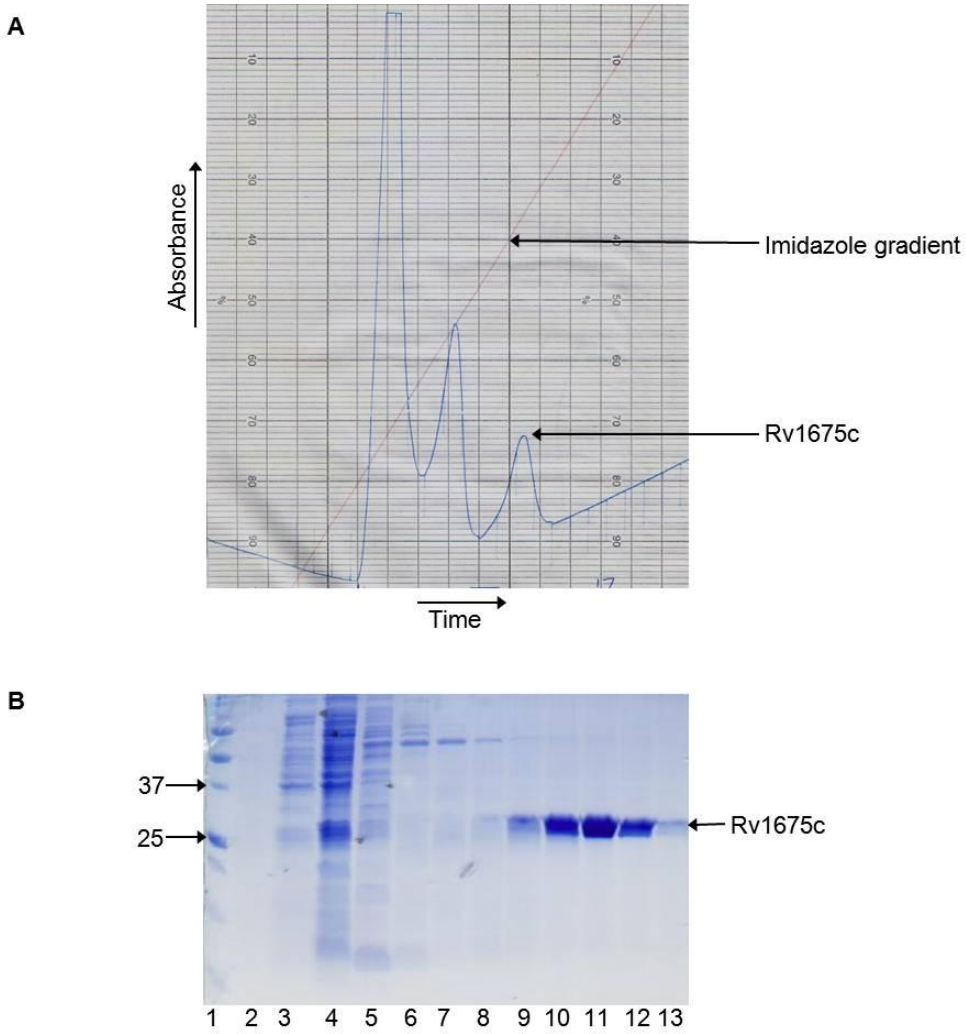

Figure 6.3: (A) Elution profile from HiTrap chelating chromatography of cell-free extract containing His-Rv1675c. Supernatant (10 ml) was applied to a Hi-Trap chelating column (1 ml) and fractionated with a linear gradient of imidazole (0-1 M). The traces show protein (A_{280}: blue line) and imidazole gradient (red line). The expected location of the Rv1675c is indicated. **(B) Histidine-tagged purification of His-Rv1675c.** Coomassie Blue-stained SDS-PAGE gel: Lane 1, Precision plus protein standards (molecular weights indicated in kDa); Lanes 2-13, Fractions collected after application of the imidazole gradient corresponding to the three peaks seen in Figure 6.2A.

6.3.3 DNA-binding of Rv1675c at the *groEL2* promoter region

Rv1675c has previously been shown to bind the *groEL2* promoter region (Gazdik *et al*., 2009). To corroborate these findings, electromobility shift assays were carried out with Rv1675c and P*groEL2* as described in Section 2.7.3. Increasing concentrations (0, 0.5, 1, 2, 4, 8 and 16 µM) of Rv1675c were incubated with ~3 ng of radiolabelled P*groEL2* (section 2.7.1), with or without 2 mM cAMP, before separation of protein-DNA complexes from free DNA. Figure 6.4 shows Rv1675c binds the P*groEL2* DNA in the presence and absence of cAMP (lanes 5-7 and 12-14). These data are consistent with the finding of Gazdik *et al*. (2009).

6.3.4 DNA-binding of Rv1675c at selected promoter regions

Electromobility shift assays (Section 2.7.3) were carried out with Rv1675c and the four promoters discussed in Section 6.1. Increasing concentrations (0, 0.5, 1, 2, 4, 8 and 16 µM) of Rv1675c were incubated with ~3 ng of the desired radiolabelled promoter DNA (P*Rv2007c*, P*Rv2032*, P*Rv3133c* or P*Rv3134c*) (Section 2.7.1), before separation of protein-DNA complexes from free DNA. Figure 6.5 shows the DNA-binding ability of Rv1675c to these promoters. Rv1675c is unable to bind P*Rv2007c* and P*Rv2032* (Figure 6.5 A and B) but does bind P*Rv*3133c and P*Rv*3134c (Figure 6.5 C and D, lanes 5-7).

6.4 Discussion

As discussed in Chapter 4, WhiB1 has been shown to be a nitric oxide-responsive transcription factor capable of binding to its own promoter (P*whiB1*) and repressing its transcription (Smith *et al*., 2010). The work in this chapter has identified a second gene regulated by WhiB1, *groEL2*. *Mycobacterium tuberculosis* has two chaperonin genes; *groEL1* (*Rv3417c*), which is dispensable and located downstream of *whiB3* (*Rv3416*), encoding a member of the Wbl family of proteins, and the essential *groEL2* (*Rv0440*) (Sassetti *et al*., 2003). Chaperonin proteins function in the sequestration and re-folding of mis-folded proteins in a chamber formed from two stacked heptameric rings of

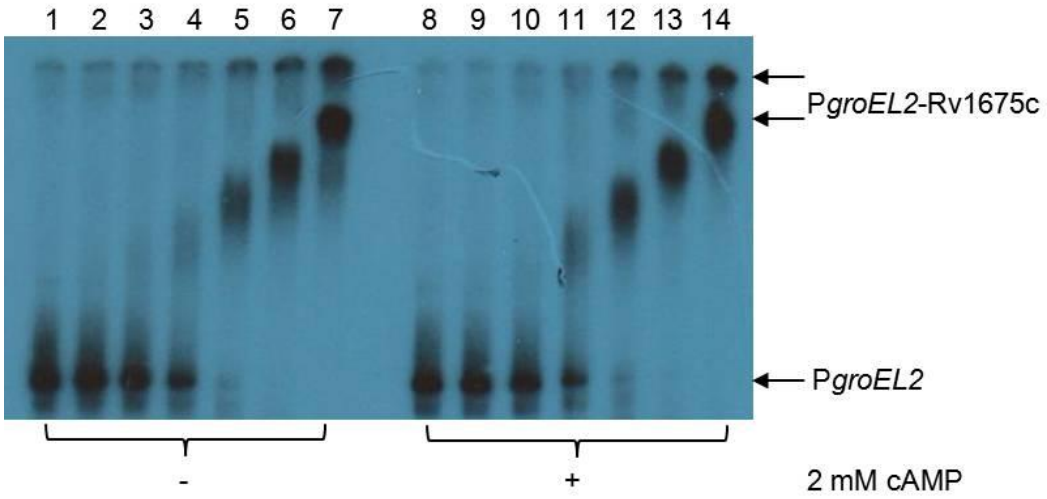

Figure 6.4: Binding of Rv1675c at the *groEL2* promoter (P*groEL2*) is independent of cAMP. Radiolabelled P*groEL2* was incubated with increasing concentrations of Rv1675c, with or without cAMP as indicated, before separation of protein-DNA complexes (P*groEL2*-Rv1675c) from free DNA (P*groEL2*) by electrophoresis. Lanes 1 and 8, no protein; lanes 2-7 and 9-14 contain, 0.5, 1, 2, 4, 8 and 16 μM Rv1675c respectively. The locations of P*groEL2* and P*groEL2*-Rv1675c are indicated.

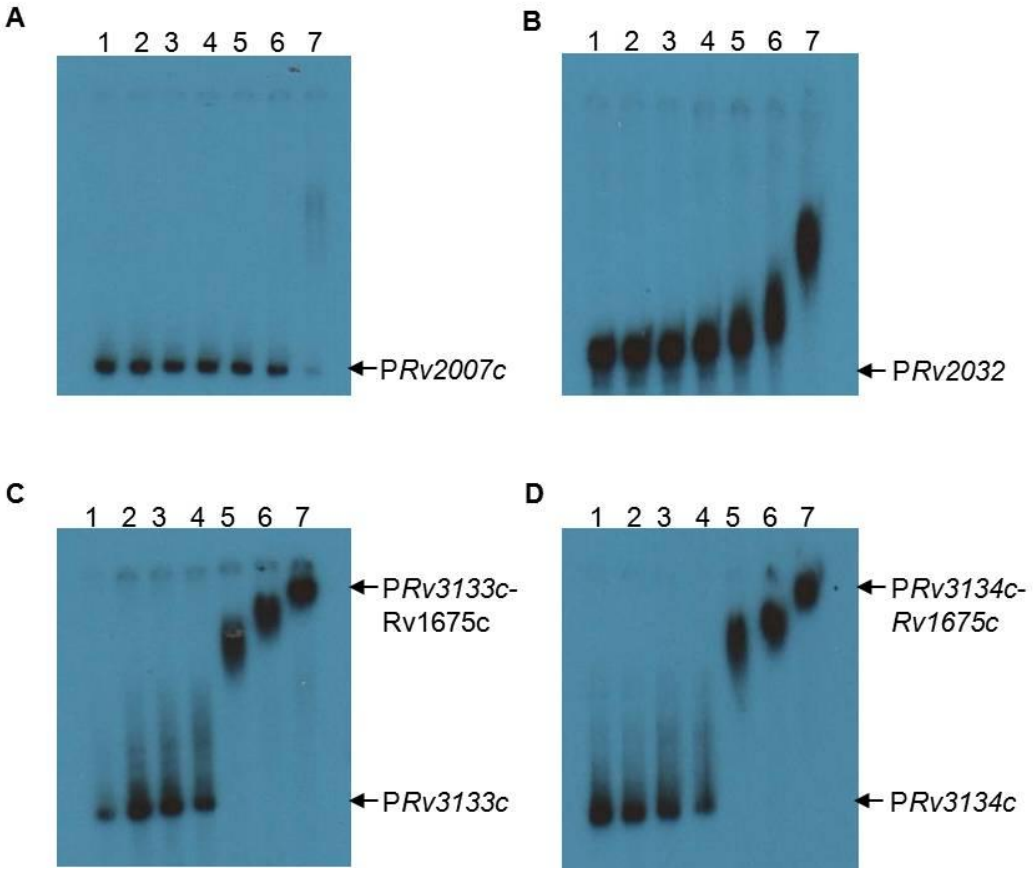

Figure 6.5: DNA-binding properties of Rv1675c with different promoters. Radiolabelled P*Rv2007c* **(A)**, P*Rv2032* **(B)**, P*3133c* **(C)** or P*3134c* **(D)** was incubated with increasing concentrations of Rv1675c before separation of protein-DNA complexes from free DNA by electrophoresis. Lanes 1, no protein; lanes 2-7 contain, 0.5, 1, 2, 4, 8 and 16 μM Rv1675c respectively. The location of free DNA (P*Rv2007c*, P*Rv2032*, P*3133c* or P*3134c*) and protein-DNA complexes (P*Rv3133c*-Rv1675c or P*Rv3134c*-Rv1675c) are indicated.

GroEL capped by GroES. Refolding can then occur in a process requiring ATP hydrolysis (Lund, 2009). GroEL2 from *M. tuberculosis* however, does not form such a structure but is dimeric and lacks ATPase activity (Qamra and Mande, 2004). GroEL2 from *M. tuberculosis* has been shown to be highly antigenic whereby monocytes having phagocytosed mycobacteria are known to present GroEL2 on their cell surface to T lymphocytes (Friedland *et al*., 1993). Cytotoxic $CD4^+$ cells may then lyse the GroEL2 expressing monocytes (Ottenhoff *et al*., 1988). GroEL2 has also been shown to stimulate the release of cytokines interleukin-10 and tumour necrosis factor-α from monocytes in a CD14-independent manner (Friedland *et al*., 1993; Lethwaite *et al*., 2001). Thus GroEL2, unlike other chaperonins, has a role in modulating the immune environment.

Here, it is shown that apo-WhiB1 binds the *groEL2* promoter region (Figure 6.1A) and that this binding is specific (Section 6.2; Stapleton *et al*., 2012). As shown for binding at the *whiB1* promoter (Chapter 4; Smith *et al*., 2010), binding at P*groEL2* saturated over a narrow range of apo-WhiB1 concentrations, consistent with cooperative interactions with the DNA. This implies the presence of more than one apo-WhiB1 binding site. The entire of the *Rv0439c-Rv0440* intergenic region was required for DNA binding by apo- and nitrosylated-WhiB1 binding, indicating its importance in forming a stable nucleoprotein complex and the likelihood of there being at least two binding sites for WhiB1 (Stapleton *et al*., 2012). DNase I footprinting identified only one locus of apo-WhiB1 binding at P*groEL2*, overlapping the -35 element, similar to that for binding at P*whiB1* (Stapleton *et al*., 2012; Smith *et al*; 2010). *In vitro* transcription assays showed apo-WhiB1 represses transcription of *groEL2*, which taken with the footprinting data, suggests that repression is by promoter occlusion (Stapleton *et al*., 2012; Figure 6.6). Due to the essential nature of the GroEL2 chaperonin, down-regulation of *groEL2* expression by WhiB1 in the presence of nitric oxide should therefore inhibit growth of *M. tuberculosis*. This may assist with entry into the dormant state. Furthermore, GroEL2 is highly antigenic and repression of its transcription by WhiB1 in the presence of nitric oxide, an important signal associated with infection, may aid in evasion of the immune response and promote the entrance into dormancy.

Regulation of *groEL2* expression has been attributed to a number of other regulatory pathways. Expression was increased upon heat shock in a process involving the repressor protein HrcA, and lowered in response to Mg(II)-starvation (Stewart *et al*.,

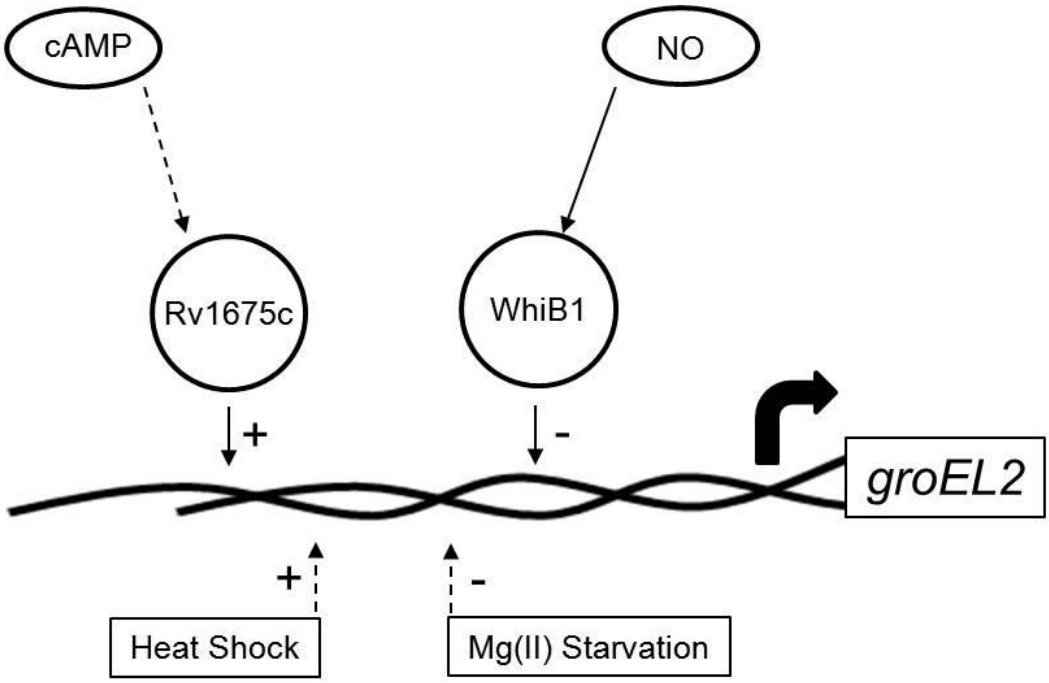

Figure 6.6: Model depicting the complex regulation of *groEL2* expression. Expression of *groEL2* is increased upon heat shock and decreased during Mg(II) starvation (Stewart *et al*., 2002; Walters *et al*., 2006). These effects on expression are indirect. Expression of *groEL2* is directly repressed by WhiB1 in response to nitric oxide *in vitro*. Rv1675c directly activates *groEL2* expression *in vitro* and this effect is independent of cAMP. An as of yet unidentified regulator may mediate the effect of cAMP on Rv1675c.

2002; Walters *et al*., 2006). The important signalling molecule cAMP has also been shown to have an effect on the regulation of expression of *groEL2*. Addition of exogeneous cAMP to *Mycobacterium bovis* BCG cultures increased the expression of a number of genes including *groEL2.* This effect was more pronounced under low oxygen conditions, suggesting a possible role for cAMP regulation during host infection (Gazdik and McDonough, 2005). This is further supported by experiments showing *groEL2* transcription was increased after 24 hour macrophage infection (Li *et al*., 2001). Rv1675c, a member of the cAMP receptor protein family, has also been shown to regulate *groEL2* expression whereby in a *Rv1675c* mutant strain of *M. bovis* BCG, expression of *groEL2* was reduced two hours into macrophage infection (Gazdik *et al*., 2009). Direct binding of Rv1675c to the *groEL2* promoter *in vitro* was also seen (Gazdik *et al*., 2009). This direct binding has been confirmed here, and was shown to be unaffected by cAMP (Section 6.3.3; Figure 6.4). *In vitro* transcription reactions showed that Rv1675c activates *groEL2* transcription and this occurs in the absence of cAMP, suggesting that Rv1675c does not directly mediate the cAMP effect on *groEL2* expression (Stapleton *et al*., 2012; Figure 6.6).

Expression of the other known target of WhiB1, *whiB1*, also responds to cAMP via the cAMP receptor protein CRP (Rv3676) (Rickman *et al*., 2005; Stapleton *et al*., 2010). Expression of *whiB1* has recently been shown to be 11-fold upregulated in the presence of cAMP (Larsson *et al.*, 2012). Activation by cAMP-CRP is however inhibited by apo-WhiB1, thus WhiB1 negatively autoregulates its own expression (Smith *et al*., 2010; Stapleton *et al*., 2010). It is therefore possible that the cAMP-mediated effects on *groEL2* expression observed *in vivo* (Gazdik and McDonough, 2005) arise, at least in part, from the CRP-mediated regulation of *whiB1*.

Work here has shown that both the known WhiB1 targets, *whiB1* and *groEL2*, are linked to cAMP signalling. cAMP is an important signalling molecule in *M. tuberculosis* gene regulation (Gazdik and McDonough, 2005; Rickman *et al*., 2009; Stapleton *et al*., 2010) and upon infection of macrophages, mycobacterial cAMP has been shown to promote bacterial survival by subverting host signalling pathways (Agarwal *et al*., 2009). The interaction between cAMP-responsive regulators and the nitric oxide-responsive WhiB1 protein may provide a mechanism to integrate the transcriptional response to two important signals associated with infection. The interplay of these regulators, as well as their effects on the expression of the essential

chaperonin GroEL2 can be further analysed to get a better understanding of gene regulation in *M. tuberculosis* infection.

Recent DNA microarray data have shown Rv1675c to negatively regulate a number of other genes, all of which are found in the DosRS regulon (D. Hunt, unpublished data). It was of interest to establish whether Rv1675c directly regulates these genes. As seen in Figure 6.5 (panels A and B), Rv1675c did not show direct binding to *Rv2007c* (*fdxA* encoding a ferredoxin) or *Rv2032* (an acr-coregulated gene of unknown function). It did however bind to *Rv3133c*, encoding the regulator DosR of the 2-component DosRS system (Figure 6.5C). Interestingly, it also bound *Rv3134c*, which encodes a gene of unknown function but may play a role in the phosphorelay of the DosRS system (Figure 6.5D). It appears likely that Rv1675c regulates the set of genes seen in the microarray data via the DosRS regulon. It could do this by binding to the promoter of *dosR* and *Rv3134c*. Further DNA-binding experiments with other genes controlled by the DosRS regulon, as well as the genes encoding the DosRS system will provide further information on the role of Rv1675c in its regulation. DNase I footprinting and *in vitro* transcription reactions will also provide a better insight into the breadth of Rv1675c influence on *M. tuberculosis* gene expression and the interplay with other regulators. The DosRS regulon is involved in the programming of the dormancy state of *M. tuberculosis*, responding to the important infection signals of nitric oxide and hypoxia (Voskuil *et al*., 2003). Non-toxic concentrations of nitric oxide induce a 48-gene regulon, via the response regulator DosR to inhibit aerobic respiration and slow replication of cells (Voskuil *et al*., 2003). The regulon is controlled by a 3-component regulatory-system with two sensor kinases, DosS (redox sensor) and DosT (hypoxia sensor), which bind nitric oxide, carbon monoxide and oxygen (Kumar *et al*., 2007) and the DosR regulator. As well as the control by these important signalling gases, there are multiple regulatory sequences upstream of *Rv3134c*, which is directly upstream of *dosR* (Leistikow *et al*., 2010). This suggests complex regulation by a number of different regulators, including Rv1675c shown here.

Work here has identified the importance of the NO-responsive transcription factor WhiB1 and the cAMP-responsive Rv1675c in regulating the essential chaperonin *groEL2* (Figure 6.6) and the role of Rv1675c in regulating the dormancy regulon. These two regulators, in response to the important infection signals of NO and cAMP, may be essential in regulating the dormancy programming of *M. tuberculosis* and thus play a

role in the infection process. Work to further understand their roles in regulating these genes, as well as their combined interactions, may provide important insights into the complex process of dormancy.

7.0 Discussion

The work presented here has identified WhiB1 as an iron-sulphur cluster binding transcription factor, requiring all four cysteine residues for cluster incorporation (Smith *et al*., 2010; 2012). The iron-sulphur cluster reacts rapidly with nitric oxide, probably forming an octa-nitrosylated cluster in a multiphasic reaction (Crack *et al*., 2011). Reaction of holo-WhiB1 with nitric oxide, converts WhiB1 from a non-DNA binding form to a form capable of binding both the *whiB1* and *groEL2* promoters (Smith *et al*., 2010; Stapleton *et al*., 2012). Apo-WhiB1, both oxidised and reduced, also bound these promoter DNAs. WhiB1 is capable of repressing its own transcription *in vitro*, and that of *groEL2* also. Thus it is concluded that the iron-sulphur cluster of WhiB1 is a sensor of nitric oxide, and that exposure to nitric oxide converts holo-WhiB1 from a non-DNA-binding form into a form capable of regulating transcription (Crack *et al*., 2011; Smith *et al*., 2010; Stapleton *et al*., 2012).

The work described here and elsewhere raises a new set of questions about the role of WhiB1 in the infection process of *M. tuberculosis*. The *whiB1* gene has been identified as essential for *M. tuberculosis* survival (Smith *et al*., 2010), thus one of the most important questions is 'why?'. Is WhiB1 itself essential or does it regulate a subset of genes which are themselves essential? The reason for the essential nature of *whiB1* is not established, but one possibility is that sufficient nitric oxide is present under the conditions tested to activate *whiB1*, possibly regulating genes essential in nitric oxide detoxification. It has been shown here that apo-WhiB1, both oxidised and reduced, as well as nitric oxide-treated holo-WhiB1 are capable of DNA binding and transcriptional repression *in vitro*. If axenic cultures do not produce sufficient nitric oxide to activate WhiB1, then its essentiality implies that the holo-form of WhiB1 may regulate as yet unidentified essential gene(s). The transcription factor IscR for example, regulates distinct groups of genes in its [2Fe-2S] holo- form and apo-form (Nesbit *et al*., 2009). The alternative forms of WhiB1 may specifically regulate overlapping sets of genes, which could explain its essential nature.

The role of WhiB1 in the global transcriptional network also remains to be fully understood. As discussed in detail in Chapter 4, there is a complex interplay between

the cAMP receptor protein, CRP^{MT} (Rv3676) and WhiB1 in controlling *whiB1* expression. Thus dual regulation of *whiB1* expression by the cAMP-responsive CRP^{MT} and the nitric oxide responsive WhiB1 protein provides a mechanism for integrating two important infection-associated signals, suggesting that in the environment of the macrophage (high nitric oxide and cAMP levels) transcription of the essential transcription factor *whiB1* will be inhibited. This is consistent with entry into the dormant state. At low nitric oxide concentrations (related to the immunocompromised state), holo-WhiB1 is formed, de-repressing *whiB1* transcription, consistent with emergence from dormancy (Smith *et al*., 2010). The WhiB1 protein may also coordinate the response to hypoxia, due to the presence of its iron-sulphur cluster thereby incorporating a third signal associated with infection into the network. Although the cluster appears stable in the presence of molecular oxygen, it may respond to reactive oxygen species such as superoxide and hydrogen peroxide that are more abundant in an aerobic environment. In low oxygen and nitric oxide levels, associated with the hypoxic granuloma and emergence from dormancy, holo-WhiB1 may activate genes for survival and then de-repress its own transcription to aid in emergence. Figure 7.1 shows WhiB1 at the centre of transcriptional regulation in response to various signals and regulators. The diagram shows several key regulators discussed in Chapter 1 and the signals they respond to, in order to alter gene expression. WhiB1, and the other WhiB proteins (except WhiB5 as it is not known what it responds to) are shown to respond at some level to the three infection signals of hypoxia/nutrient starvation, oxidative/nitric oxide stress, and cAMP. The differences in their responses to these signals indicate a different role for each of the proteins, but all may regulate a different subset of genes to promote different stages of the infection; from phagocytosis by macrophages (WhiB1, 3, 6 and 7), to entry into dormancy (WhiB1, 2, 3 and 4), and then emergence from the dormant state (WhiB1). These proteins, along with the regulators involved in dormancy (DosR/S/T, PhoPR, EHR) and cAMP signalling (CRP^{MT} – Rv3676 and Cmr – Rv1675c), are all necessary for the complex gene regulation necessary for tuberculosis pathogenesis. The data presented in Chapter 6, showing how Cmr (Rv1675c) binds upstream of the *Rv3134c* gene that is located directly upstream of the DosR regulator, and upstream of the gene encoding the DosR regulator itself (*Rv3133c*), may highlight a link between the response to cAMP and hypoxia. *In vitro* transcription assays to determine whether Cmr can activate or repress these Dos genes, will help provide further information on the integration of cAMP and hypoxia signalling. Understanding the interplay between all these regulators will provide fresh insight on how

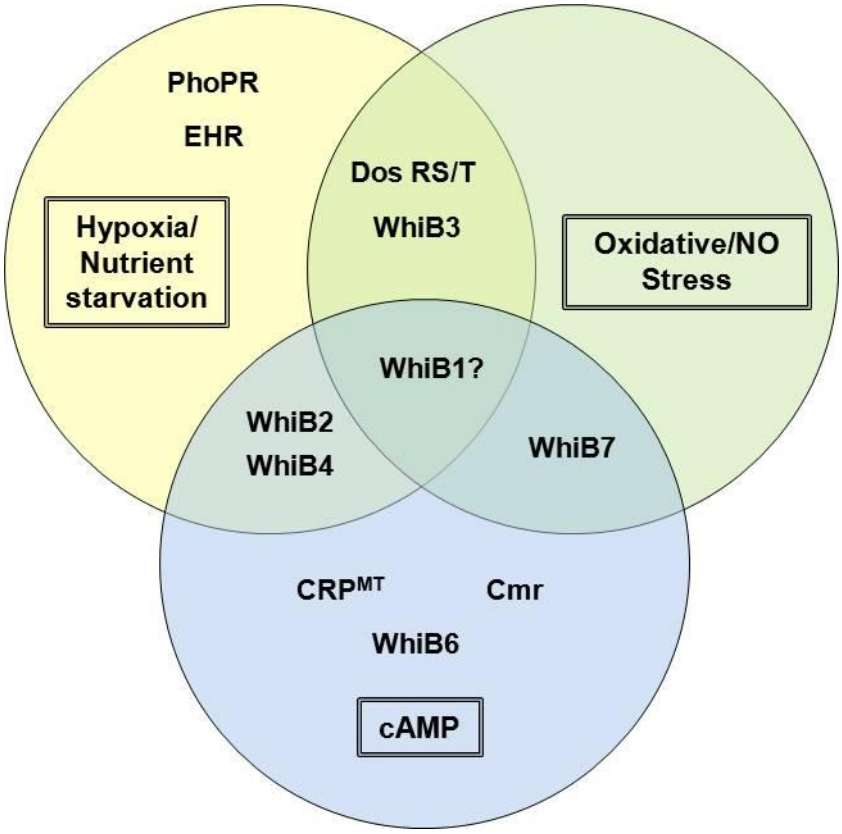

Figure 7.1: Linking the transcriptional regulators of *M. tuberculosis* and their signals. *Mycobacterium tuberculosis* undergoes extensive changes in gene expression during infection, with a number of transcriptional regulators responding to the different environments experienced. A selection of transcriptional regulators and their signals are shown here, to illustrate the complex network employed by *M. tuberculosis* to succeed as a pathogen.

M.tuberculosis enters and emerges from the persistent state, including the role of WhiB1 in this process.

In conclusion, and as discussed in Chapter 4, the essential nature of *whiB1* and the change in DNA-binding ability in response to nitric oxide has implications in the control of *M. tuberculosis* gene expression in the host environment (Smith *et al*., 2010). Although high concentrations of nitric oxide kill *M. tuberculosis* (Darwin *et al*., 2003), lower concentrations have been shown to promote entry into the persistent state (Voskuil *et al*., 2003). Nitric oxide sensing and the reprogramming of gene expression by WhiB1 could therefore contribute to developmental adaptations by *M. tuberculosis* in response to host-generated nitric oxide during infection. WhiB1 is therefore a potential target for new and more efficient treatment of tuberculosis.

8.0 References

Agarwal, N., Raghunand, T.R. and Bishai, W.R. (2006) Regulation of the expression of *whiB1* in *Mycobacterium tuberculosis*: role of cAMP receptor protein. *Microbiology*, **152**: 2749-2756.

Agarwal, N., Lamichhane, G., Gupta, R., Nolan, S. and Bishai, W.R. (2009) Cyclic AMP intoxication of macrophages by a *Mycobacterium tuberculosis* adenylate cyclase. *Nature* **460**, 98-102.

Alam, M.S., Garg, S.K. and Agrawal, P. (2007) Molecular function of WhiB4/Rv3681c of *Mycobacterium tuberculosis* H37Rv: a [4Fe-4S] cluster co-ordinating protein disulphide reductase. *Molecular Microbiology*, **63**: 1414-1431.

Alam, M.S. and Agrawal, P. (2008) Matrix-assisted refolding and redox properties of WhiB3/Rv3416 of *Mycobacterium tuberculosis* H37Rv. *Protein Expression and Purification*, **61**: 83-91.

Alam, M.S., Garg, S.K. and Agrawal, P. (2009) Studies on structural and functional divergence among seven WhiB proteins of *Mycobacterium tuberculosis* H37Rv. *FEBS Journal*, **276**: 76-93.

Bai, G., McCue, L.A. and McDonough, K.A. (2005) Characterization of *Mycobacterium tuberculosis* Rv3676 (CRP^{MT}), a cyclic AMP receptor protein-like DNA binding protein. *Journal of Bacteriology*, **187**: 7795-7804.

Bai, G., Schaak, D.D. and McDonough, K.A. (2009) cAMP levels within *Mycobacterium tuberculosis* and *Mycobacterium bovis* BCG increase upon infection of macrophages. *FEMS Immunology and Medical Microbiology*, **55**: 68-73.

Bai, G., Knapp, G.S. and McDonough, K.A. (2011) Cyclic AMP signalling in mycobacteria: redirecting the conversation with a common currency. *Cellular Microbiology*, **13**: 349-358.

Banaiee, N., Jacobs, W.R. and Ernst, J.D. (2006) Regulation of *Mycobacterium tuberculosis whiB3* in the mouse lung and macrophages. *Infection and Immunity*, **74**: 6449-6457.

Bates, D.M., Popescu, C.V., Khoroshilova, N., Vogt, K., Beinert, H., Münck, E. and Kiley, P.J. (2000) Substitution of leucine 28 with histidine in the *Escherichia coli* transcription factor FNR results in increased stability of the $[4Fe\text{-}4S]^{2+}$ cluster to oxygen. *Journal of Biological Chemistry*, **275**: 6234-6240.

Bentley, S.D., Chater, K.F., Cerdeno-Tarraga, A.M., Challis, G.L., Thomson, N.R., James, K.D., Harris, D.E., Quail, M.A., Kieser, H., Harper, D., Bateman, A., Brown, S., Chandra, G., Chen, C.W., Collins, M., Cronin, A., Fraser, A., Goble, A., Hidalgo, J., Hornsby, T., Howarth, S., Huang, C.H., Kieser, T., Larke, L., Murphy, L., Oliver, K., O'Neil, S., Rabbinowitsch, E., Rajandream, M.A., Rutherford, K., Rutter, S., Seeger, K., Saunders, D., Sharp, S., Squares, R., Squares, S., Taylor, K., Warren, T., Wietzorrek, A., Woodward, J., Barrell, B.G., Parkhill, J. and Hopwood, D.A. (2002) Complete genome sequence of the model actinomycetes *Streptomyces coelicolor* A3(2). *Nature*, **417**: 141-147.

Bentley, S.D., Brown, S., Murphy, L.D., Harris, D.E., Quail, M.A., Parkhill, J., Barrell, B.G., McCormick, J.R., Santamaria, R.I., Losick, R., Yamasaki, M., Kinashi, H., Chen, C.W., Chandra, G., Jakimowicz, D., Kieser, H.M., Kieser, T. and Chater, K.F. (2004) SCP1, a 356,023 bp linear plasmid adapted to the ecology and developmental biology of its host, *Streptomyces coelicolor* A3(2). *Molecular Microbiology*, **51**: 1615-1628.

Betts, J.C., Lukey, P.T., Robb, L.C., McAdam, R.A. and Duncan, K. (2002) Evaluation of a nutrient starvation model of *Mycobacterium tuberculosis* persistence by gene and protein expression profiling. *Molecular Microbiology*, **43**: 717-731.

Bloom, B.R. and Murray, C.J.L. (1992) Tuberculosis: Commentary on a reemergent killer. *Science*, **257**: 1055-1064.

Boon, C. and Dick, T (2002) *Mycobacterium bovis* BCG response regulator essential for hypoxic dormancy. *Journal of Bcteriology*, **184**: 6760-6767.

Bradford, M.M. (1976) A rapid and sensitive method for the quantitation of microgram quantities of protein utilizing the principle of protein-dye binding. *Analytical Biochemistry*, **72**: 248-254.

Burian, J., Ramón-Garcia, S., Sweet, G., Gómez-Velasco, A., Av-gay, Y. and Thompson, C.J. (2012) The mycobacterial transcriptional regulator *whiB7* gene links redox homeostasis and intrinsic antibiotic resistance. *Journal of Biological Chemistry*, **287**: 299-310.

Casonato, S., Sánchez, A.C., Haruki, H., González, M.R., Provvedi, R., Dainese, E., Jaouen, T., Gola, S., Bini, E., Vicente, M., Johnsson, K., Ghisotti, D., Palù, G., Hernández-Pando, R. and Manganelli, R. (2012) WhiB5: a transcriptional regulator contributing to *Mycobacterium tuberculosis* virulence and reactivation. *Infection and Immunity*, **80**: 3132-3144.

Chater, K.F. (1972) A morphological and genetic mapping study of white colony mutants of *Streptomyces coelicolor*. *Journal of General Microbiology*, **72**: 9-28.

Cole, S.T., Brosch, R., Parkhill, J., Garnier, T., Churcher, C., Harris, D., Gordon, S.V., Eiglmeier, K., Gas, S., Barry, C.E., Tekaia, F., Badcock, K., Basham, D., Brown, D., Chillingworth, T., Connor, R., Davies, R., Devlin, K., Feltwell, T., Gentles, S., Hamlin, N., Holroyd, S., Hornsby, T., Jagels, K., Krogh, A., McLean, J., Moule, S., Murphy, L., Oliver, K., Osborne, J., Quail, M.A., Rajandream, M.A., Rogers, J., Rutter, S., Seeger, K., Skelton, J., Squares, R., Squares, S., Sulston, J.E., Taylor, K., Whitehead, S. and Barrell, B.G. (1998) Deciphering the biology of *Mycobacterium tuberculosis* from the complete genome sequence. *Nature*, **393**: 537-544.

Comas, I. And Gagneux, S. (2009) The past and future of tuberculosis research. *Public Library of Science Pathogens*, **5**: e1000600.

Couture, M., Yeh, S.R., Wittenberg, B.A., Wittenberg, J.B., Ouellet, Y., Rousseau, D.L. and Guertin, M. (1999) A cooperative oxygen-binding hemoglobin from

Mycobacterium tuberculosis. *Proceedings of the National Academy of Science USA*, **96**: 11223-11228.

Crack, J.C., Green, J. and Thomson, A.J. (2004) Mechanism of oxygen sensing by the bacterial transcription factor fumarate-nitrate reduction (FNR). *Journal of Biological Chemistry*, **279**: 9278-9286.

Crack, J.C., den Hengst, C.D., Jakimowicz, P., Subramanian, S., Johnson, M.K., Buttner, M.J., Thomson, A.J. and Le Brun, N.E. (2009) Characterization of [4Fe-4S]-containing and cluster-free forms of *Streptomyces* WhiD. *Biochemistry*, **48**: 12252-12264.

Crack, J.C., Smith, L.J., Stapleton, M.R., Peck, J., Watmough, N.J., Buttner, M.J., Buxton, R.S., Green, J., Oganesyan, V.S., Thomson, A.J. and Le Brun, N.E. (2011) Mechanistic insight into the nitrosylation of the [4Fe-4S] cluster of WhiB-like proteins. *Journal of the American Chemical Society*, **133**: 1112-1121.

Crack, J.C., Green, J., Hutchings, M.I., Thomson, A.J. and Le Brun, N.E. (2012) Bacterial iron-sulfur regulatory proteins as biological sensor-switches. *Antioxidants and Redox Signaling*, doi: 10.1089/ars.2012.4511.

Cruz-Ramos, H., Crack, J., Wu, G., Hughes, M.N., Scott, C., Thomson, A.J., Green, J. and Poole, R.K. (2002) Nitric oxide-sensing by FNR: regulation of the *Escherichia coli* nitric oxide-detoxifying flavohaemoglobin, Hmp. *EMBO Journal*, **21**: 3235-3244.

Daffé, M. and Draper, P. (1998) The envelope layers of mycobacteria with reference to their pathogenicity. *Advances in Microbial Physiology*, **39**: 131-203.

Daniel, J., Deb, C., Dubey, V.S., Sirakova, T.D., Abomoelak, B., Morbidoni, H.R. and Kolattukudy, P.E. (2004) Induction of a novel class of diacylglycerol acyltransferases and triacylglycerol accumulation in *Mycobacterium tuberculosis* as it goes into a dormancy-like state in culture. *Journal of Bacteriology*, **186**: 5017-5030.

Daniel, T.M. (2006) The history of tuberculosis. *Respiratory Medicine*, **100**: 1862-1870.

Darwin, K.H., Ehrt, S., Gutierrez-Ramos, J.C., Weich, N. and Nathan, C.F. (2003) The proteasome of *Mycobacterium tuberculosis* is required for resistance to nitric oxide. *Science*, **302**: 1963-1966.

Davis, N.K. and Chater, K.F. (1992) The *Streptomyces coelicolor whiB* gene encodes a small transcription factor-like protein dispensable for growth but essential for sporulation. *Molecular and General Genetics*, **232**: 351-358.

den Hengst, C.D. and Buttner, M.J. (2008) Redox control in actinobacteria. *Biochimica et Biophysica Acta*, **1780**: 1201-1216.

Deretic, V., Singh, S., Master, S., Harris, J., Roberts, E., Kyei, G., Davis, A., de haro, S., Naylor, J., Lee, H.H. and Vergne, I. (2006) *Mycobacterium tuberculosis* inhibition of phagolysosome biogenesis and autophagy as a host defence mechanism. *Cellular Microbiology*, **8**: 719-727.

Ding, H. and Demple, B. (2000) Direct nitric oxide signal transduction via nitrosylation of iron-sulfur clusters in the SoxR transcription factor. *Proceedings of the National Academy of Science USA*, **97**: 5146-5150.

Dye, C. (2006) Global epidemiology of tuberculosis. *The Lancet*, **367**: 938-940.

Ehrlich, P. (1882) Aus dem Verein für innere Medicin zu Berlin. *Deutsche Medizinische Wochenschrift*, **8**: 269-270.

Flärdh, K., Findlay, K.C. and Chater, K.F. (1999) Association of early sporulation genes with suggested developmental decision points in *Streptomyces coelicolor* A3(2). *Microbiology*, **145**: 2229-2243.

Fowler-Goldsworthy, K., Gust, B., Mouz, S., Chandra, G., Findlay, K.C. and Chater, K.F. (2011) The actinobacteria-specific gene *wblA* controls major

developmental transitions in *Streptomyces coelicolor* A3(2). *Microbiology*, **157**: 1312-1328.

Friedland, J.S., Shattock, R., Remick, D.G. and Griffen, G.E. (1993) Mycobacterial 65-kD heat shock protein induces release of proinflammatory cytokines from human monocytic cells. *Clinical and Experimental Immunology*, **91**: 58-62.

Frigui, W., Bottai, D., Majlessi, L., Monot, M., Josselin, E., Brodin, P., Garnier, T., Gicquel, B., Martin, C., Leclerc, C., Cole, S.T., Brosch, R. (2008) Control of *M. tuberculosis* ESAT-6 secretion and specific T cell recognition by PhoP. *Public Library of Science Pathogens*, **4**: e33.

Garg, S.K., Alam, M.S., Soni, V., Kishan, K.V.R. and Agrawal, P. (2007) Characterization of *Mycobacterium tuberculosis* WhiB1/Rv3219 as a protein disulphide reductase. *Protein Expression and Purification*, **52**: 422-432.

Garg, S., Alam, M.S., Bajpai, R., Kishan, K.R. and Agrawal, P. (2009) Redox biology of *Mycobacterium tuberculosis* H37Rv: protein-protein interaction between GlgB and WhiB1 involves exchange of thiol-disulfide. *BMC Biochemistry*, **10**: 1.

Gazdik, M.A. and McDonough, K.A. (2005) Identification of cyclic AMP-regulated genes in *Mycobacterium tuberculosis* complex bacteria under low-oxygen conditions. *Journal of Bacteriology*, **187**: 2681-2692.

Gazdik, M.A., Bai, G., Wu, Y. and McDonough, K.A. (2009) Rv1675c (*cmr*) regulates intramacrophage and cyclic AMP-induced gene expression in *Mycobacterium tuberculosis*-complex mycobacteria. *Molecular Microbiology*, **71**: 434-448.

Geiman, D.E., Raghunand, T.R., Agarwal, N. and Bishai, W.R. (2006) Differential gene expression in response to exposure to antimycobacterial agents and other stress conditions among seven *Mycobacterium tuberculosis whiB*-like genes. *Antimicrobial Agents and Chemotherapy*, **50**: 2836-2841.

Gengenbacher, M. and Kaufmann, S.H.E. (2012) *Mycobacterium tuberculosis*: success through dormancy. *FEMS Microbiology Reviews*, **36**: 514-532.

Gomez, J.E. and Bishai, W.R. (2000) *whmD* is an essential mycobacterial gene required for proper septation and cell division. *Proceedings of the National Academy of Science USA*, **97**: 8554-8559.

Gonzalo-Asensio, J., Maia, C., Ferrer, N.L., Barilone, N., Laval, F., Soto, C.Y., Winter, N., Daffé, M., Gicquel, B., Martin, C. and Jackson, M. (2006) The virulence-associated two-component PhoP-PhoR system controls the biosynthesis of polyketide-derived lipids in *Mycobacterium tuberculosis*. *Journal of Biological Chemistry*, **281**: 1313-1316.

Gonzalo-Asensio, J., Mostowy, S., Harders-Westerveen, J., Huygen, K. Hernández-Pando, R., Thole, J., Behr, M., Gicquel, B. and Martin, C. (2008) PhoP: A missing piece in the intricate puzzle of *Mycobacterium tuberculosis* virulence. *Public Library of Science ONE*, **3**: e3496.

Green, J., Bennett, B., Jordan, P., Ralph, E.T., Thomson, A.J. and Guest, J.R. (1996) Reconstitution of the [4Fe-4S] cluster in FNR and demonstration of the aerobic-anaerobic transcription switch in vitro. *Biochemical Journal*, **316**: 887-892.

Gruner, I., Frädrich, C., Böttger, L.H., Trautwein, A.X., Jahn, D. and Härtig, E. (2011) Aspartate 141 is the fourth ligand of the oxygen-sensing $[4Fe\text{-}4S]^{2+}$ cluster of *Bacillus subtilis* transcriptional regulator Fnr. *Journal of Biological Chemistry*, **286**: 2017-2021.

Guo, M., Feng, H., Zhang, J., Wang, W., Wang, Y., Li, Y., Goa, C., Chen, H., Feng, Y. and He, Z.G. (2009) Dissecting transcription regulatory pathways through a new bacterial one-hybrid system. *Genome Research*, **19**: 1301-1308.

Heym, B. and Cole, S.T. (1997) Multidrug resistance in *Mycobacterium tuberculosis*. *International Journal of Antimicrobial Agents*, **8**: 61-70.

Holmgren, A. (1979) Thioredoxin catalyzes the reduction of insulin disulfides by dithiothreitol and dihydrolipoamide. *Journal of Biological Chemistry*, **254**: 9627-9632.

Homerová, D., Sevciková, J. and Kormanec, J. (2003) Characterization of the *Streptomyces coelicolor* A3(2) *wblE* gene, encoding a homologue of the sporulation transcription factor. *Folia Microbiologica (Praha)*, **48**: 489-495.

Jakimowicz, P., Cheesman, M.R., Bishai, W.R., Chater, K.F., Thomson, A.J. and Buttner, M.J. (2005) Evidence that the *Streptomyces* developmental protein WhiD, a member of the WhiB family, binds a [4Fe-4S] cluster. *Journal of Biological Chemistry*, **280**: 8309-8315.

Jervis, A.J., Crack, J.C., White, G., Artymiuk, P.J., Cheesman, M.R., Thomson, A.J., Le Brun, N.E. and Green, J. (2009) The O_2 sensitivity of the transcription factor FNR is controlled by Ser24 modulating the kinetics of [4Fe-4S] to [2Fe-2S] conversion. *Proceedings of the National Academy of Science USA*, **106**: 4659-4664.

Kang, S.H., Huang, J., Lee, H.N., Hur, Y.A., Cohen, S.N. and Kim, E.S. (2007) Interspecies DNA microarray analysis identifies *wblA* as a pleiotropic down-regulator of antibiotic biosynthesis in *Streptomyces*. *Journal of Bacteriology*, **189**: 4315-4319.

Keiser, T.L., Azad, A.K., Guirado, E., Bonacci, R. and Schlesinger, L.S. (2011) A comparative transcriptional study of the putative mannose donor biosynthesis genes in virulent *Mycobacterium tuberculosis* and attenuated *Mycobacterium bovis* BCG strains. *Infection and Immunity*, **79**: 4668-4673.

Kennedy, M.C., Antholine, W.E. and Beinert, H. (1997) An EPR investigation of the products of the reaction of cytosolic and mitochondrial aconitases with nitric oxide. *Journal of Biological Chemistry*, **272**: 20340-20347.

Konar, M., Alam, M.S., Arora, C. and Agrawal, P. (2012) A cell division associated protein WhiB2/Rv3260c of *Mycobacterium tuberculosis* H37Rv has properties of a chaperone. *The FEBS Journal*, **279**: 2781-2792.

Kumar, A., Toledo, J.C., Patel, R.P., Lancaster, J.R. and Steyn, A.J. (2007) *Mycobacterium tuberculosis* DosS is a redox sensor and DosT is a hypoxia sensor. *Proceedings of the National Academy of Sciences USA*, **104**: 11568-11573.

Laemmli, U.K. (1970) Cleavage of structural proteins during the assembly of the head of bacteriophage T4. *Nature*, **227**: 680-685.

Larsson, C., Luna, B., Ammerman, N.C., Maiga, M., Agarwal, N. and Bishai, W.R. (2012) Gene expression of *Mycobacterium tuberculosis* putative transcription factors *whiB1-7* in redox environments. *Public Library of Science ONE*, **7**: e37516.

Leistikow, R.L., Morton, R.A., Bartek, I.L., Frimpong, I., Wagner, K. and Voskuil, M.I. (2010) The *Mycobacterium tuberculosis* DosR regulon assists in metabolic homeostasis and enables rapid recovery from nonrespiring dormancy. *Journal of Bacteriology*, **192**: 1662-1670.

Lewthwaite, J.C., Coates, A.R., Tormay, P., Singh, M., Mascagni, P., Poole, S. Roberts, M., Sharp, L. and Henderson, B. (2001) *Mycobacterium tuberculosis* chaperonin 60.1 is a more potent cytokine stimulator than chaperonin 60.2 (Hsp 65) and contains a CD14-binding domain. *Infection and Immunity*, **69**: 7349-7355.

Li, M.S., Monahan, I.M., Waddell, S.J., Mangan, J.A., Martin, S.L., Everett, M.J. and Butcher, P.D. (2001) cDNA-RNA subtractive hybridization reveals increased expression of mycocerosic acid synthase in intracellular *Mycobacterium bovis* BCG. *Microbiology*, **147**: 2293-2305.

Lund, P.A. (2009) Multiple chaperonins in bacteria – why so many? *FEMS Microbiology Reviews*, **33**: 785-800.

Matteelli, A., Migilori, G.B., Cirillo, D., Centis, R., Girard, E. and Raviglion, M. (2007) Multidrug-resistant and extensively drug-resistant *Mycobacterium tuberculosis*: epidemiology and control. *Expert Review of Anti-Infective Therapy*, **5**: 857-871.

Maxam, A.M. and Gilbert, W. (1980) Sequencing and end-labelled DNA with base specific chemical cleavage. *Methods in Enzymology*, **65**: 499-560.

McCue, L.A., McDonough, K.A. and Lawrence, C.E. (2000) Functional classification of cNMP-binding proteins and nucleotide cyclases with implications for

novel regulatory pathways in *Mycobacterium tuberculosis*. *Genome Research*, **10**: 204-219.

McDonough, K.A. and Rodriguez, A. (2011) The myriad roles of cyclic AMP in microbial pathogens: from signal to sword. *Nature Reviews Microbiology*, **10**: 27-38.

McVittie, A. (1974) Ultrastructural studies on sporulation in wild-type and white colony mutants of *Streptomyces coelicolor*. *Journal of General Microbiology*, **8**: 291-302.

Molle, V., Palframan, W.J., Findlay, K.C. and Buttner, M.J. (2000) WhiD and WhiB, homologous proteins required for different stages of sporulation in *Streptomyces coelicolor* A3(2). *Journal of Bacteriology*, **182**: 1286-1295.

Morris, R.P., Nguyen, L., Gatfield, J., Visconti, K., Nguyen, K., Scnappinger, D., Ehrt, S., Liu, Y., Heifets, L., Pieters, J., Schoolnik, G. and Thompson, C.J. (2005) Ancestral antibiotic resistance in *Mycobacterium tuberculosis*. *Proceedings of the National Academy of Science USA*, **102**: 12200-12205.

Mukamolova, G.V., Turapov, O.A., Young, D.I., Kaprelyants, A.S., Kell, D.B. and Young, M. (2002) A family of autocrine growth factors in *Mycobacterium tuberculosis*. *Molecular Microbiology*, **46**: 623-635.

Nesbit, A.D., Giel, J.L., Rose, C.D. and Kiley, P.J. (2009) Sequence specific binding to a subset of IscR-regulated promoters does not require IscR Fe-S cluster ligation. *Journal of Molecular Biology*, **387**: 28-41.

Nikaido, H. and Jarlier, V. (1991) Permeability of mycobacterial cell wall. *Research in Microbiology*, **142**: 437-443.

Noss, E.H., Pai, R.K., Sellati, T.J., Radolf, J.D., Belisle, J., Golenbock, D.T., Boom, W.H. and Harding, C.V. (2001) Toll-like receptor 2-dependent inhibition of macrophage class II MHC expression and antigen processing by 19-kDa lipoprotein of *Mycobacterium tuberculosis*. *Journal of Immunology*, **167**:910-918.

Orme-Johnson, W.H. (1973) Iron-sulfur proteins: structure and function. *Annual Review of Biochemistry*, **42**: 159-204.

Ottenhoff, T.H.M., Kale, B., van Embden, J.D.A., Thole, J.E.R. and Kiessling, R. (1988) The recombinant 65-kD heat shock protein of *Mycobacterium bovis* bacillus Calmette-Guerin/*M. tuberculosis* is a target molecule for $CD4^+$ cytotoxic T lymphocytes that lyse human monocytes. *Journal of Experimental Medicine*, **168**: 1947-1952.

Ouellet, H., Ouellet, Y., Richard, C., Labarre, M., Wittenberg, B., Wittenberg, J. and Guertin, M. (2002) Truncated hemoglobin HbN protects *Mycobacterium bovis* from nitric oxide. *Proceedings of the National Academy of Science USA*, **99**: 5902-5907.

Park, H.D., Guinn, K.M., Harrell, M.I., Liao, R., Voskuil, M.I., Tompa, M., Schoolnik, G.K. and Sherman, D.R. (2003) Rv3133c/*dosR* is a transcription factor that mediates the hypoxic response of *Mycobacterium tuberculosis*. *Molecular Microbiology*, **48**: 833-843.

Pathania, R., Navani, N.K., Gardner, A.M., Gardner, P.R. and Dikshit, K.L. (2002) Nitric oxide scavenging and detoxification by the *Mycobacterium tuberculosis* haemoglobin, HbN in *Escherichia coli*. *Molecular Microbiology*, **45**: 1303-1314.

Pérez, E., Samper, S., Bordas, Y., Guilhot, C., Gicquel, B. and Martin, C. (2001) An essential role for *phoP* in *Mycobacterium tuberculosis* virulence. *Molecular Microbiology*, **41**: 179-187.

Qamra, R. and Mande, S.C. (2004) Crystal structure of the 65-kilodalton heat shock protein, chaperonin 60.2, of *Mycobacterium tuberculosis*. *Journal of Bacteriology*, **186**: 8105-8113.

Raghunand, T.R. and Bishai, W.R. (2006a) *Mycobacterium smegmatis whmD* and its homologue *Mycobacterium tuberculosis whiB2* are functionally equivalent. *Microbiology*, **152**: 2735-2747.

Raghunand, T.R. and Bishai, W.R. (2006b) Mapping essential domains of *Mycobacterium smegmatis* WhmD: insights into WhiB structure and function. *Journal of Bacteriology*, **188**: 6966-6976.

Reed, M.B., Gagneux, S., Deriemer, K., Small, P.M. and Barry, C.E. (2007) The W-Beijing lineage of *Mycobacterium tuberculosis* overproduces triglycerides and has the DosR dormancy regulon constitutively upregulated. *Journal of Bacteriology*, **189**: 2583-2589.

Reents, H., Gruner, I., Harmening, U., Böttger, L.H., Layer, G., Heathcote, P., Trautwein, A.X., Jahn, D. and Härtig, E. (2006) *Bacillus subtilis* Fnr senses oxygen via a [4Fe-4S] cluster coordinated by three cysteine residues without change in the oligomeric state. *Molecular Microbiology*, **60**: 1432-1445.

Rengarajan, J., Bloom, B.R. and Rubin, E.J. (2005) Genome-wide requirements for *Mycobacterium tuberculosis* adaptation and survival in macrophages. *Proceedings of the National Academy of Science USA*, 102: 8327-8332.

Rich, E.A., Torres, M., Sada, E., Finegan, C.K., Hamilton, B.D. and Toossi, Z. (1997) *Mycobacterium tuberculosis* (MTB)-stimulated production of nitric oxide by human alveolar macrophages and relationship of nitric oxide production to growth inhibition of MTB. *Tubercle and Lung Disease*, **78**: 247-255.

Rickman, L., Scott, C., Hunt, D.M., Hutchinson, T., Menéndez, M.C., Whalan, R., Hinds, J., Colston, M.J., Green, J. and Buxton, R.S. (2005) A member of the cAMP receptor protein family of transcription regulators in *Mycobacterium tuberculosis* is required for virulence in mice and controls transcription of the *rpfA* gene coding for a resuscitation promoting factor. *Molecular Microbiology*, **56**: 1274-1286.

Rohde, K.H., Abramovitch, R.B. and Russell, D.G. (2007a) *Mycobacterium tuberculosis* invasion of macrophages: linking bacterial gene expression to environmental cues. *Cell Host and Microbe*, **2**: 352-364.

Rohde, K., Yates, R.M., Purdy, G.E. and Russell, D.G. (2007b) *Mycobacterium tuberculosis* and the environment within the phagosome. *Immunological Reviews*, **219**: 37-54.

Russell, D.G. (2001) *Mycobacterium tuberculosis*: Here today, and here tomorrow. *Nature Reviews Molecular Cell Biology*, **2**: 569-586.

Russell, D.G. (2007) Who put the tubercle in tuberculosis? *Nature Reviews Microbiology*, **5**: 39-47.

Russell, D.G., Cardona, P.J., Kim, M.J., Allain, S. and Altare, F. (2009) Foamy macrophages and the progression of the human tuberculosis granuloma. *Nature Immunology*, **10**: 943-948.

Russell, D.G., Barry, C.E. and Flynn, J.L. (2010) Tuberculosis: What we don't know can, and does, hurt us. *Science*, **328**: 852-856.

Rustad, T.R., Harrell, M.I., Liao, R. and Sherman, D.R. (2008) The enduring hypoxic response of *Mycobacterium tuberculosis*. *Public Library of Sciences ONE*, **3**: e1502.

Rustad, T.R., Sherrid, A.M., Minch, K.J. and Sherman, D.R. (2009) Hypoxia: a window into *Mycobacterium tuberculosis* latency. *Cellular Microbiology*, **11**: 1151-1159.

Rybniker, J., Nowag, A., van Gumpel, E., Nissen, N., Robinson, N., Plum, G. and Hartmann, P (2010) Insights into the function of the WhiB-like protein of mycobacteriophage TM4 – a transcriptional inhibitor of WhiB2. *Molecular Microbiology*, **77**: 642-657.

Saini, V., Farhana, A. and Steyn, A.J.C. (2012) *Mycobacterium tuberculosis* WhiB3: A novel iron-sulfur cluster protein that regulates redox homeostasis and virulence. *Antioxidants and Redox Signaling*, **16**: 687-697.

Sassetti, C.M., Boyd, D.H. and Rubin, E.J. (2003) Genes required for mycobacterial growth defined by high density mutagenesis. *Molecular Microbiology*, **48**: 77-84.

Sassetti, C.M. and Rubin, E.J. (2003) Genetic requirements for mycobacterial survival during infection. *Proceedings of the National Academy of Science USA*, **100**: 12989-12994.

Schnappinger, D., Ehrt, S., Voskuil, M.I., Liu, Y., Mangan, J.A., Monahan, I.M., Dolganov, G., Efron, B., Butcher, P.D., Nathan, C. and Schoolnik, G.K. (2003) Transcriptional adaptation of *Mycobacterium tuberculosis* within macrophages: Insights into the phagosomal environment. *Journal of Experimental Medicine*, **198**: 693-704.

Sherman, D.R., Voskuil, M., Schnappinger, D., Liao, R., Harrell, M.I. and Schoolnik, G.K. (2001) Regulation of the *Mycobacterium tuberculosis* hypoxic response gene encoding α-crystallin. *Proceedings of the National Academy of Science USA*, **98**: 7534-7539.

Singh, A., Guidry, L., Narasimhulu, K.V., Mai, D., Trombley, J., Redding, K.E., Giles, G.I., Lancaster, J.R. and Steyn, A.J.C. (2007) *Mycobacterium tuberculosis* WhiB3 responds to O_2 and nitric oxide via its [4Fe-4S] cluster and is essential for nutrient starvation survival. *Proceedings of the National Academy of Science USA*, **104**: 11562-11567.

Singh, A., Crossman, D.K., Mai, D., Guidry, L., Voskuil, M.I., Renfrow, M.B. and Steyn, A.J. (2009) *Mycobacterium tuberculosis* WhiB3 maintains redox homeostasis by regulating virulence lipid anabolism to modulate macrophage response. *Public Library of Science Pathogens*, **5**: e1000545.

Sirakova, T.D., Dubey, V.S., Deb, C., Daniel, J., Korotkova, T.A., Abomoelak, B. and Kolattukudy, P.E. (2006) Identification of a diacylglycerol acyltransferase gene involved in accumulation of triacylglycerol in *Mycobacterium tuberculosis* under stress. *Microbiology*, **152**: 2717-2725.

Smith, I. (2003) Mycobacterium tuberculosis pathogenesis and molecular determinants of virulence. *Clinical Microbiology Reviews*, **16**: 463-496.

Smith, L.J., Stapleton, M.R., Fullstone, G.J.M., Crack, J.C., Thomson, A.J., Le Brun, N.E., Hunt, D.M., Harvey, E., Adinolfi, S., Buxton, R.S. and Green, J (2010) *Mycobacterium tuberculosis* WhiB1 is an essential DNA-binding protein with a nitric-oxide-sensitive iron-sulfur cluster. *Biochemical Journal* **432**: 417-427.

Smith, L.J., Stapleton, M.R., Buxton, R.S. and Green, J (2012) Structure-function relationships of the *Mycobacterium tuberculosis* transcription factor WhiB1. *Public Library of Science ONE*, **7**: e40407.

Sohaskey, C.D. and Wayne, L.G. (2003) Role of *narK2X* and *narGHJI* in hypoxic upregulation of nitrate reduction by *Mycobacterium tuberculosis*. *Journal of Bacteriology*, **185**: 7247-7256.

Soliveri, J.A., Gomez, J., Bishai, W.R. and Chater, K.F. (2000) Multiple paralogous genes related to the *Streptomyces coelicolor* developmental regulatory gene *whiB* are present in *Streptomyces* and other actinomycetes. *Microbiology*, **146**: 333-343.

Spiro, S. (2007) Regulators of bacterial responses to nitric oxide. *FEMS Microbiology Reviews*, **31**: 193-211.

Stapleton, M.R., Haq, I., Hunt, D.M., Arnvig, K.B., Artymiuk, P.J., Buxton, R.S. and Green, J. (2010) *Mycobacterium tuberculosis* cAMP receptor protein (Rv3676) differs from the *Escherichia coli* paradigm in its cAMP binding and DNA binding properties and transcription activation properties. *Journal of Biological Chemistry* **285**: 7016-7027.

Stapleton, M.R., Smith, L.J., Hunt, D.M., Buxton, R.S. and Green, J. (2012) *Mycobacterium tuberculosis* WhiB1 represses transcription of the essential chaperonin GroEL2. *Tuberculosis*, **92**: 328-332.

Stewart, G.R., Wernisch, L., Stabler, R., Mangan, J.A., Hinds, J., Laing, K.A., Young, D.B. and Butcher, P.D. (2002) Dissection of the heat-shock regulon in *Mycobacterium tuberculosis* using mutants and microarrays. *Microbiology*, **148**: 3129-3138.

Stewart, G.R., Robertson, B.D. and Young, D.B. (2003) Tuberculosis: A problem with persistence. *Nature Reviews Microbiology*, **1**: 97-105.

Steyn, A.J., Collins, D.M., Hondalus, M.K., Jacobs, W.R., Kawakami, R.P. and Bloom, B.R. (2002) *Mycobacterium tuberculosis* WhiB3 interacts with RpoV to affect host survival but is dispensable for in vivo growth. *Proceedings of the National Academy of Science USA*, **99**: 3147-3152.

Sutton, V.R., Mettert, E.L., Beinert, H. and Kiley, P.J. (2004) Kinetic analysis of the oxidative conversion of the $[4Fe\text{-}4S]^{2+}$ cluster of FNR to a $[2Fe\text{-}2S]^{2+}$ cluster. *Journal of Bacteriology*, **186**: 8018-8025.

Sweeney, W.V. (1980) Proteins containing 4Fe-4S clusters: an overview. *Annual Review of Biochemistry*, **49**: 139-161.

Swindells. S. (2012) New drugs to treat tuberculosis. *F1000 Medicine Reports*, **4**: 12 (doi: 10.3410/M4-12).

Talaat, A.M., Lyons, R., Howard, S.T. and Johnston, S.A. (2004) The temporal expression profile of *Mycobacterium tuberculosis* infection in mice. *Proceedings of the National Academy of Science USA*, **101**: 4602-4607.

Thelander, L. (1973) Physiochemical characterization of ribonucleoside diphosphate reductase from *Escherichia coli*. *Journal of Biological Chemistry*, **248**: 4591-4601.

Tucker, N.P., Hicks, M.G., Clarke, T.A., Crack, J.C., Chandra, G., Le Brun, N.E., Dixon, R. and Hutchings, M.I. (2008) The transcriptional repressor protein NsrR senses nitric oxide directly via a [2Fe-2S] cluster. *Public Library of Science ONE*, **3**: e3623.

Tufariello, J.M., Chan, J. and Flynn, J.L. (2003) Latent tuberculosis: mechanisms of host and bacillus that contribute to persistent infection. *The Lancet Infectious Diseases*, **3**: 578-590.

Via, L.E., Lin, P.L., Ray, S.M., Carrillo, J., Allen, S.S., Eum, S.Y., Taylor, K., Klein, E., Manjunatha, U., Gonzales, J., Lee, E.G., Park, S.K., Raleigh, J.A., Cho, S.N., McMurray, D.N., Flynn, J.L. and Barry, C.E. (2008) Tuberculosis granulomas are hypoxic in guinea pigs, rabbits, and nonhuman primates. *Infection and Immunity*, **76**: 2333-2340.

Vieira, O.V., Botelho, R.J. and Grinstein, S. (2002) Phagosome maturation: aging gracefully. *Biochemical Journal*, **366**: 689-704.

Voskuil, M.I., Schnappinger, D., Visconti, K.C., Harrell, M.I., Dolganov, G.M., Sherman, D.R. and Schoolnik, G.K. (2003) Inhibition of respiration by nitric oxide induces a *Mycobacterium tuberculosis* dormancy program. *Journal of Experimental Medicine*, **198**: 705-713.

Voskuil, M.I., Visconti, K.C. and Schoolnik, G.K. (2004) *Mycobacterium tuberculosis* gene expression during adaption to stationary phase and low-oxygen dormancy. *Tuberculosis*, **84**: 218-227.

Wadee, A.A., Kuschke, R.H. and Dooms, T.G. (1995) The inhibitory effects of *Mycobacterium tuberculosis* on MHC class II expression by monocytes activated with riminophenazines and phagocyte stimulants. *Clinical and Experimental Immunology*, **100**: 434-439.

Walters, S.B., Dubnau, E., Kolesnikova, I., Laval, F., Daffe, M. and Smith, I. (2006) The *Mycobacterium tuberculosis* PhoPR two-component system regulates genes essential for virulence and complex lipid biosynthesis. *Molecular Microbiology*, **60**: 312-330.

Wardrop, S.L., Watts, R.N. and Richardson, D.R. (2000) Nitrogen monoxide activates iron regulatory protein 1 RNA-binding activity by two possible mechanisms: effect on the [4Fe-4S] cluster and iron mobilization from cells. *Biochemistry*, **39**: 2748-2758.

World Health organisation (2011) Global Tuberculosis Control. WHO Press, Geneva, WHO/HTM/TB/2011.16.

Young, D.B., Perkins, M.D., Duncan, K. and Barry, C.E. (2008) Confronting the scientific obstacles to global control of tuberculosis. *Journal of Clinical Investigation*, **118**: 1255-1265.